# The use of photogrammetry in the measurement of the deformation of a box girder bridge.

A thesis submitted to the University of London for the degree of Doctor of Philosophy.

By

P.J.Scott.

Department of Photogrammetry and Surveying,
University College London.

April 1977.

## Abstract.

A comprehensive series of calibrations of a Galileo-Santoni Special "A" stereometric camera pair was carried out in preparation for the structural deformation measurement of a model box girder bridge. The calibrations are described here. A goniometer was built for the infinite focus calibration which in turn was required as a basis for comparison of the close focus calibrations. A new method of calibrating the cameras at less than 4m object distance was then devised, which proved capable of very high precision. It forms the only truly original part of this work.

Results of all the calibrations were then examined and an unexpected change in principal distance was found at the close focus. The change is shown to be dependent on the positions of the entrance and exit pupils. The opportunity is taken to explain an effect known as the variation of principal distance with object distance, and to show that this variation is, in fact, non-existent.

A simulation of the structural project was created in the laboratory and photographed. The photogrammetric results were obtained first using the maker's value of the principal distance, then using the principal distance derived from the infinite focus calibration and finally from the values obtained in the actual close focus calibration. The three results demonstrate the increase in accuracy obtained by calibration, and also the importance of the lens effect described above.

Details are given of the photogrammetric process used on the box girder bridge. Finally, a critical appraisal is made of the use of photogrammetry in a project such as this.

# Contents.

I gratefully acknowledge the indispensable help of the following people:

Professor E. H. Thompson for his inspiration.

Mr. C. C. Newth for the construction of the goniometer, for his patience, his screwdrivers and things.

Mr. E. H. Wickens for his practical advice, and hours and hours of general assistance.

Mr. T. K. Rylance for his computer knowledge, his survey network adjustment programs and his box girder observations.

Mr. J. A. Knight and Mr. R. M. Hepburn for their box girder observations.

Mr. D. R. Gordon and Dr. I. A. Harley for ideas, discussions, advice and criticism.

Mr. I. J. Dowman and the staff of the Department for encouragement and discussions.

Miss J. Gurr for technical advice on the box girder photography.

Mr. K. B. Atkinson for undertaking the ghastly job of proof reading.

Mr. G. H. Owens for his patience,

and, most importantly, A, P, and M because they were always happy to see me come home.

## Introduction.

The purpose of this project was to develop a photogrammetric system for structural deformation measurement of a 1:12 scale model of a box girder bridge. The stringent accuracy requirements necessitated a comprehensive series of calibrations. The Galileo Santoni camera which was calibrated was chosen for the measurement because of its long focal length, and the fact that the very small minimum aperture made it possible to photograph the bridge at close range while still accommodating the great depth of field required. Numerical details are given in Chapter 8, together with the results of a test of the accuracy of the methods used for the actual box girder measurement.

In this thesis the cameras are first described. The theory of calibration by goniometer is then set down, followed by a description of the goniometer built for the project, and the results of the infinite focus calibration. A new method of camera calibration at object distances of less than 4m is then described and a theory developed concerning the increase of principal distance at close focus. The theory and calibrations are justified by photogrammetric measurement of a test object similar to a section of the box girder. Finally a brief description of the methods used on the actual bridge measurement is given.

Plate 2. The fiducial cross on glass in the brass mount. Note the optic fibre.

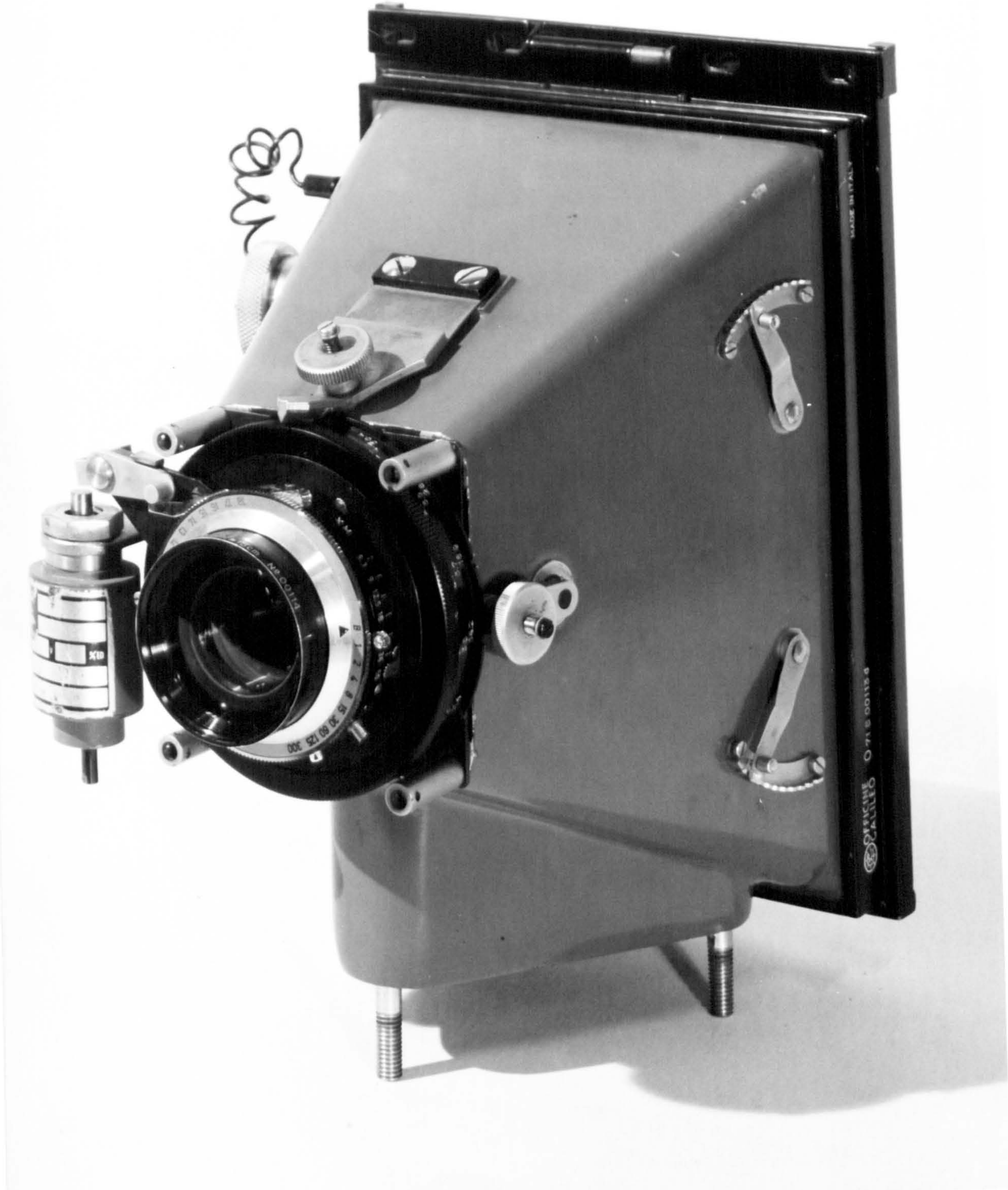


Plate 1. One of the stereometric cameras.


Plate 3. The camera on the A.8. stage plate.

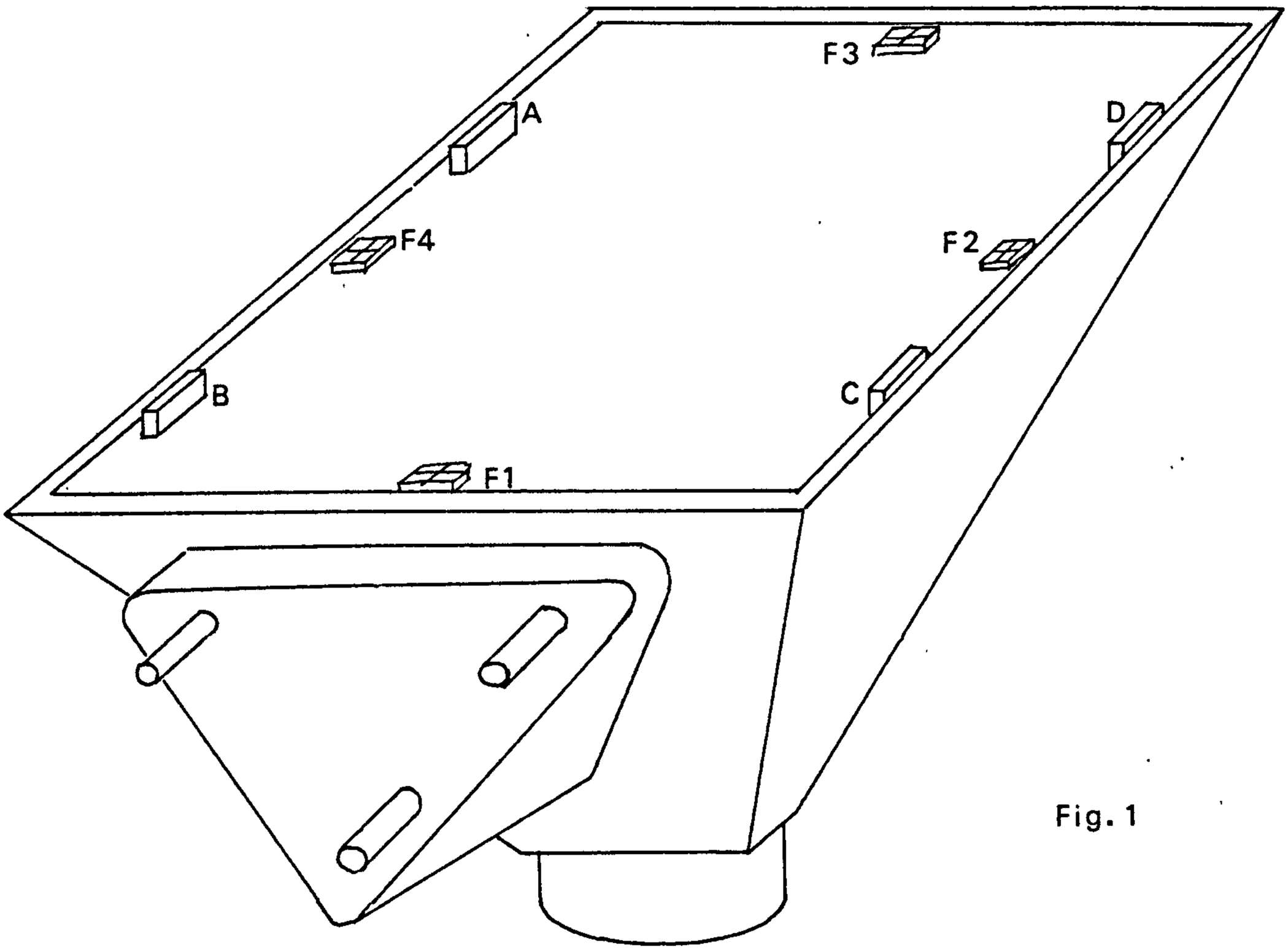


Fig. 1

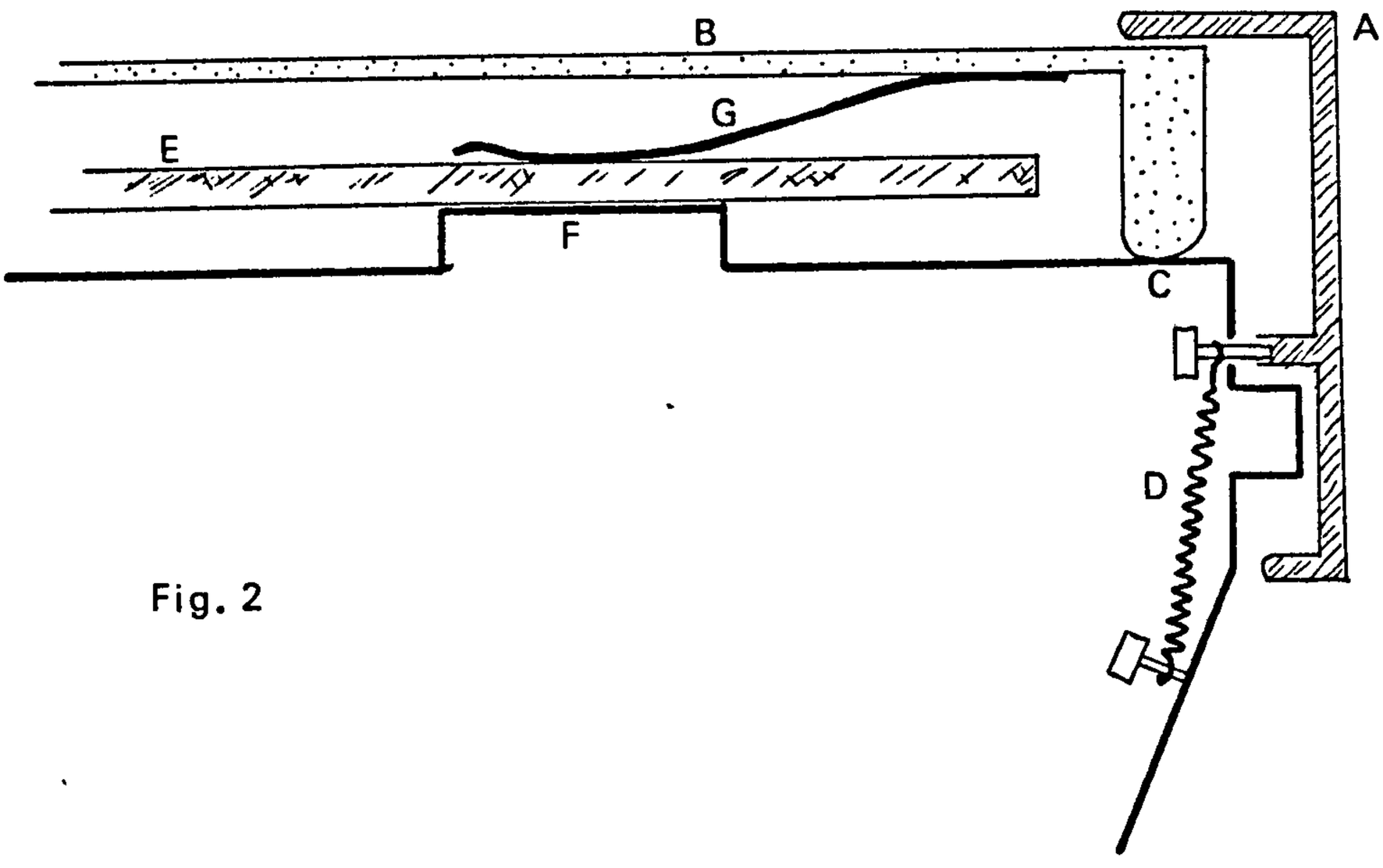


Fig. 2

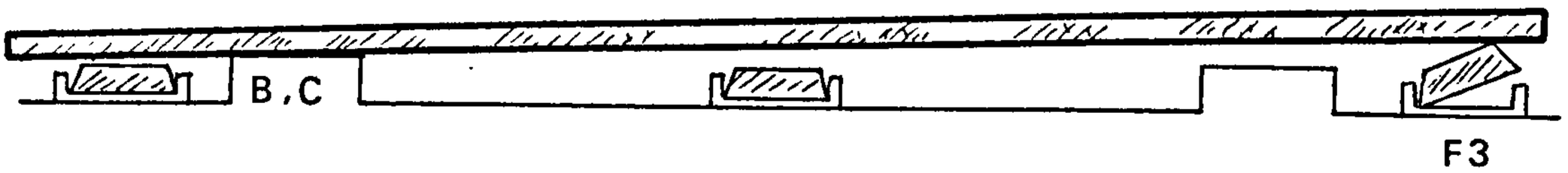


Fig. 3

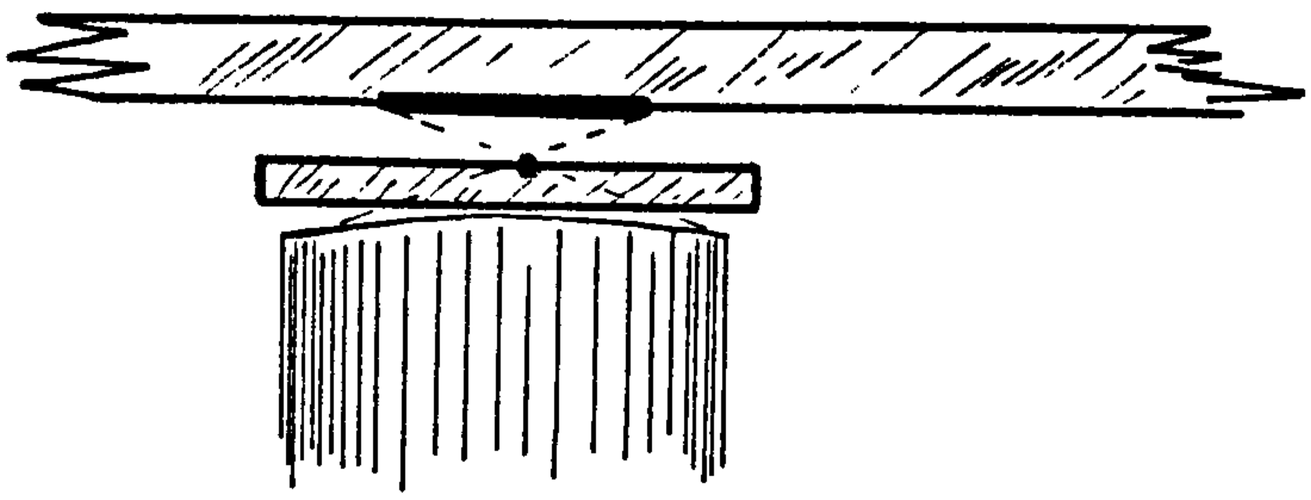

Fig. 4

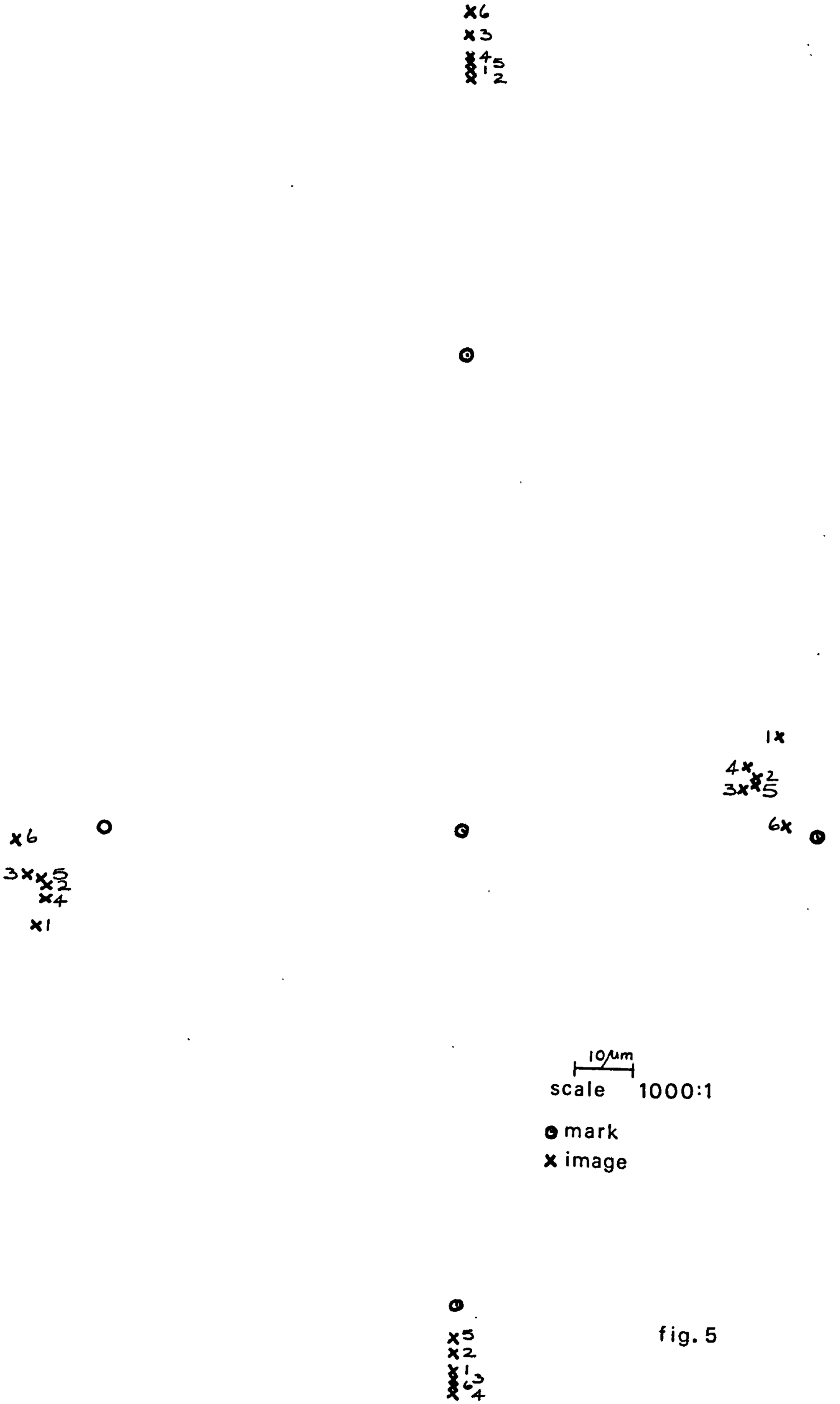
x6
x3
x4
x5
x1
x2
x6
3x
x5
x2
x4
x1
1x
4x
x2
3x
x5
6x
10/um
scale 1000:1
mark
image
x5
x2
x1
x3
x4

fig. 5

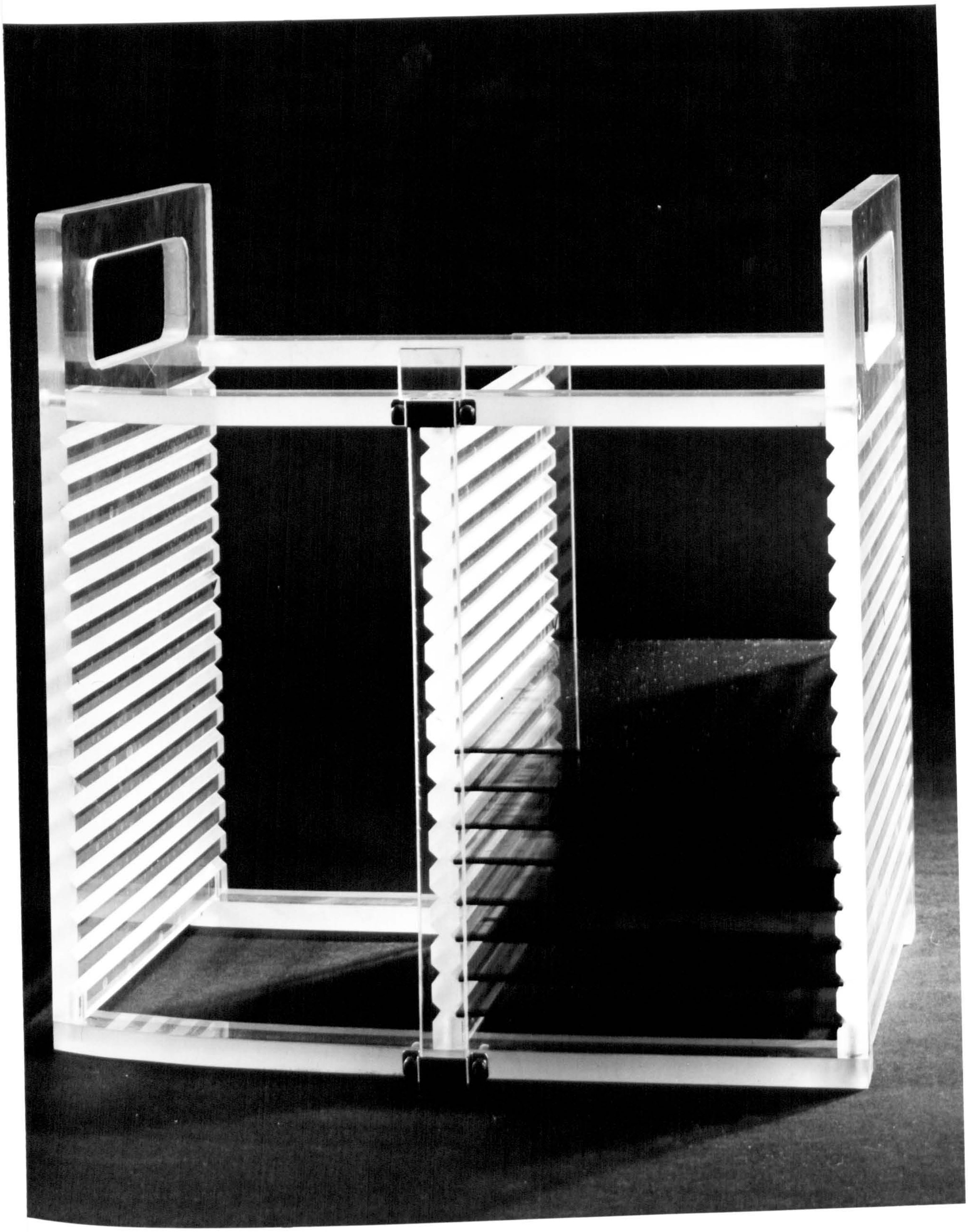

Plate 4. The bulk-processing plate rack.

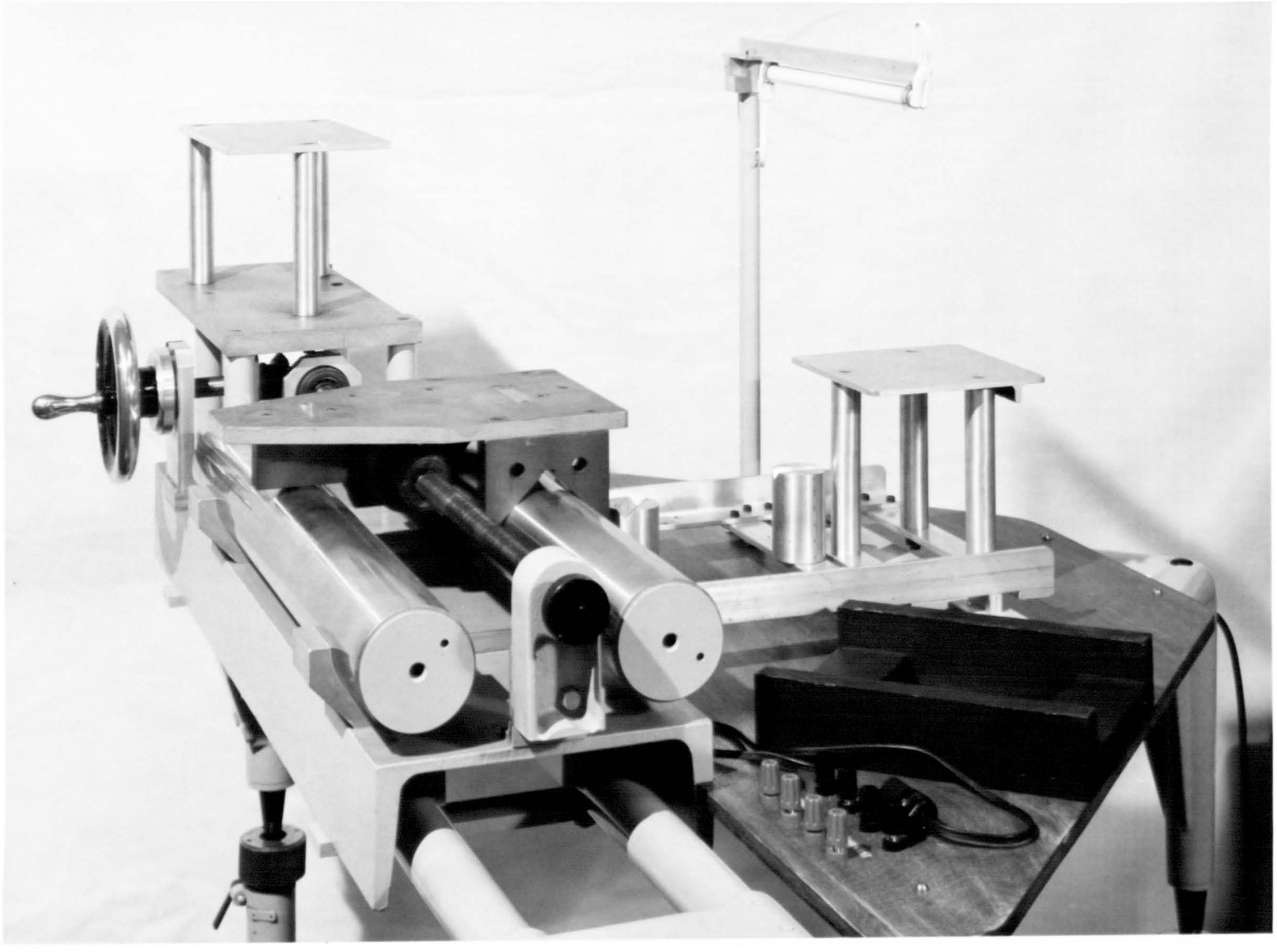

Plate 5. The slide on its base.

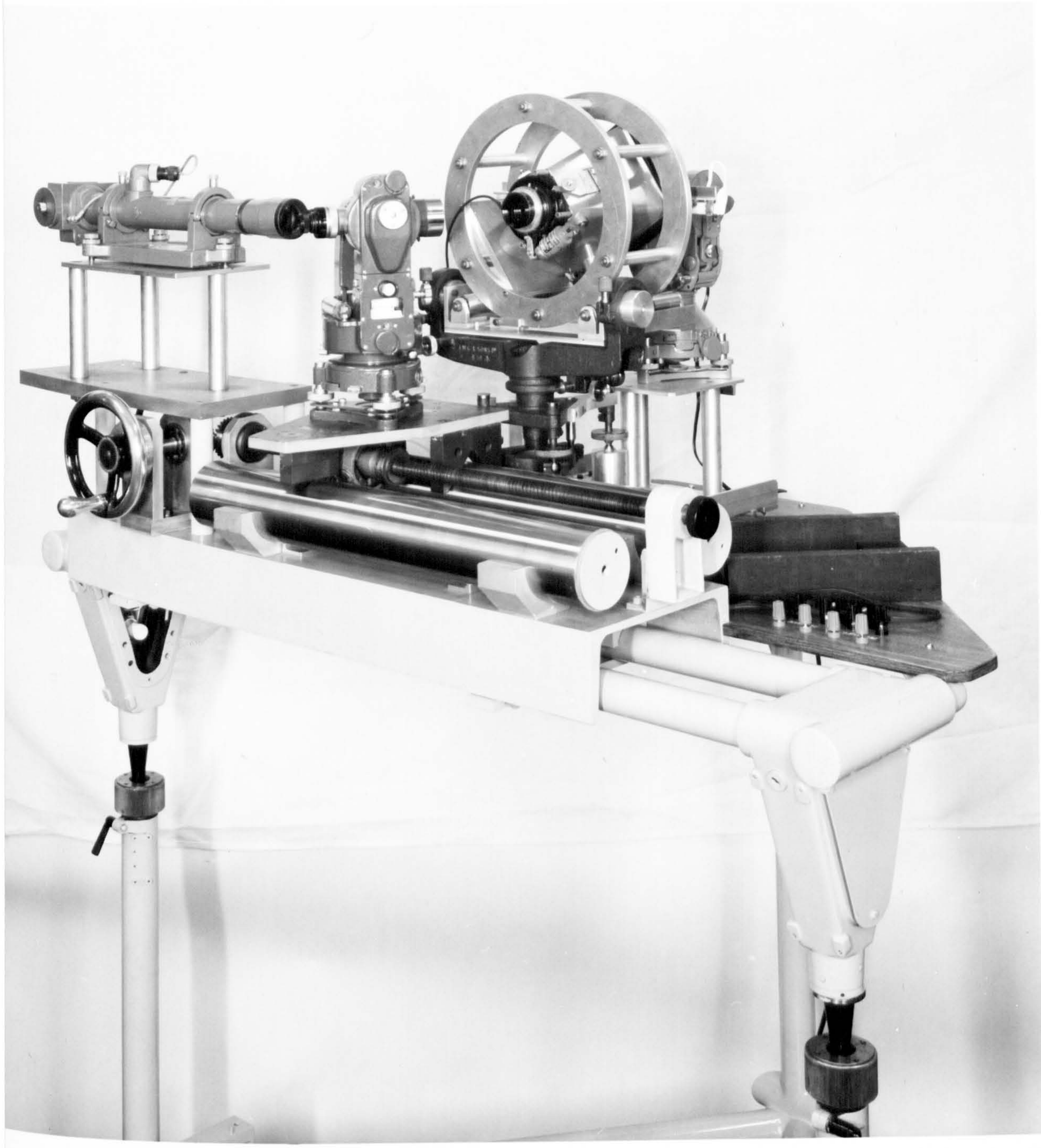

Plate 6. The goniometer on the base frame.

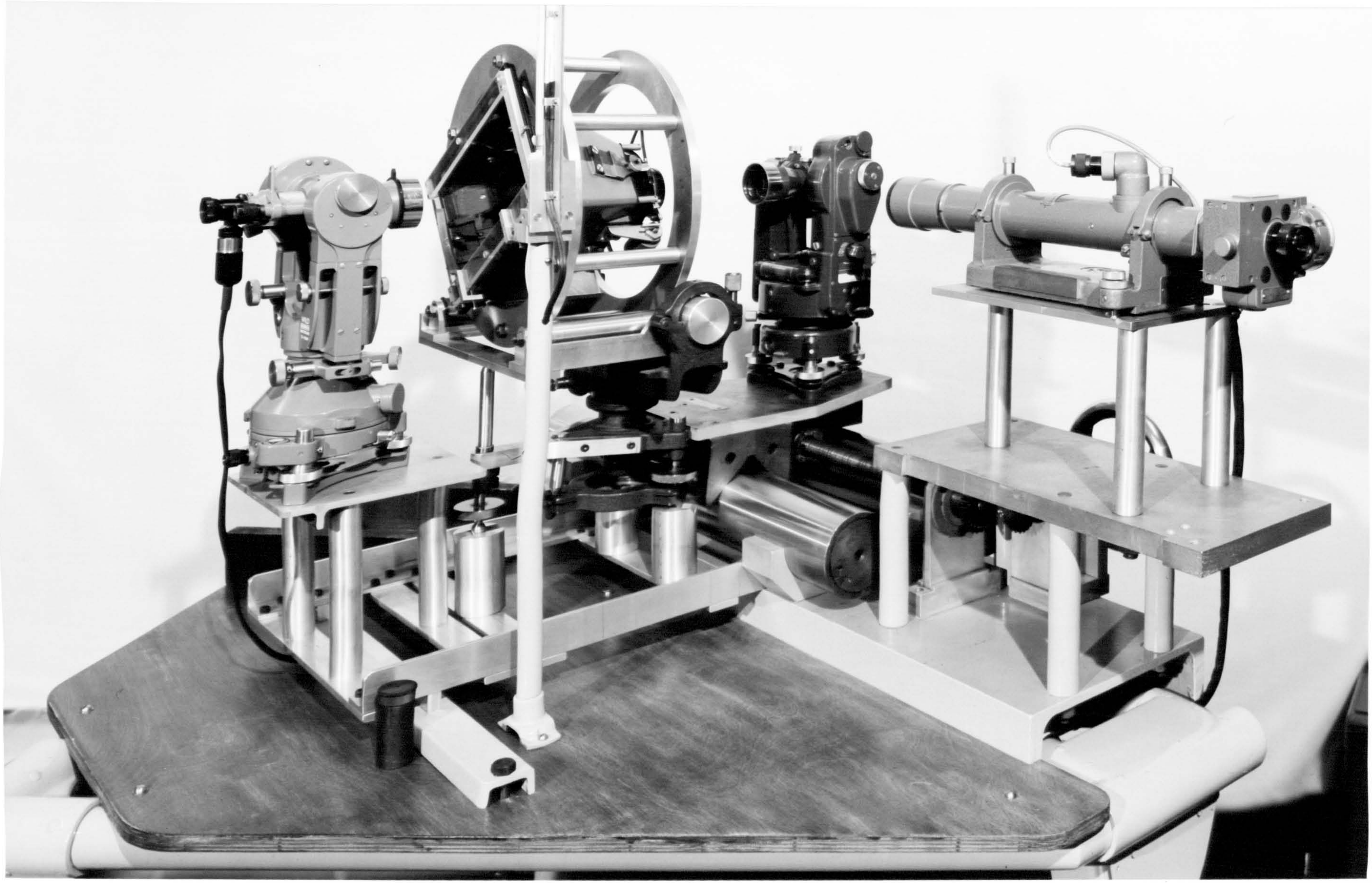

Plate 7. The completed instrument. Note the rear autocollimator. The vertical fluorescent tube is lowered to the horizontal position to illuminate the diagonal when observing.

Plate 8. The camera, cage, roller assembly and tribrach. Note the extended rear footscrew.

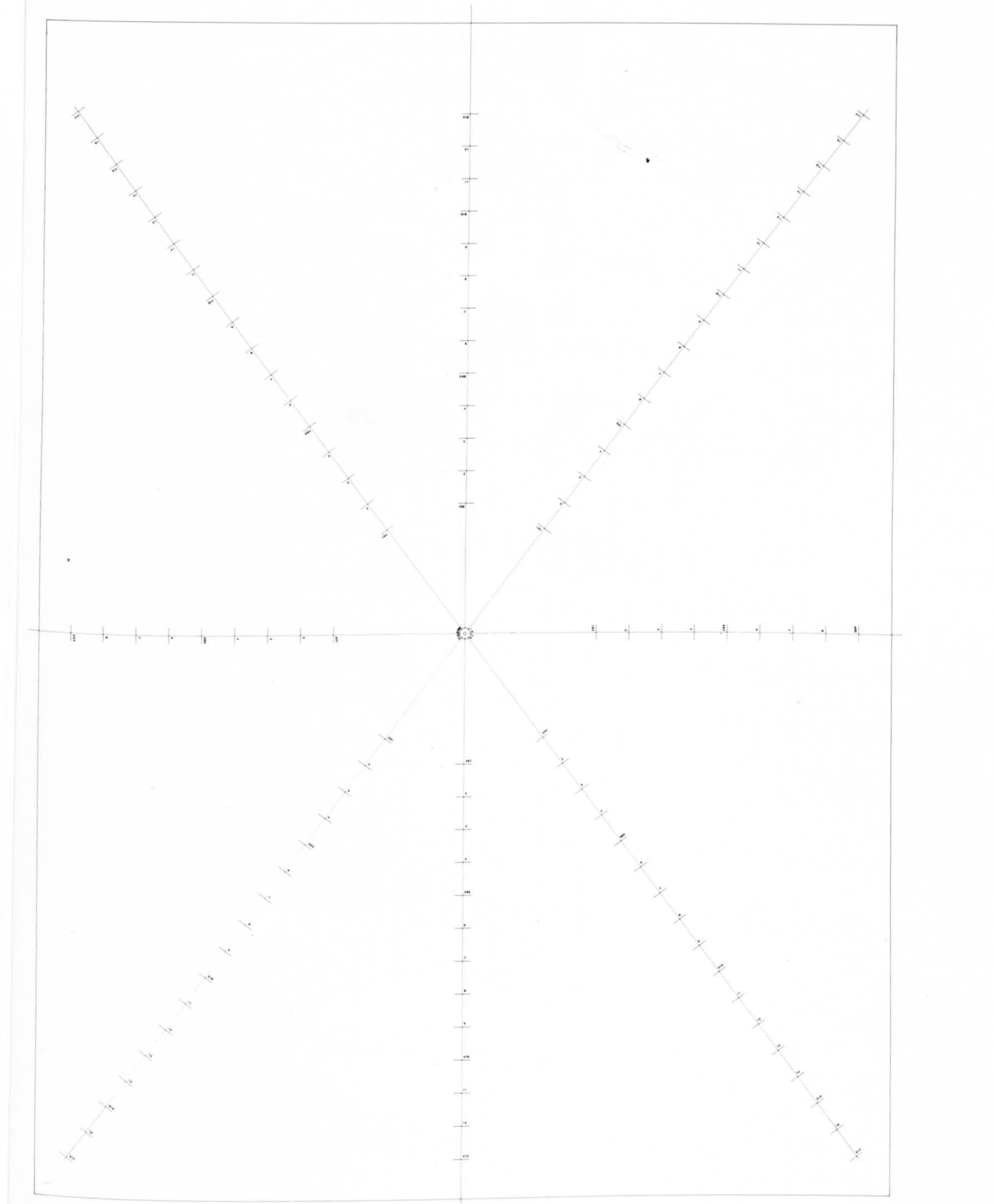

Plate 8a. The graticule on the glass plate.

# Chapter 1.

## The Galileo Santoni "A" cameras.

### Introduction.

The cameras which were used in the structural deformation project are described. Results of a test on fiducial mark reproduction are given. A system of bulk processing of photographic glass plates in the darkroom is then presented.

### General description

The Galileo Santoni "A" stereometric cameras were bought by the Department of Photogrammetry and Surveying, University College London, in 1967. The basic equipment consists of a pair of cameras, two mounting bars of 0,56m and 2m, and a tripod. A mounting base for a single camera has since been made in the Department.

Each camera has a nominal focal length of 150mm, and uses glass plates of 130 x 180mm, with an effective picture size of 120 x 160mm. The lens has apertures from f/6,3 to f/50, and shutter speeds from 1s to 1/300s, as well as manual time exposure. One of these cameras is shown in plate 1.

### The lens and shutter.

The lens is mounted on a screw thread. The camera can be focussed by advancing the lens on this thread through 12 steps of 0,4mm each. A spacer of 5,4mm, or one of 10,8mm, can be inserted between the lens and the camera body. This gives a total of 36 principal distance settings. The smallest object distance possible is 1,6m.

The shutter can be released by means of a cable release. When the cameras are used as a pair, both

shutters can be released simultaneously by means of the electrical solenoid switches which are fitted.

The cameras are referred to throughout by their serial numbers. 113s refers to the "sinistra" or left hand camera, and 113d to the "dextra" or right hand camera. These cameras have lenses 115 and 114 respectively.

The picture plane.

The picture plane is defined by four machined metal staqes, shown as A-D in figure 1. The photoqraphic qlass plate is brought into contact with these stages by a system of springs described later in the chapter.

Each camera has four fiducial marks, shown as F1-F4 in figure 1. They are numbered clockwise when viewed from the perspective centre, with F1 on the side of the camera's mounting screws. F1 is identified in the photoqraph by the clear strip which always appears on the negative along the mounting screw edqe, because the plate is blinded by the plate holder frame.

The fiducials are in the form of a cross etched onto a 4x4mm qlass plate, cemented into a brass mount, as shown in plate 2. A singqle light source in a housing on the camera body is used to illuminate the fiducials usinq fibre optics. One is clearly seen in plate 2.

The plate location system.

The qlass plates are loaded into plate holders in a dark room. Each plate holder can hold one plate, and it has a slidinq shield to exclude light during transit.

The photoqraphic plate loading and location system is shown in fiqure 2. A metal plate holder frame, A, on the back of the camera body, holds the plate holder, B, and is lowered until B comes into contact with the camera body at C. Four springs, D, supply the force.

At this stage, the photographic plate, E, is pressed against the focal plane stage, F, by four leaf springs, G. These weak leaf springs, and not the stronger coil springs, locate the plate in the focal plane. The cameras are equipped with 24 plate holders. On inspection of the leaf springs, several were found to be flattened against the back of the holder, and were thus not functioning. They were bent outwards to bring them into action again. Previous to this, many plates had blurred fiducial images. The problem did not recur after the springs had been bent. The blurring thus indicates that the plate had not been brought into contact with the picture plane. The springs are definitely a weak design feature, and they should be tested frequently.

It is worth mentioning that one of the plate holders was modified to make the coil springs D pull down the plate itself, but they were too strong and actually warped the plate.

Adjustment of the fiducial marks.

Before proceeding with the calibrations described later, one of the fiducials, F3 on 113s, had to be repositioned as it protruded 0,1mm beyond the picture plane ABCD in figure 1. This meant that when the glass plate was pressed toward the picture plane, it would be supported by the two stages B and C, and F3, as shown in figure 3. The plate would obviously never lie in the intended plane. Moreover all the fiducial images were blurred because of the lack of contact, as shown in figure 4. The large gap between mark and plate allowed the image to scatter, since the fibre optic was so close to the mark itself.

The small fiducial glass was removed by dissolving the cement securing it in the mount, and it was then correctly positioned and reset.

A qlass plate with a rectanqular qraticule was placed in the picture plane and fitted over F1, F2 and F4. The brass mount of F3 was now loosened and shifted to make the fiducial axis F1-F3 normal to the F2-F4 axis.

Investigation into the fiducial mark reproduction.

The test to be described here cannot be used to improve results cbtained frcm the camera, but it does help to determine a limit of possible accuracy. The experiment involved coordinatinq the actual fiducials in the camera, and comparinq them aqainst the coordinates of the images they made on the plates.

To coordinate the marks in the camera, the plate holder frame was removed so that the four machined stages of the picture plane could stand on the staqe plate of a plottinq instrument. The plotter used was a digitised Wild A8, and the camera is shown in position in plate 3. The procedure was as follows:

1. Without alterinq the z coordinate, pointings were made to all fiducials, and the x and y coordinates read. The round was repeated five times.

2. The camera was removed, and a calibrated qrid plate clamped onto the staqe plate.

3. Coordinates of a qrid intersection in the vicinity of each fiducial were read, and repeated five times.

4. Joins were calculated between the qrid intersections to qive a scale factor from model coordinates to plate coordinates.

5. The scale factor was applied to the coordinates of the fiducials.

6. The coordinates of the fiducials (and later of the imaqes on each plate) were used to intersect the defined principal point. All coordinates were then

reduced to this point as origin, and rotated onto the long axis F1-F3 as the zero direction.

Eighteen plates were now exposed to the fiducial marks in the camera, in groups of three. For each new group the camera's axis was set in a different attitude to test for any change in the image separations with camera movement.

The results are presented graphically in figure 5. The displacements from mark to image are plotted to an enlarged scale. The six groups of plates agree fairly well with each other, and the four mean shifts from the marks to their own images appear to be random in size and direction. Not only has the separation distance changed on each axis but the angle of intersection has altered as well. The most important point is that the actual intersection of the fiducial marks is not necessarily the same as that of the images. As is seen later, the infinite focus calibration uses the marks themselves as the reference for the principal point. It is therefore possible that the principal point used in practice on a photograph is in error. The close range calibration uses the images as a reference and the results should thus agree with photographs used in practice.

The investigation is inconclusive as there seems to be no way of deciding which mark, if any, is correct.

Bulk processing.

During the above test, a small investigation was conducted into the simultaneous processing of large numbers of plates. Research done on processing of glass plates indicates a tendency for the emulsion to creep if the plates are vertical. It would seem essential, therefore, to process plates horizontally. This means that a definite limit is imposed on the number of plates which can be processed at one time, governed by the area

of the available processing dish.

Initial calculations concerning the approaching box girder bridge test showed that each of the estimated 25 load stages would require 25-30 plates, which would mean that more than 200 hours of processing time would be required if plates were to be processed singly.

It was felt that some form of bulk processing should be attempted. A rack was designed which could hold 32 plates in two stacks, at 10mm spacings. It is shown in plate 4. The plates are horizontal. Three fibre glass 7 gallon water tanks were obtained, and used for the standard developer, wash and fix steps of developing.

The method was tested using the 18 plates in the above test. All photographs were of the same test target, consisting of three line maps of the London area.

It must be pointed out that the developer cannot reach the centre of the plate as readily as it can reach the edge. This produces an uneven image, less dense towards the centre of the plate. Also, agitation sets up eddy currents, which produce a ripple effect on the density. In photogrammetric projects where premarked targets are used, however, this effect is not critical as long as the targets are observable. This test, therefore, was designed to discover whether the fall-off was so bad as to prevent observation.

In fact, despite a slight fall-off in the extreme corners of the plate, where two members of the rack prevented easy circulation, the results were thoroughly satisfactory, and the lines of the map stood out equally well all over the plate. The camera has a marked vignetting effect at the picture edges, and it would seem that the two effects largely cancel each other.

Agitation was achieved by raising and lowering the rack slowly but continuosly, and allowing gravity to cause the circulation. Fixing time was increased by a factor of

three. It is not sure whether this is necessary. Washing requires considerably longer, and drying requires a constant stream of air. If the rack is left to stand in still air, the plates may take up to 72 hours to dry, but in the air stream this is considerably reduced.

Including loading of the plates into the rack, dark room time was about 30 minutes, excluding mixing of chemicals, and cleaning up afterwards. This immediately cut estimates of dark room time on the box girder test down to no more than one hour per load stage (with increased number of plates) or some 25-30 hours altogether.

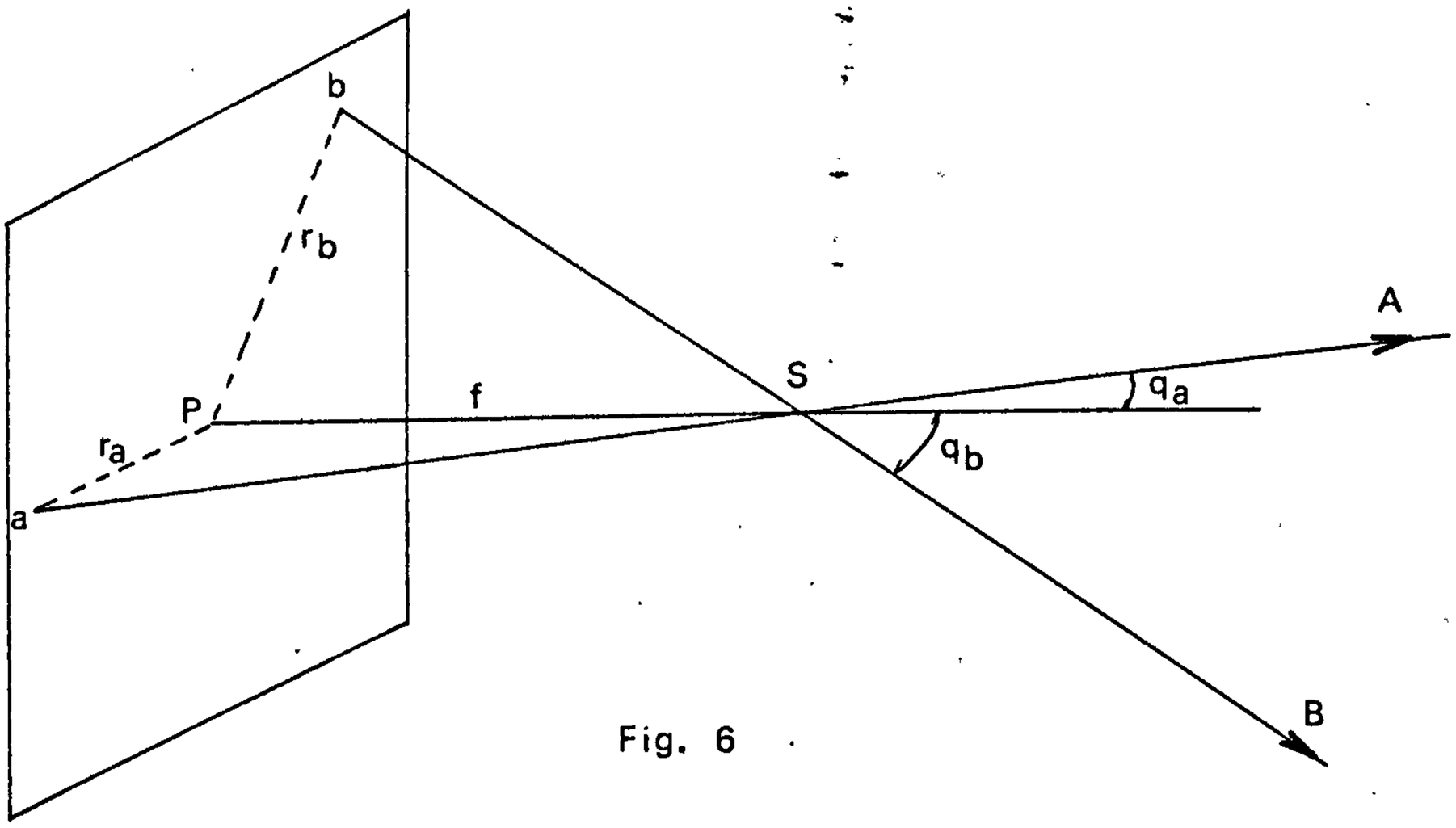


Fig. 6

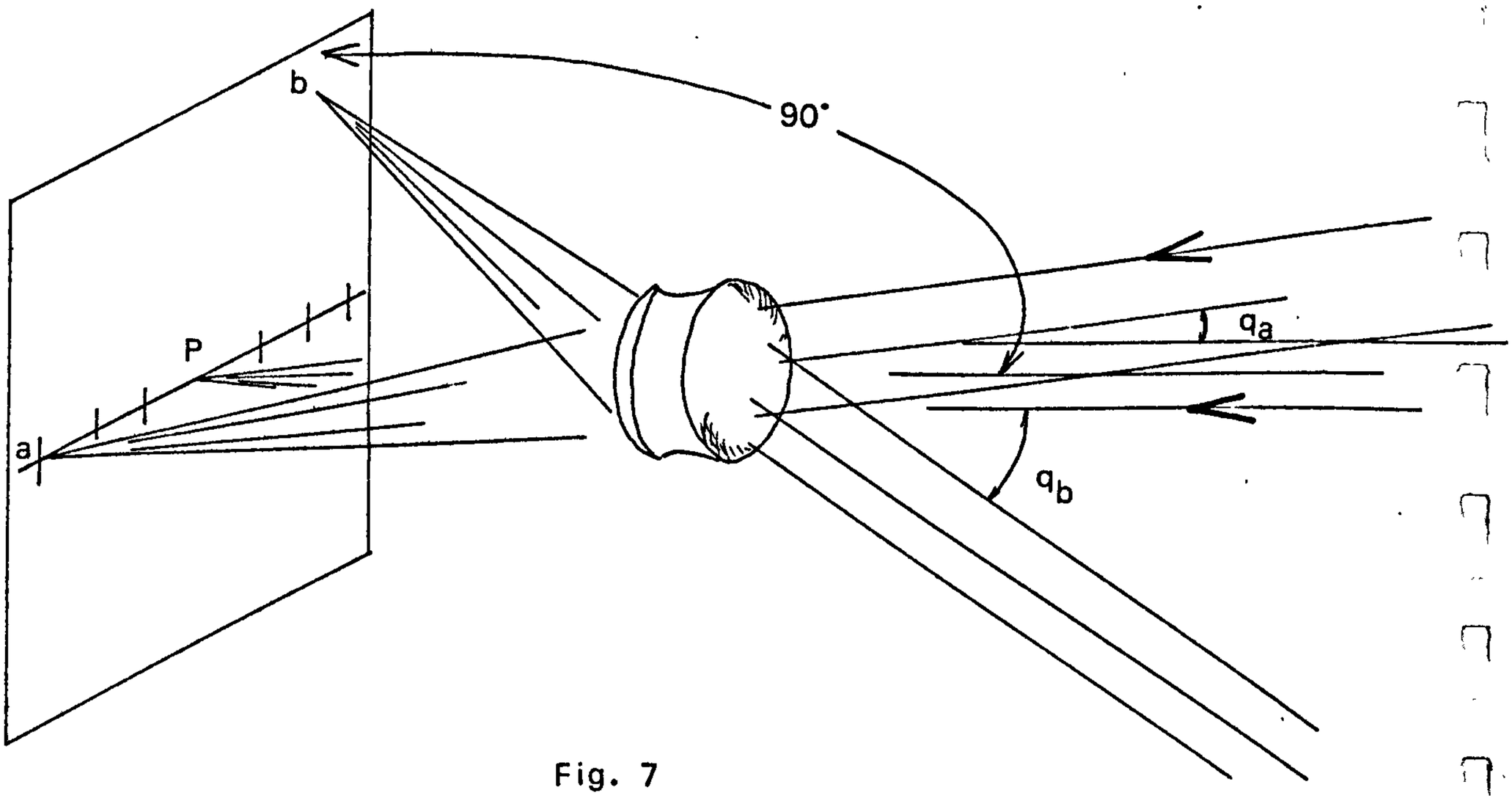


Fig. 7

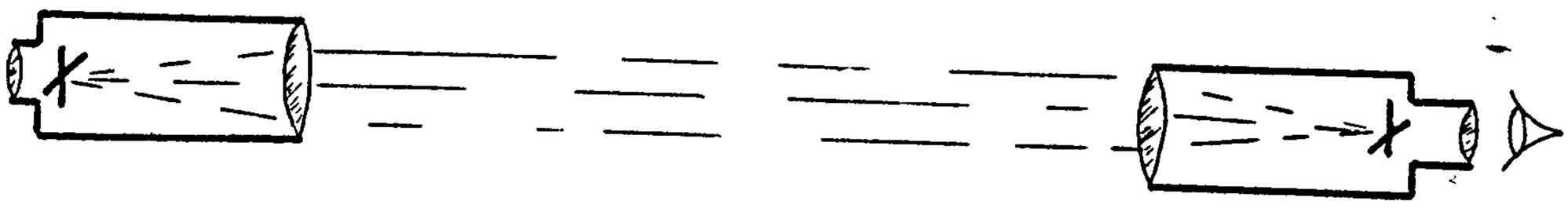

Fig. 8a

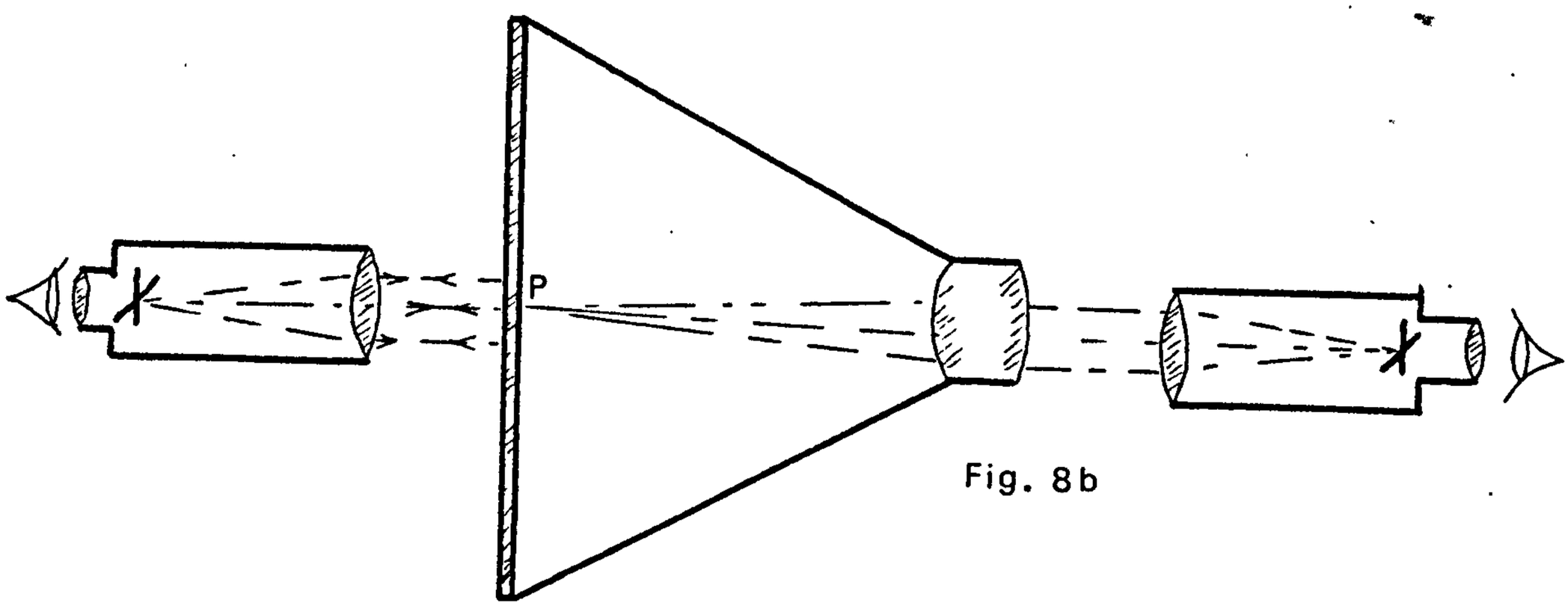


Fig. 8b

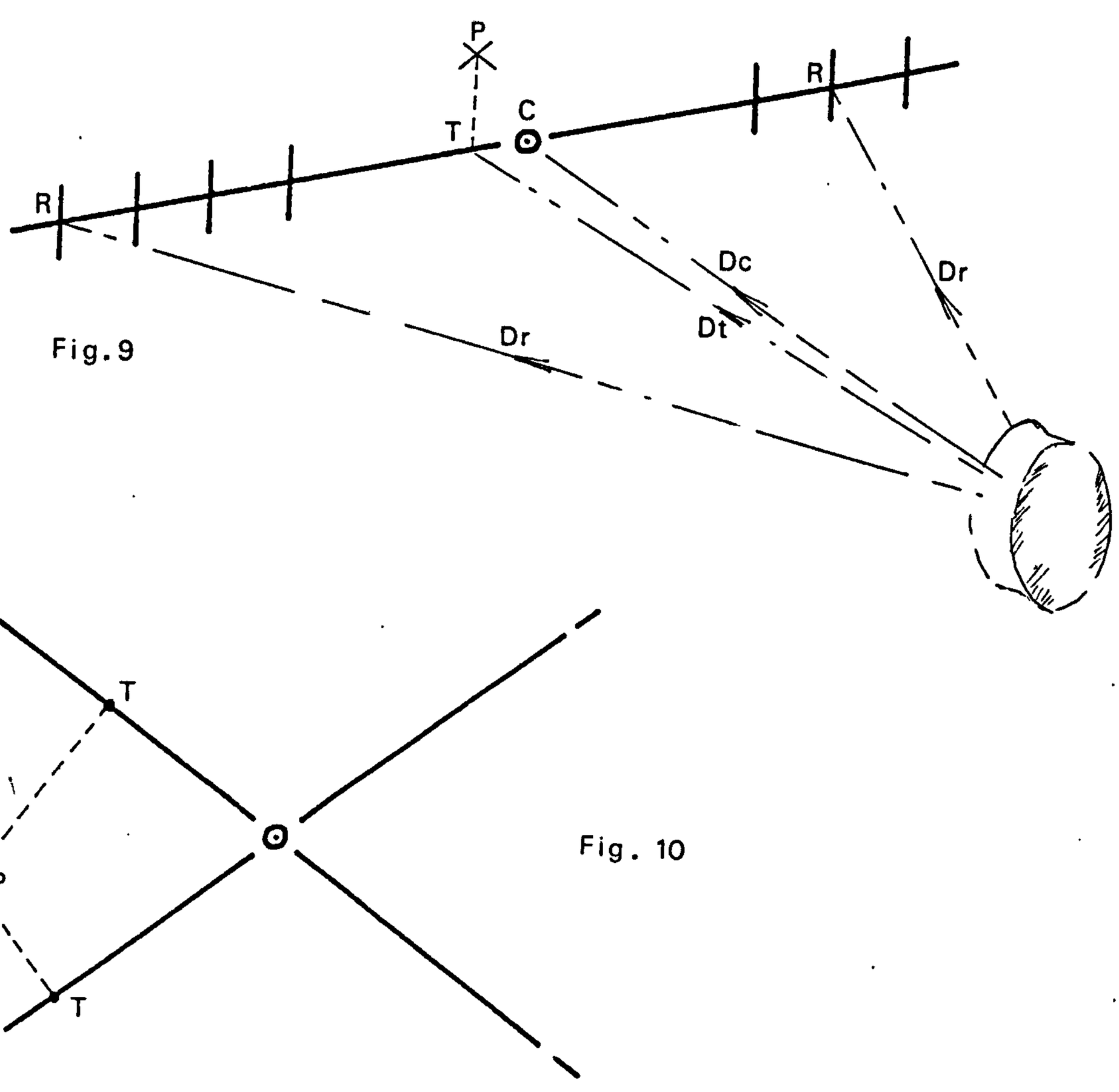


Fig.9




Fig. 10

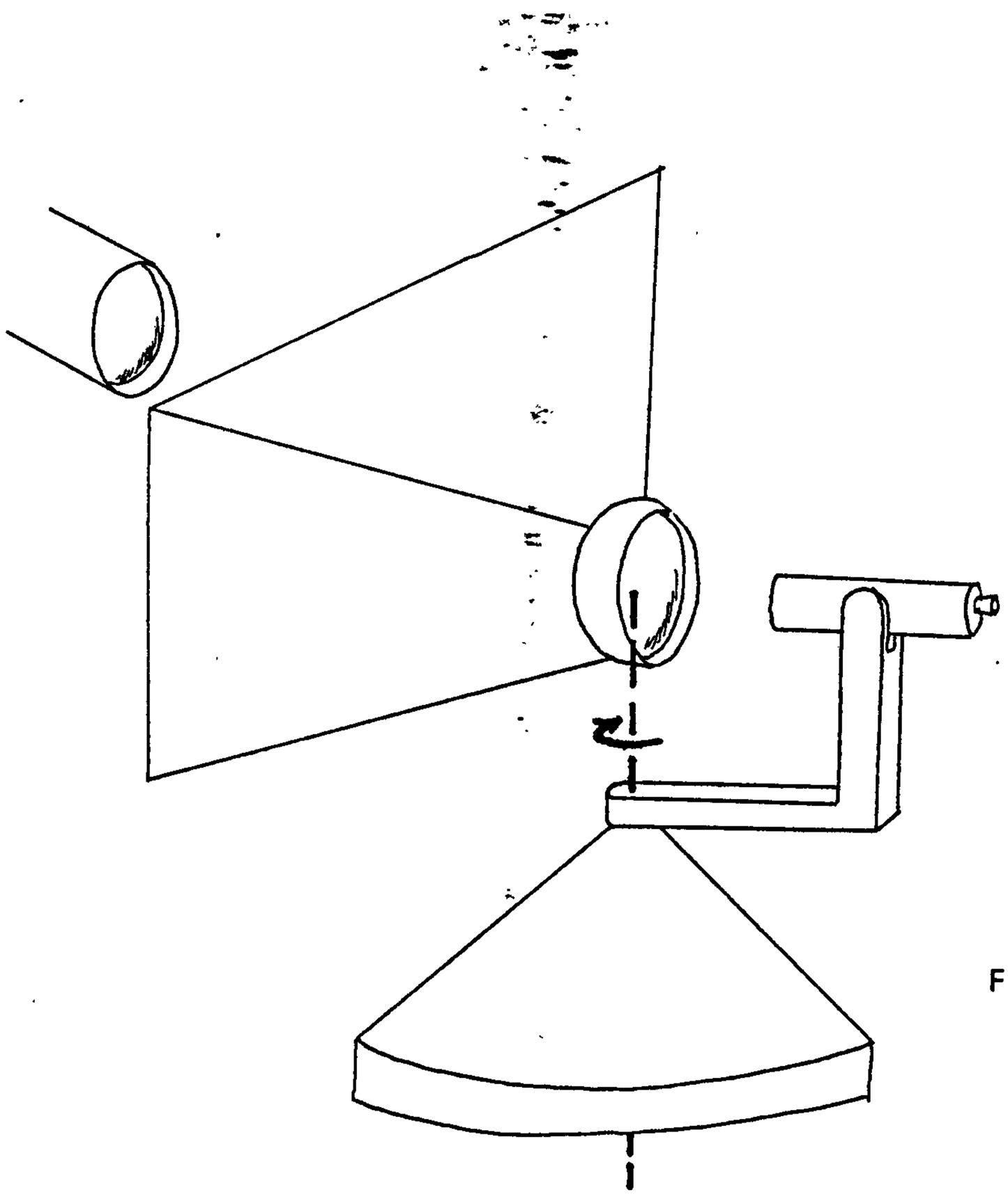

Fig. 11

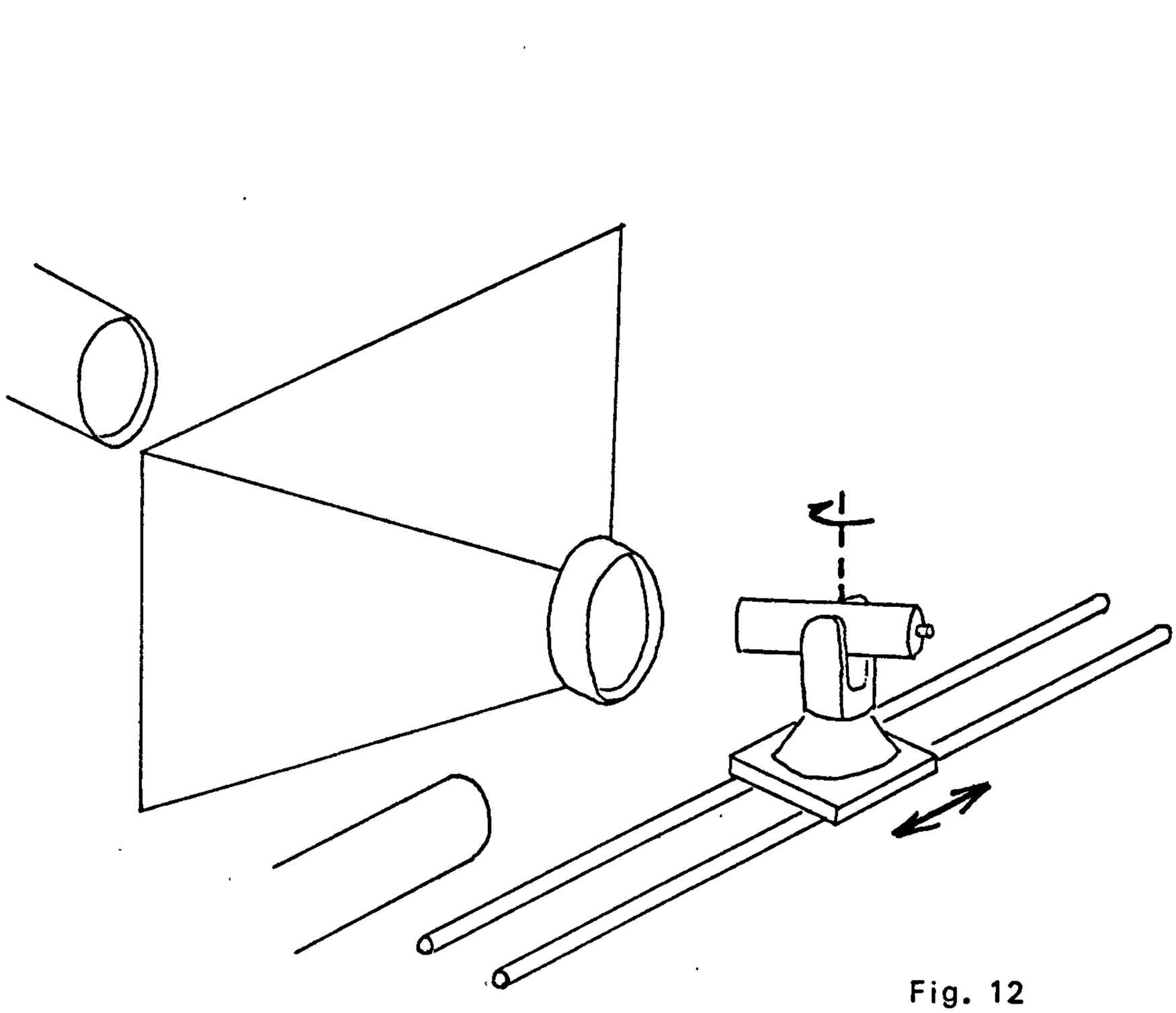

Fig. 12

# Chapter 2.

## The theory of the camera and its calibration.

### Introduction.

Since the camera has been explained in Thompson (1957) , it is not intended to present the theory in minute detail. The purpose of this chapter is to define terms, and to show how the calibration method used in this work is derived from the basic theory.

Many rigorous methods of photogrammetric restitution equate the photographic process to a central projection of a three dimensional object onto a plane. A lens, however, cannot be considered as a single point. The elements of the central projection must, therefore, be defined, and an unambiquous comparison must be made with the camera.

### Comparison with the central projection.

Consider the diagram, figure 6, of the central projection menticned above. The two essential elements are the plane of projection, and the perspective centre, S. The normal through S to the plane, called the principal axis, meets the plane at P, referred to as the principal point. The distance PS, called the principal distance, is denoted f. For all projected points such as A and B it is clear that

$$ra.\cot qa = rb.\cot qb = f \qquad (1)$$

where r and q are defined in the figure.

This, then, is the simple requirement of the metric camera i.e

$$r.\cot q = f \qquad (2)$$

where f is a constant. The purpose of a calibration is to define an origin for all r and hence q, and thereafter to determine the value of f,

and its variation, if any. The variation can be treated in any satisfactory manner during the restitution process, but this is beyond the scope of the actual calibration.

Since S does not exist in the lens, P cannot be defined in the camera as it was in the central projection. A point similar to P must be chosen as the origin for all r and q. Consider a camera focussed for infinity, as shown in figure 7.

The images of objects at infinity are formed by the lens on a surface which may be called the image surface. A perfect lens has a plane image surface. This lens does not exist, and in practice the surface has a complex curvature. The picture plane of a camera approximates closely to the image surface to keep the image as sharp as possible. The camera has some mechanical means of defining the picture plane, and of ensuring that the photographic emulsion coincides with it. Obviously the picture plane is equivalent to the plane of projection in figure 6.

Two beams of sensibly parallel light from objects A and B form an image in this plane at a and b. qa and qb can be considered as the angles made by the beams with the normal to the plane, and, if P is defined, ra and rb can be measured from P as origin. f can now be calculated for each r.

The logical position for P is the image point of a light beam originally normal to the picture plane. This point, usually termed the point of autocollimation, has the advantage of being defined physically. It is, therefore, unique, and can be recovered with a high degree of accuracy. It is also exactly analogous to the point P in the central projection.

A practical interpretation of the theory.

The method presented here is not new, but is described to explain the apparatus which was constructed.

As shown above, some means of measuring incident angles q for defined radial distances r is required. From these observations, values of f for each r, and hence the variation in f, can be calculated. Furthermore, the equipment should be able to define the point of autocollimation P as described above.

In this method a plane glass plate is substituted for the picture plane of the camera. Radial lines etched on it are fitted over the fiducial marks. Their intersection, therefore, is the principal point as defined by the fiducials on a photograph. The radials have graduations along them. The distances of these graduations from the intersection are known.

The camera is set up with its axis horizontal. One of the radials in the picture plane is also made horizontal by rotating the camera about its axis. All measurements are now made in the horizontal plane defined by the axis and the radial.

Let one of the graduations on the horizontal radial be point a in figure 7. The beam from a will pass through the lens and emerge as a parallel beam of light. If a theodolite, focussed for infinity, is set in the beam, the observer will see point a. The direction Dr can thus be measured.

To locate P, an autocollimator is mounted behind the camera, as shown in figure 8. With the camera removed, the theodolite is aligned onto the projected image of the cross hairs from the autocollimator (see figure 8a). If the camera is now placed in the beam as shown in figure 8b, the glass plate will reflect the projected beam. When the picture plane is set normal to the beam, an observer at the autocollimator sees the reflected image of the cross hairs superimposed on the direct image. The picture plane is now normal to the theodolite's line of sight as well. An observer there will thus see the point P, as shown in figure 9. This point is, in general, not on the

radial. Let T be the foot of the perpendicular from P onto the radial. The horizontal direction to T is thus the same as that to P. This direction, Dt, is now used as origin for all q.

Directions Dc, Dr are now observed to the intersection C, which is the defined principal point, and each graduation R in turn, as shown in figure 9. Let the directions increase clockwise. Let distances along the diagonal be measured from C as origin, positive as the directions increase. Let Lr and Lt be the distances of R and T.

From the diagram:

$$Lt = f.\tan(Dt - Dc) \qquad (3)$$

Then, for each R,

$$f = (Lr - Lt).\cot(Dr - Dt) \qquad (4)$$

The maker's value of the focal length may be substituted for the unknown f in 3, as (Dt - Dc) should not exceed two minutes of arc.

Each line of radials in turn is made horizontal, and the directions observed. The position of T is found on each diagonal, and the coordinates of P deduced from these, as shown in figure 10, by erecting perpendiculars from both points T.

From all the lines there will be statements of the variation of f with radial distance from P. These will show the symmetric and asymmetric nature of the deviation of the camera from the mathematical standard.

Rotation about the front node.

It will be noticed that the above description implies that the theodolite rotates about a vertical axis through the front node of the camera lens. In some types of

instrument this is the case as shown in figure 11. These types are necessarily very expensive, as they are completely specialised. A variation can be constructed using a standard theodolite and collimator. The theodolite is mounted on a horizontal slide, as shown in figure 12. The slide is roughly parallel to the picture plane. When a pointing is made to a new graduation, the theodolite must be translated on the slide until the line of sight once more enters the entrance pupil of the camera. Since the translation may upset the orientation, each observation must be paired with a pointing to the collimator mounted in a fixed position, with its line of sight approximately parallel to the direction of movement of the slide.

The instrument described above is loosely referred to as a goniometer. The following chapter describes how one was constructed in the Department.

<u>Reference.</u>

Thompson,E.H., 1957. The geometrical theory of the camera and its application in photogrammetry. Photogrammetric Record 2(10) : 241-263.

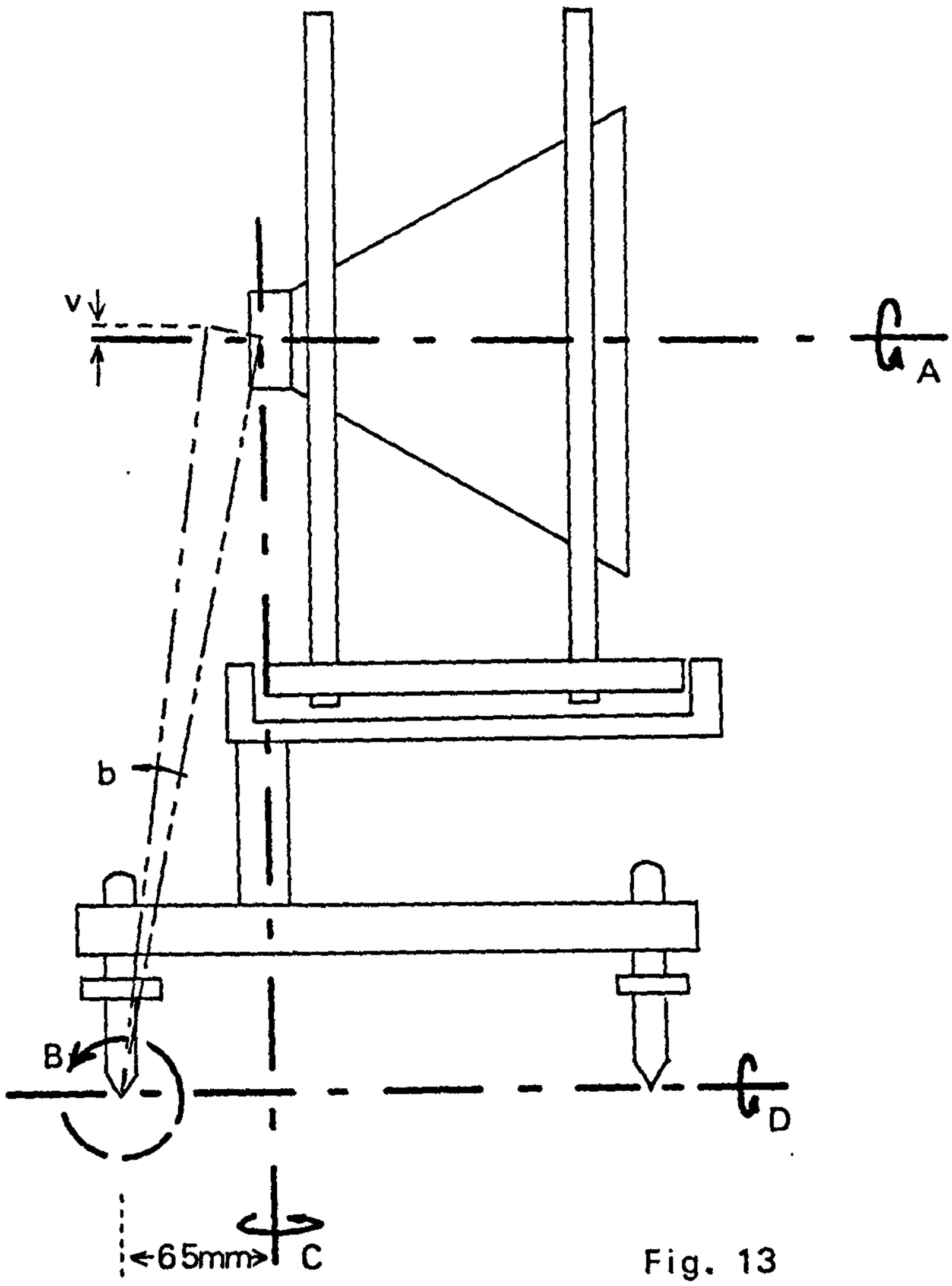


Fig. 13

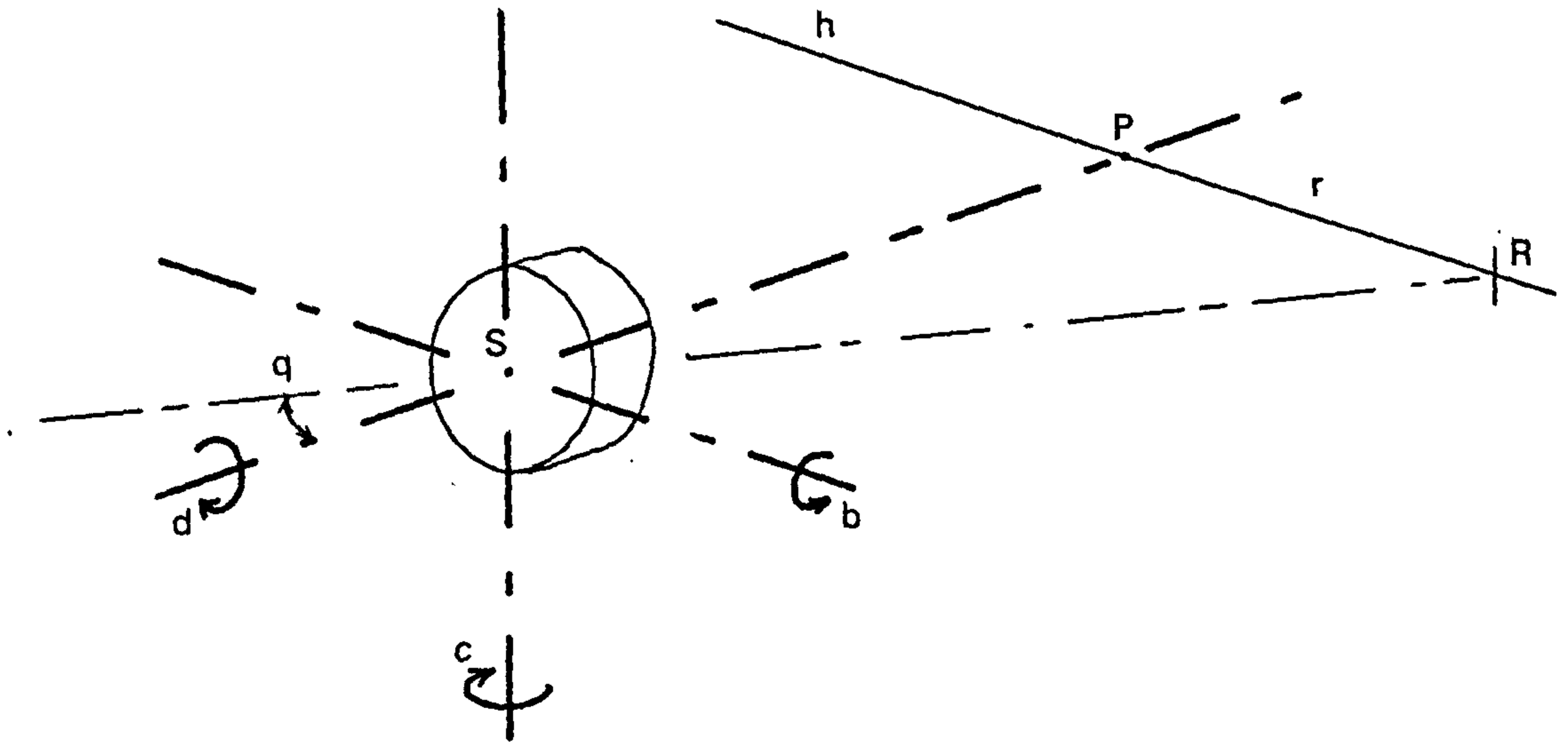


Fig. 14

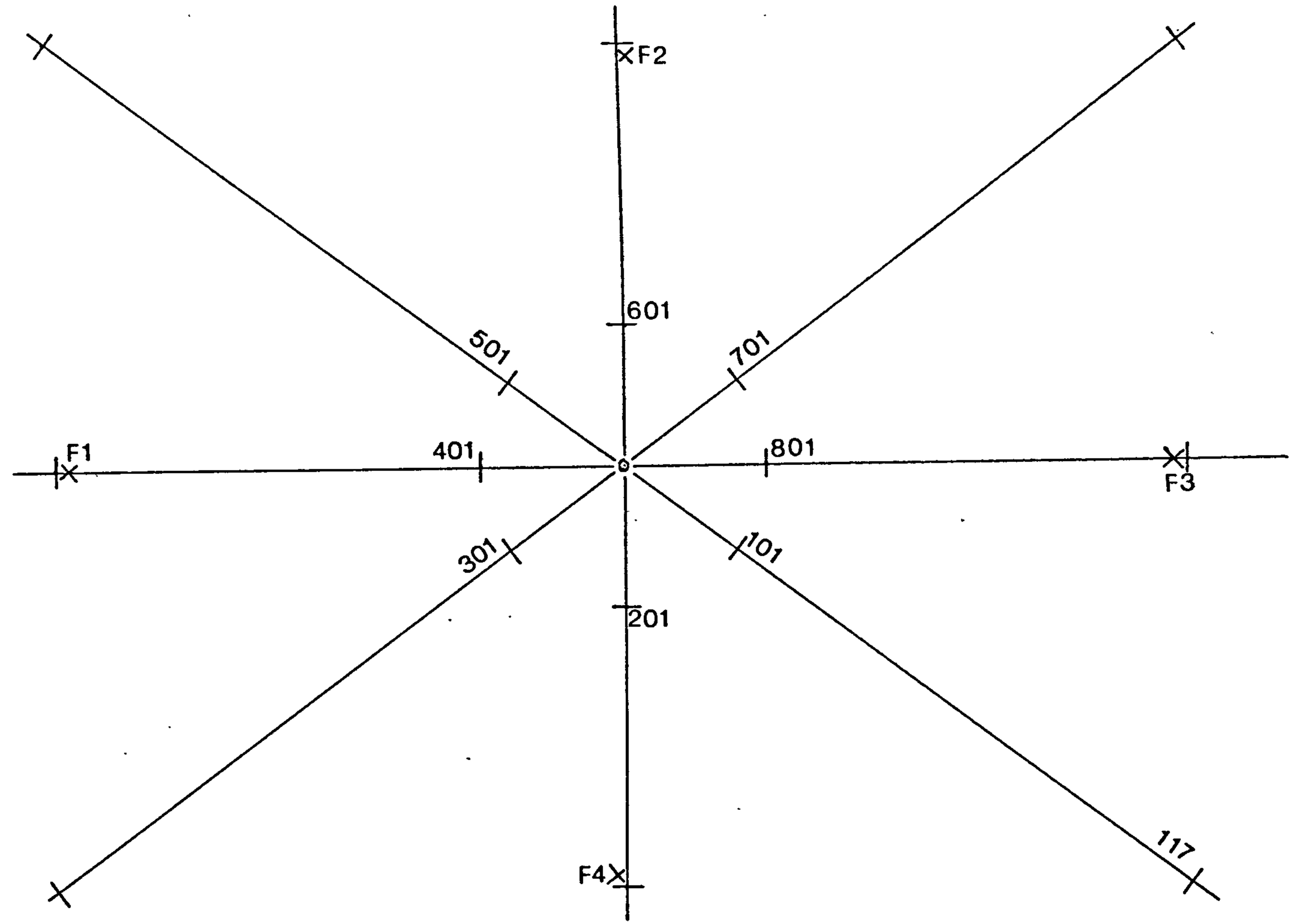


Fig. 15

# Chapter 3.

# The construction of the goniometer.

## Introduction.

The instrument constructed for this project uses existing material from previous experiments, and was very cheap to make. It was designed specifically for the Santoni camera, and a considerable amount of time, though little money, would have to be spent in adapting it for another camera.

For the purpose of the description the instrument can conveniently be subdivided into four components:

a. The horizontal slide and base,
b. The camera mount,
c. The collimators and measuring theodolite,
d. The graduated plate and holder.

## A. The horizontal slide and base.

A sturdy slide, supported on two parallel hard chrome 80mm diameter by 590mm cylinders was available from a previous project. It is shown in plate 5. The table is guided by a handwheel and 2,5mm pitch lead screw. It has two V blocks in contact with one cylinder, and a plane block in contact with the other. The two cylinders are mounted on a 0,86m long channel iron section.

The stability of the slide was tested by mounting a theodolite on the slide table, levelling it, and pointing it at a fixed collimator aligned approximately parallel to the direction of travel of the slide. When the slide was translated from end to end, the plate bubble varied by less than 60" in any direction. The line of sight varied by a maximum of 12" in a horizontal direction.

At one end of the base is a solid horizontal table. As explained below, a platform was added on top to support the reference collimator.

An aluminium frame was built out from the channel iron base to support the camera mount and rear collimator. The complete assembly is supported on the base frame of a dismantled stereoplotter, as shown in plates 5 and 6.

B. The camera mount.

A cylindrical cage, shown in plate 8, was built to hold the camera. The axes of the cylinder and the camera are coincident. The cage rests on a roller assembly which allows it to rotate through 360° about its own axis A, shown in figure 13. It can be clamped in any position. Using this rotation, the picture plane radial to be observed can be set approximately in the horizontal plane.

The roller assembly in turn is mounted on the base of a disused subtense bar. The base has three footscrews and a vertical axis with clamp and tangent screw. The vertical axis supplies one of the rotations necessary to align the picture plane normal to the autocollimator. The entrance pupil of the camera lens is set directly over the vertical axis, and no translation of the lens thus results from the rotation.

Setting the lens over the vertical axis placed the centre of gravity of the unit very close to the rear footscrew. It has thus been extended beyond the picture plane, as can be seen in plate 8.

The second rotation required for alignment of the picture plane is effected by the rear footscrew, which rotates the camera about a horizontal axis B passing through the two front footscrews. These footscrews are 65mm in front of the vertical axis C and the rotation thus translates the lens as shown in figure 13. The horizontal component of the translation is unimportant as it simply alters the separation of camera and theodolite. The

vertical component will, however, move the camera's entrance pupil off the theodolite's line of sight by v = b.65mm where b is the amcunt of the rotation. b is never more than 1º from the zero position where C is vertical, and thus v is not more than 1,2mm. Since the entrance pupil of the theodolite is 40mm in diameter, the translation can be ignored.

The fine rotation to level the radial under observation is made using the two front footscrews. It thus takes place about an axis D through the rear footscrew. The translation produced at the camera lens by this rotation is obviously mainly horizontal, and can be counteracted by moving the theodolite slide until its line of sight once more enters the entrance pupil of the camera.

The tribrach stands on three blocks with radiating V grooves, as can be seen in plate 7. The blocks are attached to the aluminium frame built out from the side of the channel iron base.

C. The collimators and measuring theodolite.

1. The reference collimator is a Hilger and Watts 450mm focal length collimator. To bring it up to the collimating height of the measuring theodolite on the slide table, a platform was built onto the existing fixed table at one end of the slide. Radiating grooves were cut in the platform to accommodate the footscrews. The collimator has its own lighting source. It is aligned sensibly parallel to the direction of the slide. It is seen in position in plates 6 and 7.

2. The rear collimator is a Wild T2 single second theodolite with an autocollimating eyepiece. A 4V transformer is used as the power supply. The theodolite is mounted on a platform built onto the aluminium frame mentioned earlier. Its height of collimation is the same as that of the measuring theodolite. The base of its

tribrach is plane, and no attempt is made to secure it to the platform, its weight creating enough friction to avoid movement. It is seen in plate 7.

3. The measuring theodolite is a standard Hilger and Watts single second microptic theodolite, used with artificial illumination of the circles. Its base is also plane and it stands on the sliding table unsecured. No relative movement between theodolite and table was ever detected during observations. It is seen on the slide in plates 6 and 7.

D. The graduated plate and holder.

To hold the graduated plate in the picture plane, a small frame was made of perspex to fit into the camera's photographic plate clamp. The frame has three adjusting screws with counteracting leaf springs. These are used for setting the vertical and horizontal lines of the graticule exactly over the fiducial marks.

The graticule must include the following:

1. Vertical and horizontal lines to fit over the fiducial marks. Their intersection is the defined principal point, C.
2. Diagonal lines with graduations whose distances from C are known.

It was decided to draw this grid onto draughting film at 6 times required scale and to reduce it photographically. This was necessary to achieve a line of less than 0,04mm thickness. To allow the graticule to be drawn directly in ink, the plotting pencil of the Thompson-Watts plotter's coordinatograph was modified to hold a draughting pen.

The vertical and horizontal lines were first drawn onto the film, using the x and y scan of the coordinatograph. They were not continued through the intersection point, but stopped 2mm away from it. The intersection was marked by a circular dot, a target which

remains symmetrical whichever radial is made horizontal. Each of the lines was graduated at 30mm intervals so that extra radials were available for observation if necessary.

The film was now rotated to bring one of the diagonals into the y direction of the coordinatograph. The centre mark was set onto the line of y scan and the diagonal was drawn. It was interrupted over the centre point as before. Both radials were graduated at 30mm intervals as the previous lines had been. The procedure was repeated for the second diagonal.

The completed graticule was photographically reduced to true scale on lith-film. The negative was commercially copied in hard chrome onto a 130 x 180mm piece of optically flat glass. A print from the negative can be seen in plate 8a.

Conclusion.

The instrument is shown in its final state in plates 6 and 7. Chapter 4 describes the observing procedure and presents calibration results for both cameras.

# Chapter 4.

## Calibration at infinity: observations and results.

### Introduction.

The general principles of observing and calculating a full calibration are outlined. The results of calibrations on both cameras are then presented, and a mathematical expression for variation of principal distance is developed from these results.

### Observations: the general principles.

An operator's manual for the goniometer has been written, and is therefore available in the Department. Since the method of operation is peculiar to the instrument, only the general principles are presented here.

1. Since the measuring theodolite measures angles in the horizontal plane, great care must be taken to set the autocollimator's line of sight horizontal, thus ensuring that the camera's axis is horizontal after autocollimation against the glass plate. For this reason, the vertical index error of the measuring theodolite is determined by observation to the reference collimator. The theodolite is then set truly horizontal and both collimators, in turn, are adjusted onto its cross hairs.

2. To prepare the camera for observation, it is placed in the cage and the plate is clamped in the picture plane. With the aid of a fiducial microscope, the graticule is fitted over the fiducial marks. This procedure is discussed later in the chapter.

3. The direction to the autocollimator is observed, and referred to the reference collimator. The cage is now placed on the rollers, and rotated to make one of the picture plane diagonals approximately horizontal. To

align the camera exactly before observing the diagonal now involves rotations about the three axes B, C and D described in Chapter 3. Since the camera is focussed for infinity, translations of the lens produced by these rotations can be ignored, and the three axes can be considered to pass through the front node of the camera lens, as shown in figure 14.

The plane in which observations are required is defined by the normal to the plate PS, and the diagonal under observation, h. Consider an emergent angle q as defined by the point of autocollimation P and a graduation R of radial distance r. Consider further the effect of rotational errors b, c and d about B, C and D respectively on the angle q.

3a. Any error b in rotation about B places the plane of observation outside the horizontal plane, which is the measuring theodolite's plane of reference. The same effect dq would be introduced into the measured angle if the theodolite were dislevelled by -b i.e.

$$dq = 0,25\ b^2 \sin 2(90 - q)$$
$$= 0,25\ b^2 \sin 2q$$

The rotation about B is defined by the levelling of the autocollimator's line of sight, and subsequently by the act of autocollimating this line against the glass. Since the autocollimator has been levelled against the measuring theodolite, it is reasonable to assume that the axis is within 10" of the horizontal plane i.e.

$$dq''max. = \frac{0,25 \times 10 \times 10 \times 1}{206265}$$

when $q = 45°$. This is clearly negligible.

3b. The rotation about D to make h horizontal is made while traversing the slide table from side to side

and observing differences in height between the ends of the diagonal. An error d in this rotation simply rotates h out of the horizontal plane by d, thus effectively altering a measured radial distance r to r.cos d, the projection of r into the horizontal plane, i.e.

$$r' = r.\cos d$$
$$= r(1 - d^2/2) \text{ when d is small.}$$

With the maximum value of r of 100mm, and a nominal required accuracy in r of ±0,002mm (to be commensurate with future analytical projects conducted with the camera)

$$r - r' = r.d^2/2$$
$$\text{i.e } 0,002 = 50 \times d^2$$
$$\text{or } d = 0,006 = 20' \text{ of arc}$$

This is clearly within the capability of the observer to detect, as it represents a difference in height of 1,2mm between the extremities of the diagonal. A difference of 0,1mm is clearly visible. The effect of any residual error d can therefore be ignored.

3c. The rotation about C is made to set the principal axis PS parallel to the direction of the autocollimator. The direction of PS cannot be measured directly as P is not physically defined by a mark on the plate. The direction of the autocollimator was observed by the measuring theodolite before the camera was placed on the rollers. Any error c in the rotation, while not changing the observed direction, changes all other directions SR by c, thus effectively creating an origin shift dr = f.c in P since all q are deduced from the direction Dt to SP as origin. For dr not to exceed 0,002mm, and f = 150mm

$$c = \frac{0,002}{150}$$

$$= 3''$$

This rotation must therefore be very accurate indeed, and is cbviously the one tc be made last of the three. When observinq the diaqonal, frequent checks are made on the autocollimation. Any shift necessitates complete re-observation of the diaqonal.

## The origin of the calibration

In theory, the calibration is referred to the point of autocollimation. Although the point is unique, it is itself referred during the calibration to the centre mark on the plate. Practically, it is very difficult to fit the qraticule lines over the fiducials exactly, since they cover the fiducials completely. The central mark therefore will not assume the same position when the plate is resited. In addition the fiducial axes in both cameras are not exactly orthoqonal. The vertical qraticule line must be evenly disposed cn either side of the fiducial axis as shown in fiqure 15. The qlass plate should thus be positioned once only for the calibration so that only one origin is used for all radial lines observed.

In between observinq diagonals the positioning of the plate is checked and, if a shift is found, the whole calibration must be started aqain. Some estimate of the accuracy with which the plate can be positioned was obtained by the followinq method:

1. The qlass plate was set over the fiducials as accurately as possible.

2. The point T, the projection of P onto the observed diaqonal, was located on horizontal and vertical lines. P was intersected by erecting perpendiculars to the lines at these points T.

3. The plate was then removed and the process repeated six times.

The results from camera 113s in Appendix A1 are shown as points P3 to P8. They indicate a spread of around

0,03mm in the determinations. The means of the intersected points P1 and P2 can also be included. They are the results obtained from the two full calibrations described below, where the point of autocollimation was determined from all four radial lines. P1 and P2 also indicate that the individual points T for a single setting of the plate are correct to within 0,005mm.

Calibrating the glass plate.

The glass plate was placed in the stereccomparator with the horizontal and vertical lines sensibly parallel to the x and y axes of the instrument. The extremities of these lines were coordinated, as well as the central mark. Joins between the extremities made it possible to intersect the true fiducial axis intersection which appeared to be about 0,009mm from the central mark. Eight observations were made to each of these five points.

All vertical line graduations were measured in the y direction only tc ascertain their radial distances from the central mark. The horizontal line was measured in the x direction only.

Each diagonal in turn was then set parallel to the x axis of the comparator and the graduations measured in the same way. Four observations were made to each graduation.

The lines are numbered sequentially starting with the smallest value of radial distance on the line, as shown in figure 15. The first line is numbered 101 to 117 and is referred to as the 100 line. A single diagonal is called the 100-500 diagonal or the 300-700 diagonal.

Results of calibrations of both cameras.

The complete set of observations consists of reading both diagonals, and the shorter horizontal and vertical lines. The method of calculation has been set out in Chapter 3. The results of both cameras are presented here, and they are then developed into a form which is

satisfactory for analytical calculations.

The calibrations of both cameras are presented in graphical form in Appendices A3 and A4. The location of the points T (figure 9) on each calibration are shown in Appendices A1 and A2. There is an extremely large variation in the principal distance in both cameras. Clearly it must be taken into account for all but the most imprecise work.

The asymmetry of the results makes the point of autocollimation useless as an origin. Most of the asymmetry of a curve such as the 300-700 diagonal in 113s (Appendix A3) can be removed by choosing a new origin a distance dr from the point T3 according to the following development:

$$f = r.\cot q$$

and from this $df = dr.\cot q - r.\mathrm{cosec}^2 q\ dq$

For small dq, $dq = dr/f$

By substitution for the trigonometrical functions,

$$df = \frac{dr\ f}{r} - \frac{r(r^2 + f^2)\ dr}{r^2\ f}$$

and after sme simplification,

$$df = \frac{-r\ dr}{f}$$

The required change in principal distance df can be scaled between the centre and either extremity of the curve, where r = 100mm. In the 300 line, as shown by the broken line, df = +0,113mm and thus

$$dr = \frac{-150 \times 0{,}113\text{mm}}{100}$$

$$= -0{,}170\text{mm}$$

This origin shift is shown as the distance T3-U3 in Appendix A1. It is now used to calculate df for all the values of f on the graph. The curve based on this origin

is shown in Appendix A5. Similarly a new origin U1 is chosen on the 100-500 diagonal. U1 and U3 uniquely define a new origin of symmetry V in the picture plane, at the intersection of the perpendiculars to the diagonals at U1 and U3. By dropping perpendiculars from V onto the horizontal and vertical lines at U2 and U4, the origin shift for these lines, T2-U2 and T4-U4, may be found. Appendix A6 shows the corresponding curve for 113d.

All curves now show a more symmetrical pattern. In these cameras, the distortion pattern appears to be parabolic. All the values of f based on the new origin can thus be used in a set of equations of the form

$$f = a.r^2 + b$$

and the parabola of best fit found by least squares. It is shown in Appendices A5 and A6.

Each camera was calibrated twice, with the glass plate beinq repositioned each time. The origins of the second calibrations are shown as the points V' in Appendices A1 and A2. Graphs of the second calibrations are not shown. The parameters a and b of the parabolas calculated in the four calibrations are as follows:

| camera | a x $10^4$ | b (mm) |
|---|---|---|
| 113s - 1 | -0,242 | 150,457 |
| 113s - 2 | -0,235 | 150,446 |
| Mean | -0,238 | 150,452 |
| | | |
| 113d - 1 | -0,251 | 150,302 |
| 113d - 2 | -0,260 | 150,324 |
| Mean | -0,255 | 150,313 |

Study of Appendix A6 will show that there is still some asymmetry remaining. Successive lines from 100 to 800 oscillate about the parabola. This is caused by the comparatively large range of f in the 100 line which has upset the choice of a point of symmetry. The 100-500

diagonal still shows very little symmetry. In a lens of such poor distortion characteristics, little advantage will be gained by attempting to find a more compatible origin.

Use of the parabola in analytical calculations.

A suitable value of f must be chosen from the parabola. In these calibrations, all observations were weighted by the tangent of the incident angle q and the mean values of f found to be h = 150,325mm and 150,185mm for 113s and 113d respectively.

Now the adjustment from curve to mean value is

$$Cf = h - a.r^2 - b$$

This is changed to the radial distance adjustment on the photograph by multiplying by r/f:

$$Cr = \frac{r.h}{f} - \frac{r^3.a}{f} - \frac{r.b}{f}$$

$$= \frac{r.(h - b)}{f} - \frac{r^3.a}{f}$$

Obviously, x and y coordinates measured on a comparator would have to be adjusted in the same ratio as the radial distance i.e:

$$\frac{Cx}{x} = \frac{Cy}{y} = \frac{Cr}{r}$$

and from this,

$$Cx = \frac{x.Cr}{r}$$

$$= \frac{x.(h - b - r^2.a)}{f}$$

and $$Cy = \frac{y.(h - b - r^2.a)}{f}$$

Writing $\frac{h - b}{f} = d$ and $\frac{-a}{f} = e$,

$$Cx = x.(d + e.r^2)$$

and $$Cy = y.(d + e.r^2)$$

The value h may be substituted for f in the calculation of d and e with no significant loss of accuracy. d and e are thus constants.

Calculation of the adjusted coordinates now involves the following steps:

1. Obtain the coordinates of the defined principal point from the fiducial mark coordinates.

2. Deduce from these the coordinates of the chosen origin of symmetry V by applying the shifts C-U2 and C-U4 in the direction of the fiducial axes shown in Appendices A1 and A2.

3. Reduce all observed coordinates to the new origin.

4. Calculate radial distances $r^2 = x^2 + y^2$.

5. Substitute in the above formulae for Cx and Cy.

6. Apply these corrections to the coordinates on the new origin.

The computer program written for this purpose requires the shifts C-U2 and C-U4, and the parameters d and e. It has been designed to accept an unlimited number of observations to all points, to mean them and then to reduce the means as in steps 1 - 6 above. It then prints the results and punches sets of cards for use in a single picture resection program described later, and the Department's existing relative orientation program if required. The parameters d and e, and the shifts from the defined principal point in the direction of fiducial marks F1 and F2 respectively are given below.

| Camera | d | e | C - F1 (mm) | C - F2 (mm) |
|---|---|---|---|---|
| 113s | $-0,844 \times 10^{-3}$ | $0,158 \times 10^{-6}$ | +0,130 | -0,223 |
| 113d | $-0,851 \times 10^{-3}$ | $0,170 \times 10^{-6}$ | -0,062 | +0,034 |

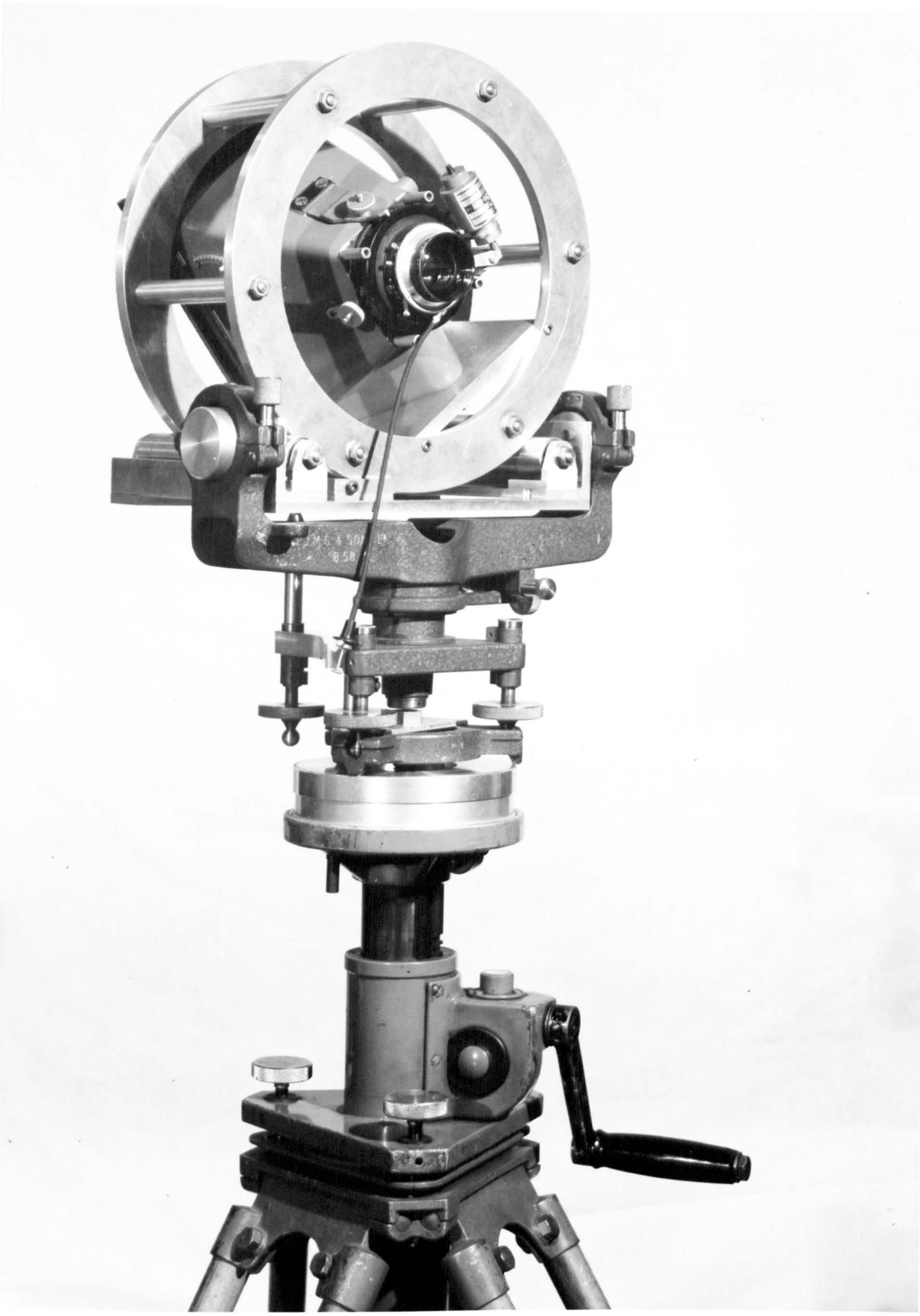

Plate 9. The camera on the roller assembly mounted on the racking tripod for the calibration.

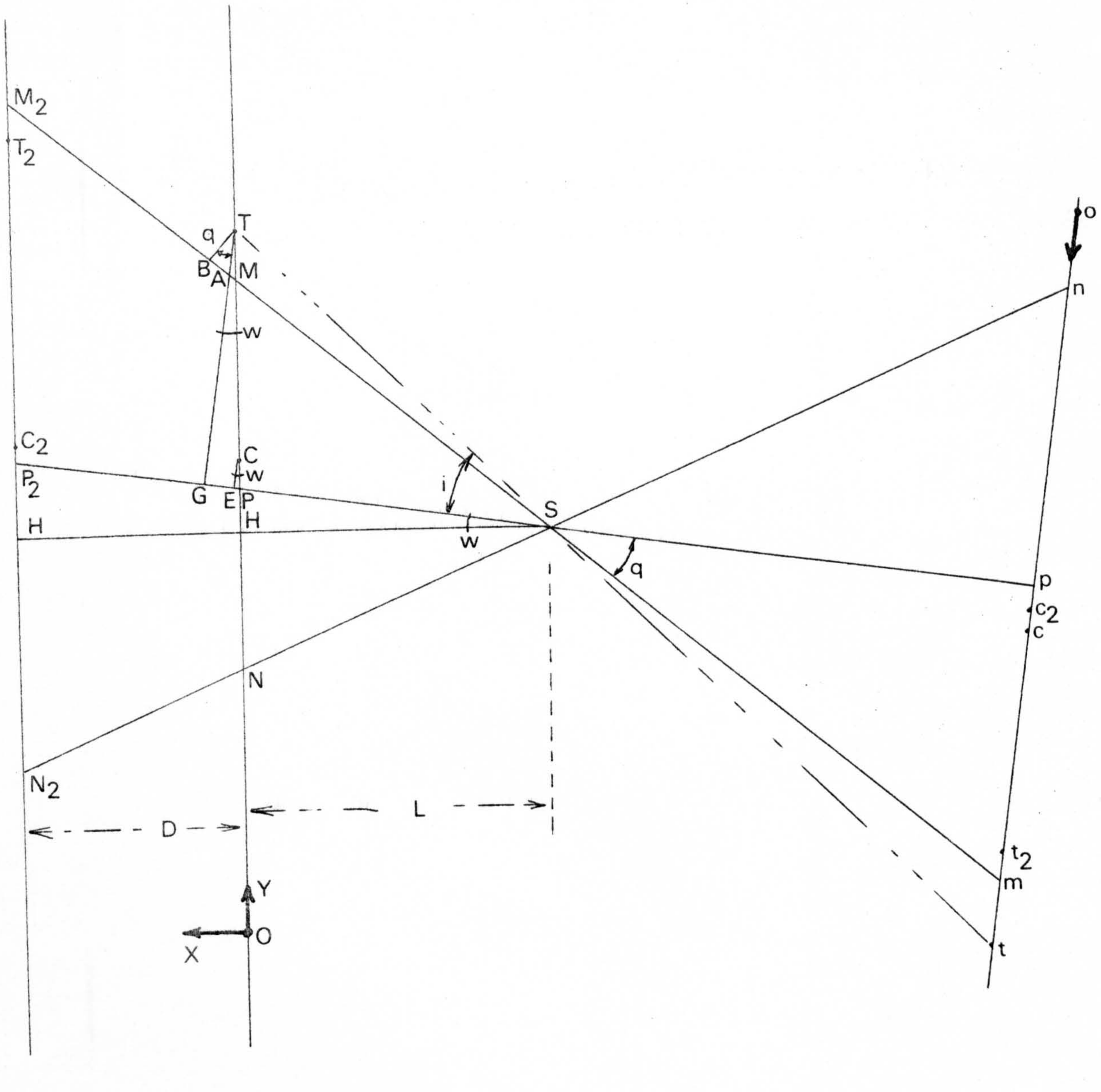


Fig. 16

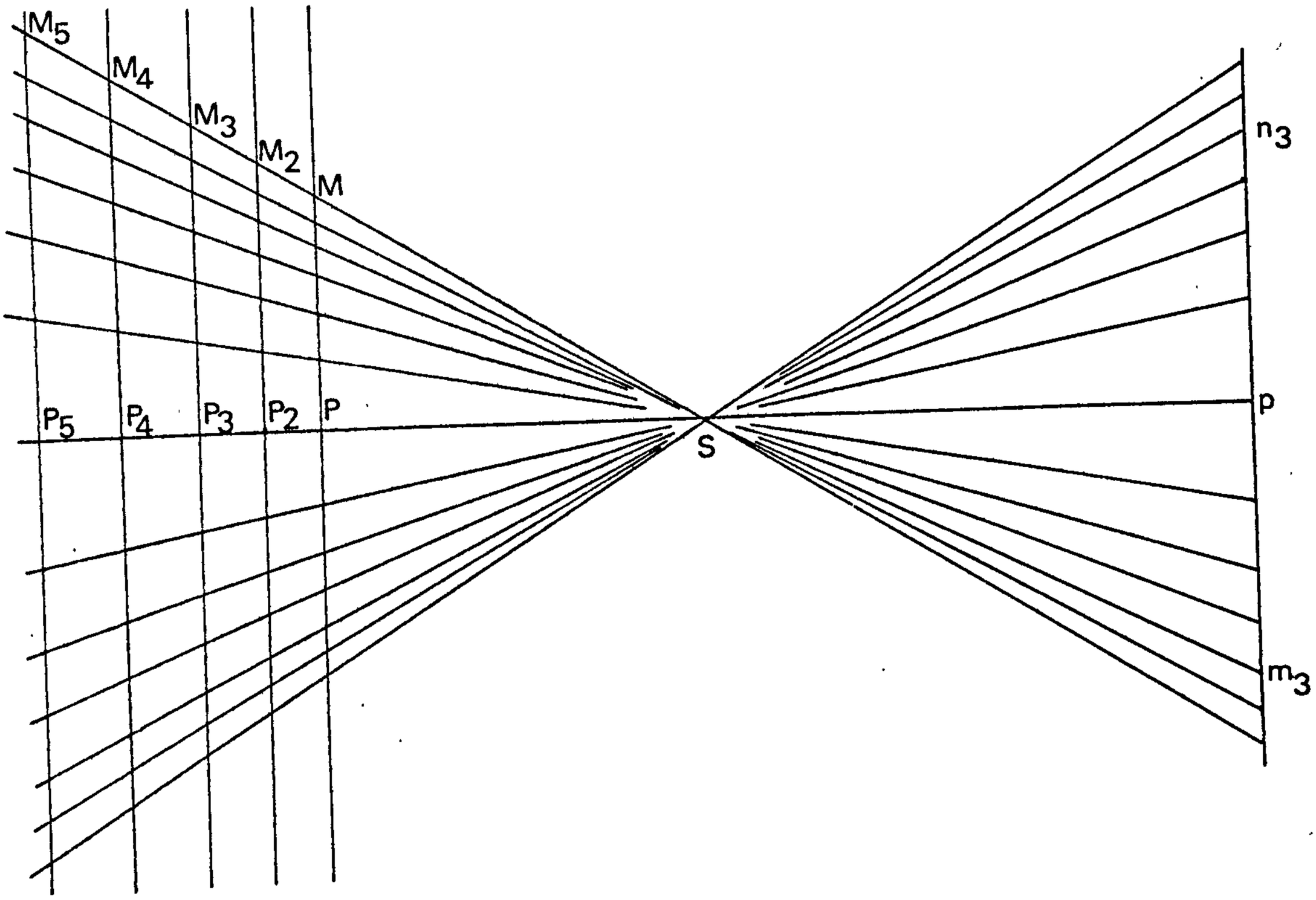


Fig. 17

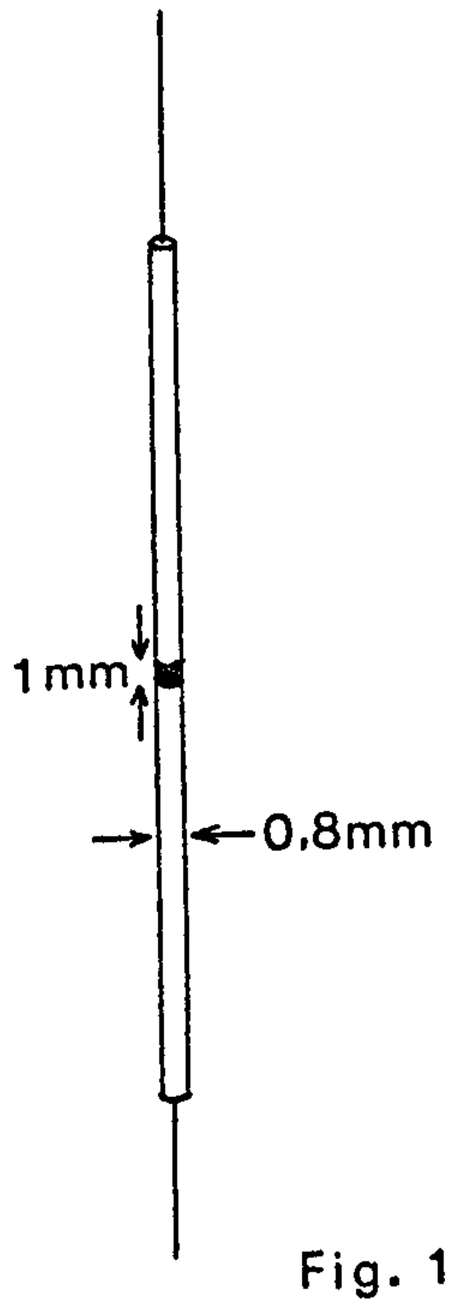


Fig. 18

# Chapter 5.
# Close ranqe camera calibration: a new method.

## Introduction.

A camera calibration method for object distances of 1 - 4m is described. It was developed to resemble the qoniometer method of calibration at infinite focus, and supplies a statement of variation in principal distance alonq a line radial from the principal point. Since it is obviously impossible to use the pcint of autocollimation as oriqin, the principal point defined by the fiducial marks is used as a preliminary oriqin. A new origin of symmetry is then selected from these observations as before.

## The theory of the calibration.

Consider a camera with its axis approximately horizontal. It is assumed for the moment that the principal distance f is free of distortion, and that the perspective centre S is thus a unique point. Let the axis be inclined at an angle w to the horizontal plane.

The perspective centre S and the principal point p define a vertical plane, shown in figure 16. Two plumbwires are hunq in this plane at the near and far limits of the camera's depth of field. A two dimensional coordinate system for targets on the wires is defined with its oriqin at O on the first wire. The X axis is horizontal, positive away from S, while the Y axis is vertical, positive upwards. X coordinates are thus zero for the first wire and D for the seccnd, where D is the horizontal separation of the wires.

Imaqine three lines in the plane, each passing througqh S, two from near the extremities of the picture plane, and the third coinciding with the camera's axis pS. Let six tarqets be positioned on the wires, approximately on the intersections of these three lines with the wires.

Four of the six targets are shown at heights (or Y values) T, T2, C and C2 in the figure.

The coordinates of S are (L,H) where |L| is the horizontal distance from S to the first wire. These coordinates must be found before f can be calculated. The method of finding them is to locate imaginary lines MM2 and NN2 from the targets near them, and to use the lines to intersect S. The formulae all use L,f and w which must therefore be known approximately. The solution is reiterated until their values converge.

Image distances p, c, c2, t2, t are measured along the image line from some arbitrary origin o. The distances are positive downward to agree with increasing Y values. The calculation is now conveniently divided into three parts:

1. P and P2, the projections of p onto the wires, are derived from the targets at C and C2. The tilt angle w is then calculated from P and P2.

2. Lines M2M and N2N, radial from S, are located from targets at T2, T and so on. S is then intersected from these lines.

3. f is evaluated for each of the outside targets at T, T2 and so on.

The steps are now explained in full.

1. Location of P, P2 and w.

Drop a perpendicular from C cnto pS produced as shown. In similar triangles SEC and Spc,

$$\frac{SE}{EC} = \frac{Sp}{c - p}$$

Thus with due regard for signs,

$$\frac{-L.\sec w + (C - P)\sin w}{(C - P)\cos w} = \frac{f}{c - p}$$

and from this,

$$P = C + \frac{(c - p)\, L.\sec^2 w}{f - (c - p)\tan w}$$

Having evaluated P and P2, it is clear that

$$\tan w = \frac{P2 - P}{D}$$

2. Location of M2M, N2N and S:

Consider only the line M2M:

Find the mean m of the image distances t and t2 as shown in figure 16. Let the incident angle of mS be q as shown.

Now calculate the height M cf the projection of m onto the first wire, as follows:

Drop perpendiculars TAG and TB onto pS and mS produced.

Now in triangles TBA and TBM

$$AT = BT.\sec q$$
$$= (T - M) \cos(q + w) \sec q$$
$$= (T - M) (\cos w - \tan q \sin w)$$

Thus in similar triangles TAS and tmS

$$\frac{AT}{SG} = \frac{t - m}{f}$$

or, by substitution

$$\frac{(T - M) (\cos w - \tan q \sin w)}{-L.\sec w + (T - P) \sin w} = \frac{t - m}{f}$$

Rearranging this, and substituting $\tan q = (m - p) / f$

$$M = T + \frac{(t - m) (L.\sec^2 w - (T - P) \tan w)}{f - (m - p) \tan w}$$

Using this form, M, M2, N and N2 are obtained. They may now be used to express line M2M in the form

$$Y = m'X + m''$$

where $m' = \frac{M2 - M}{D}$ and $m'' = M$

Similarly N2N is expressed in the form

$$Y = n'X + n''$$

Then S(L,H) is obtained from the intersection of these lines:

$$H = m'L + m'' = n'L + n''$$

from which $L = \frac{n'' - m''}{m' - n'}$

3. Calculation of f:

For a target at T, since w is known, the incident angle i can be deduced:

$$\tan(i + w) = \frac{T - H}{-L}$$

Then $f = (t - p) \cot i$

It will have been noticed that the line N2N is theoretically unnecessary, as the line P2P could have been used to intersect S. The former does, however, make the intersection angle at S more favourable.

The practical application.

As outlined above, the method is in a simple form. There are two major factors which complicate it in practice.

A. Errors in observations make it necessary to increase the number of targets used for locating the three lines. This will not only serve as a check on mistakes, but also improve the accuracy of the final result. For this purpose, extra wires are distributed through the depth of field between the wires at the limits as shown in figure 17. Instead of two target images t and t2, there are thus five images t, t2 . . t5 which yield a single mean m, and five heights M, M2 . . M5. These are not exactly in line as they are affected by errors in t, T and so on. They are used instead to determine the best fitting line through them, using the five observations of the form $m'X + m'' = Y$.

Since m' is the slope of the line, the five points P, P2 . . P5 may be used in a similar set of equations to determine w. Furthermore, if the value X = L is substituted in the expression for this line, a new value of H is obtained. Because of observational error it will

not be exactly the same as that obtained by the intersection described above. It is, however, in sympathy with the points P, P2 . . P5. The difference between the values is discussed in Chapter 6.

B. Since the calibration must determine variations in principal distance across the field of view, several extra groups of targets must be placed on other radial lines between mS and nS. These lines are paired at equal radial distances above and below the axis, as shown in figure 17. Each pair of lines (for example n3S and m3S) gives another determination of the coordinates of S. The individual results vary because of the variation in the entrance pupil, and also because of observaticnal error. The final coordinates may be selected by suitable weighting of the individual results.

Principal distance variation.

Once the final coordinates of S have been calculated, a principal distance is obtained for each target. There are thus five values grouped at each of the defined mean radial distances. A mathematical expression for f can be developed from the full set of values across the field of view.

Conclusion.

Chapter 6 describes the practical procedure of a full calibration and analyses the results obtained.

# Chapter 6.

## Close ranqe calibration: observations and results.

### Introduction.

Details of the practical method of observations are qiven, followed by the calibraticn results for both cameras at two object distances. These results are given in the same mathematical form as those of the infinite focus calibrations.

### The practical procedure.

1. Setting out the test field.

Thirteen targets were mcunted on a 4m length of 0,25mm diameter stainless steel wire. They were made from the plastic insulating sheath of electrical flex and were 0,8mm in diameter. Each target was a 1mm lenqth of black sheath between two 30-40mm sections of white sheath, as shown in fiqure 18. Five such wires were made, and a 2kq weight attached to each. When the wires were positioned, each weight was suspended in an oil bath.

A theodolite was set up at the camera station and used to aliqn the wires as closely as possible without obscuring the rear targets. The wires were spaced at object distances of 1,8m, 2,0m, 2,3m, 2,7m and 3,2m. For each chosen radial distance r of a qroup of target images, a vertical angle was set on the theodolite, and a target on each wire moved onto the line of sight.

2. Coordinating the targets.

Three well disposed theodolite stations were placed around the wires. Only one side of the triangle was measured. Two arcs of horizontal angles were measured at each station to the other stations and the wires. The stations were then coordinated and the wires intersected

from them. Error figures at the wires indicated that the derived distances from joins between the wires had a standard deviation of 0,07mm.

The heights of all 65 targets were now measured from two of the stations using vertical angles. This method ensured that any scale error in the single measured distance (and hence in the horizontal coordinates) was transferred into the vertical coordinate as well. Angles subtended at the perspective centre were consequently not distorted because of the scale factor. Comparison of the two height differences between successive pairs of targets indicated a standard deviation of 0,07mm. The coordinates used in all the calculations below were therefore rounded off to the nearest 0,1mm.

3. Photography.

Camera 113s was now focussed for 2,3m by inserting the 10,8mm spacer between the lens and the body. It was then mounted in the goniometer's camera mount assembly which was in turn attached to a racking tripod as shown in plate 9. A ground glass screen was set in the picture plane, and the camera adjusted on the footscrews, the tripod and the rollers until the images of the central targets (c, c2, . . c5 in chapter 5) were as close to the defined principal point as possible, and one of the picture plane diagonals was approximately vertical. A photograph was now taken.

The camera was rotated on the rollers to make the second diagonal vertical, and a second photograph taken. The procedure was then repeated for 113d.

Calibration at a smaller object distance.

The complete experiment was repeated with the cameras refocussed on 1,6m by advancing the lens a further 4,8mm on its thread. The wires were redistributed for this calibration at object distances of 1,2m, 1,4m, 1,6m, 1,8m

and 2,1m, and all the targets reset onto the required lines. They were then ccordinated as before.

Observations on the stereoccmparator.

Each plate in turn was placed on the comparator stage plate with the imaqe lines parallel to the x axis of the instrument. Fiducial marks were observed, and the x coordinate obtained for each target image. The set of observations was then repeated as a check. The plate was positioned so that the x coordinate increased with the height of the target, as required in Chapter 5.

Calculations and results.

The two sets of observations were meaned, and the defined principal point intersected from the fiducial images. A computer proqram was written which followed the calculation method set out in Chapter 5. Each plate was calculated using the defined principal point as origin and a curve fitted to the 60 values of f across the diagonal. These values appeared to lie on a parabola as before, and the curve used was of the form

$$f = ar^2 + qr + b$$

The r values are neqative for images above the principal point, and the term qr thus indicates any asymmetry in the curve. The parameter q is the slope of a line similar to the broken line joininq the curve extremities on the 300-700 diaqonal in Appendix A3. A new origin can be located from the term accordinq to the development on p.28:

$$dr = \frac{-f\ df}{r}$$

The required df at a radial distance r to make the curve symmetrical is (-qr) and thus

$$dr = \frac{f\ qr}{r}$$

$$= f.q$$

This is equivalent to changinq the x coordinate of the oriqin by (-f.q)

All the plates were now recomputed on their new origins. Only the results based on this origin are included in Appendix B. Some explanatory notes on the presentation of these will now be given. A summary of the most important results will follow, together with some discussion on the accuracy.

Explanation of the results.

The results in Appendix B are fairly well annotated, but some extra points are made here.

A. The x and y coordinates of the defined principal point are followed by the new origin's x value. The y coordinates of all five image lines are then given to ensure that the lines are as close to the principal point as possible.

B. Whenever a line is fitted through the five P or M points, residuals are quoted in millimetres between line heights at X = 0, X = D and so on, and the point heights themselves. The residuals are always clearly labelled together with the standard deviation of a single point height.

C. The parameters m', m", n' and n" of each pair of lines (MS and NS) are defined in turn, followed by the deduced coordinates L and H. The six individual results are weighted by the sum of the absolute slopes (|m'| + |n'|). The weighted mean appears below, with the slope w. The value X = L is then substituted in the equation of the fitted axis line P P1 . . P5 to obtain another value for H. It is this value which is used to calculate f for the targets. The reason is discussed in full later in the chapter.

D. Values of f are calculated for all 60 targets, and used to fit the curve described above. The parameters appear on the seccnd page of the results, followed by the required shift to the origin of symmetry. A table then gives the calculated value of f for each target, together

with its radial distance, the tangent of the incident angle and the height residual, which is a measure of the accuracy of the curve fit. It is calculated by the following method: residuals for each target in turn are taken out between the calculated f and the curve value at that radial distance. They are then multiplied by r/f to convert them to the equivalent radial distance residuals. These are multiplied by the factor (-L + X) / f to convert them from picture scale to the quoted height residuals at the scale of the wires. The 60 height residuals across the diagonal yield a standard deviation of the curve fit which is quoted directly below the table of calculated f values.

E. For plotting purposes there follows a table of curve values at the mean radial distance of each group. None of these curves has been plotted here. Details are also given in the same table of the M and T values of all targets.

F. Once origins of symmetry have been located, the identification number of the second plate in each pair is made negative. The program then fits a composite curve of the form

$$f = ar^2 + b$$

over all 120 values of the two diagonals. This is the form used in the infinite focus results. The parameters for the curve are given after the second plate, followed by curve values of f at set intervals for plotting. Finally a standard deviation of the 120 height residuals calculated from the composite curve is given.

Summary of the results.

The graphs in Appendix C1 - C4 show the observed principal distances from each pair of plates, together with the composite curve. The table below gives the curve parameters a and b for the four pairs of plates, along with the standard deviations from the composite curve. The weighted mean principal distance is also given as

before. The parameters are in the same form as those of the infinite focus results, but should not be compared directly, as a ray at a given incident angle will have different values of r at each principal distance. A direct comparison between the three calibrations will be made in the following chapter.

| Focus/Camera | | a x $10^4$ | b (mm) | Std.Deviation (mm) | Mean P.D (mm) |
|---|---|---|---|---|---|
| 2,3m | 113s | -0,269 | 161,452 | 0,10 | 161,315 |
| | 113d | -0,291 | 161,278 | 0,10 | 161,130 |
| 1,6m | 113s | -0,363 | 166,389 | 0,10 | 166,193 |
| | 113d | -0,358 | 166,187 | 0,11 | 165,993 |

The program described in Chapter 4 which removes radial distortion from coordinates observed on the comparator requires the two derived parameters d and e as well as the shifts from the defined principal point to the chosen origin. The shifts were obtained by plotting the difference between the x coordinates of the two origins and constructing normals to the diagonals as before. The four parameters are given below.

| Focus/Camera | | d | e | C - F1 (mm) | C - F2 (mm) |
|---|---|---|---|---|---|
| 2.3m | 113s | $-0.849 \times 10^{-3}$ | $0,167 \times 10^{-6}$ | 0,193 | -0,218 |
| | 113d | $-0,919 \times 10^{-3}$ | $0,181 \times 10^{-6}$ | -0,087 | 0,048 |
| 1,6m | 113s | $-0,1179 \times 10^{-2}$ | $0,218 \times 10^{-6}$ | 0,120 | -0,218 |
| | 113d | $-0,1169 \times 10^{-2}$ | $0,216 \times 10^{-6}$ | -0,138 | 0,072 |

Discussion on the accuracy.

A. It will be shown in Chapter 7 that the perspective centre in the object space can be expected to vary by 0,2mm across the field of view. The variations of about 2 mm in the 1,6m focus values of L are thus disturbing, particularly as they are consistent, and are not reflected in the 2,3m results. They suggest a residual scale change between horizontal and vertical coordinates on the wires, but the method of observing was designed specifically to avoid this. Since the purpose of the calibration was to improve the forthcoming box girder test results which would use the 2,3m setting, the large variations in the 1,6m results have been accepted, but it is admitted that they should be investigated further.

The six values of H vary in all cases over a range entirely commensurate with the standard deviations of the two intersecting lines.

B. Significantly the fitted intersecting lines and the composite curves at both object distances have much the same standard deviation. If the camera's limit had been reached, a drop in accuracy would be noticed at the larger object distance. It would seem therefore that the limit is established by the accuracy to which the targets have been coordinated.

C. Any residual error in H will have its maximum effect where T - H is smallest, and its effect is seen as an equal and opposite displacement of the graph of f on either side of the principal point as shown in several of the diagonals in Appendix C. Chapter 5 described two possible methods of calculating H. Now the two formulae for calculating f are

$$\tan(i + w) = \frac{T - H}{-L + X}$$

from which i is obtained, and

$$f = (t - p) \cot i$$

Since p defines the axis, and was used to calculate w, the

value of H calculated from substituting in the axis equation is more likely to be in sympathy with the formulae. To substantiate this, all the calibrations were first calculated using the intersected value of H. Several of the plates showed the discontinuity described above. The plate observaticns were then recalculated using the axis equation value of H. All origins of symmetry remained the same, as is expected considering the symmetrical nature of the discontinuity. The fitted composite curve parameters changed by an amount which altered the curve values of f by a maximum of 0,002mm anywhere on the curve. On the three plates where the discontinuity had been worst, however, the axis value of H reduced the effect significantly, and all three plates showed an improvement of 30% in the standard deviations of height residuals, which brought them into line with the other five plates. It is consequently this value which has been used in the results printed here.

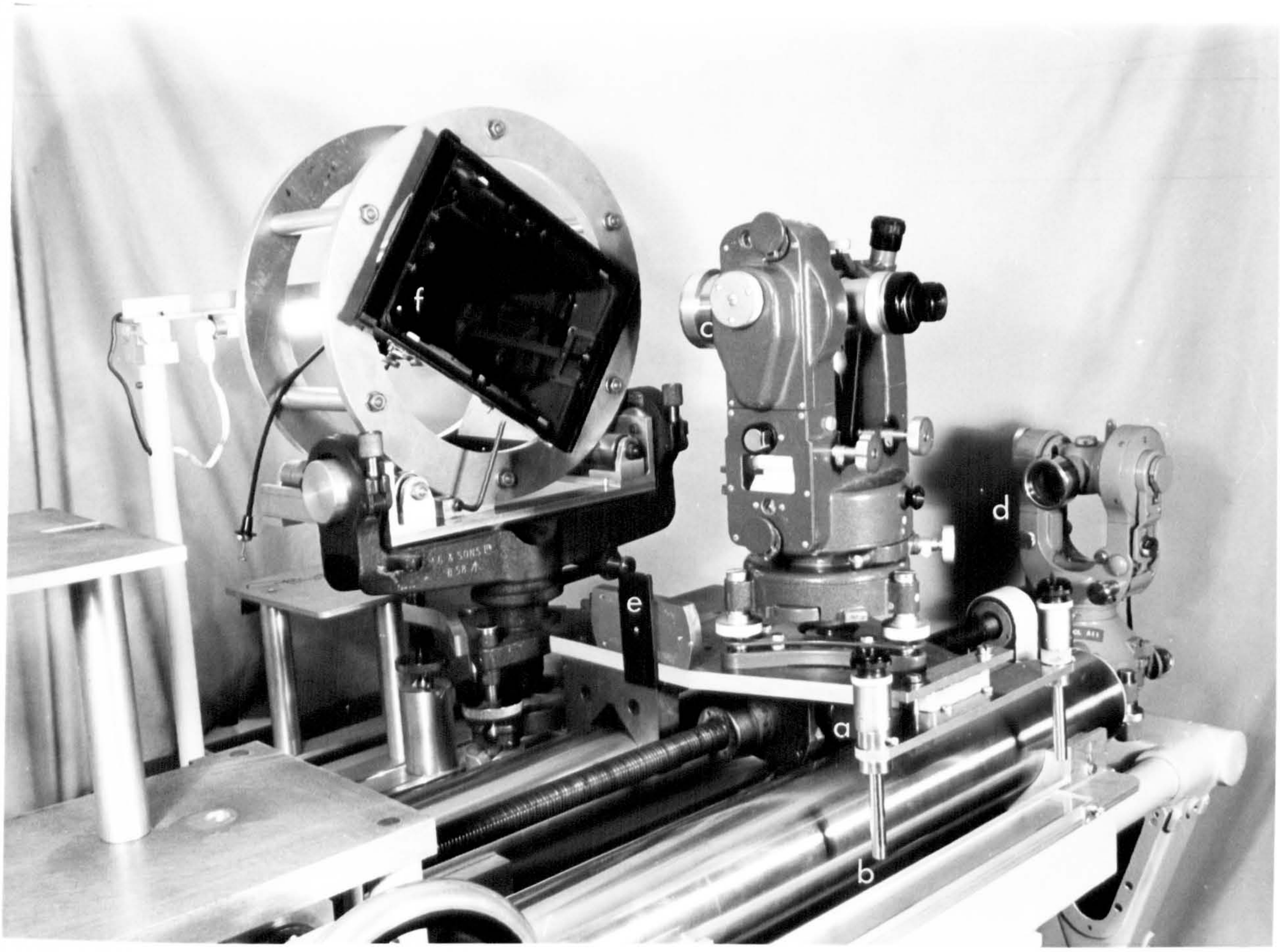


Plate 10. Location of the exit pupil.

a) Reading microscopes
b) Glass scale
c) Converging lens
d) Autocollimating theodolite
e) Mirror
f) Exit pupil

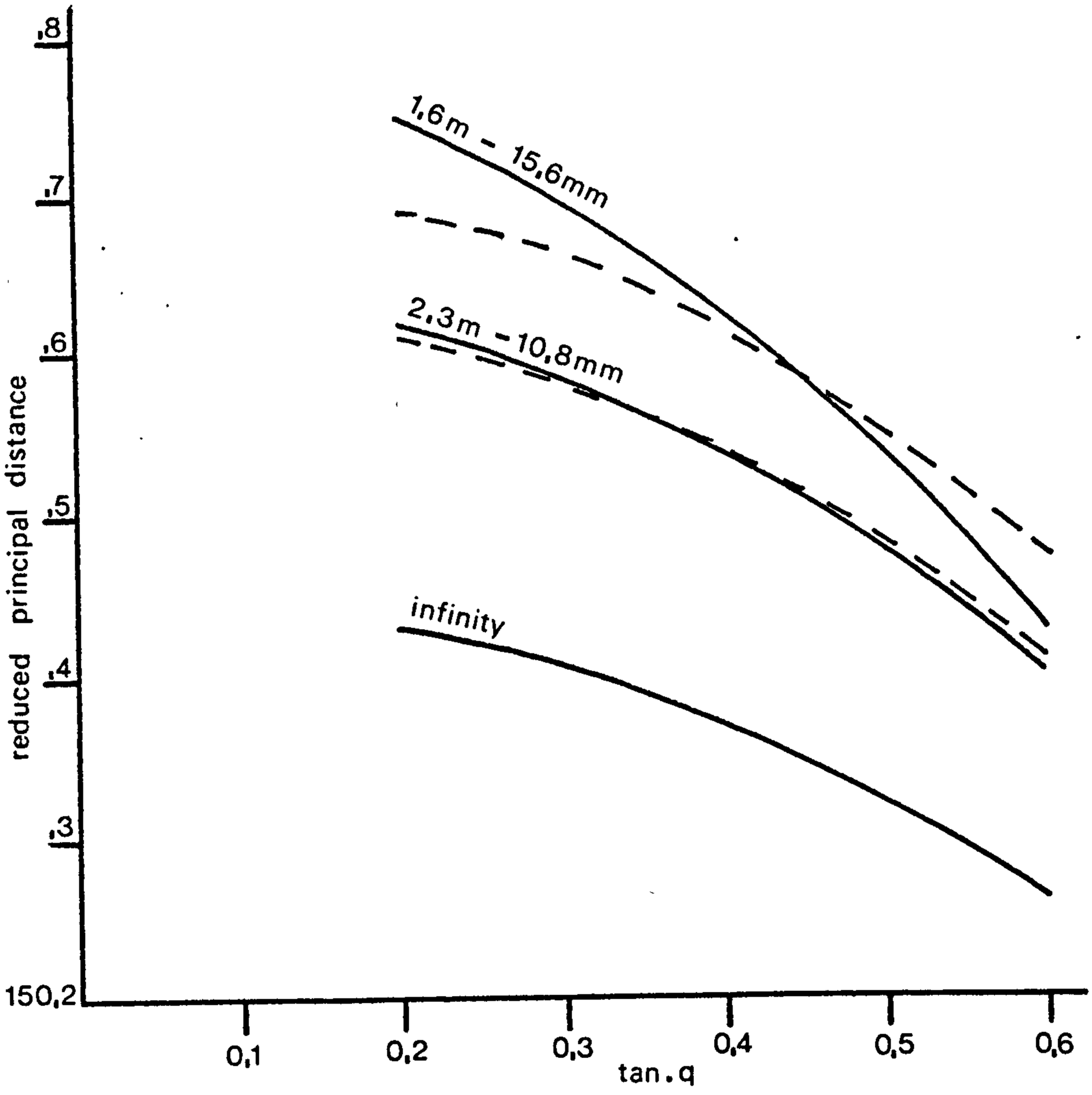
reduced principal distance
,8
,7
,6
5
4
3
150,2
1,6m - 15,6mm
2,3m - 10,8mm
infinity
0,1
0,2
0,3
0,4
0,5
0,6
tan.q

Fig. 19 113 s

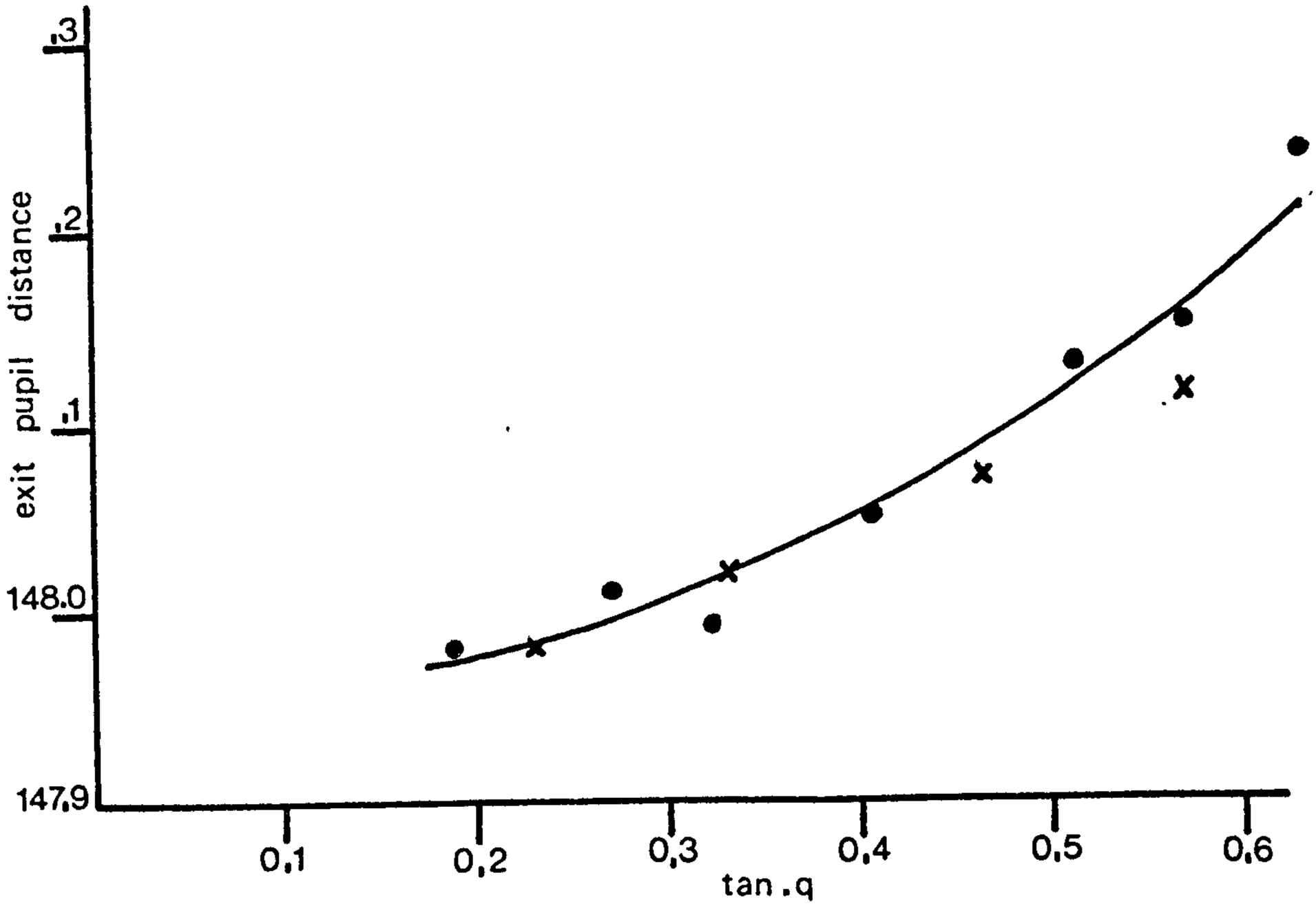
exit pupil distance
3
2
1
148.0
147,9
0,1
0,2
0,3
0,4
0,5
0,6
tan.q

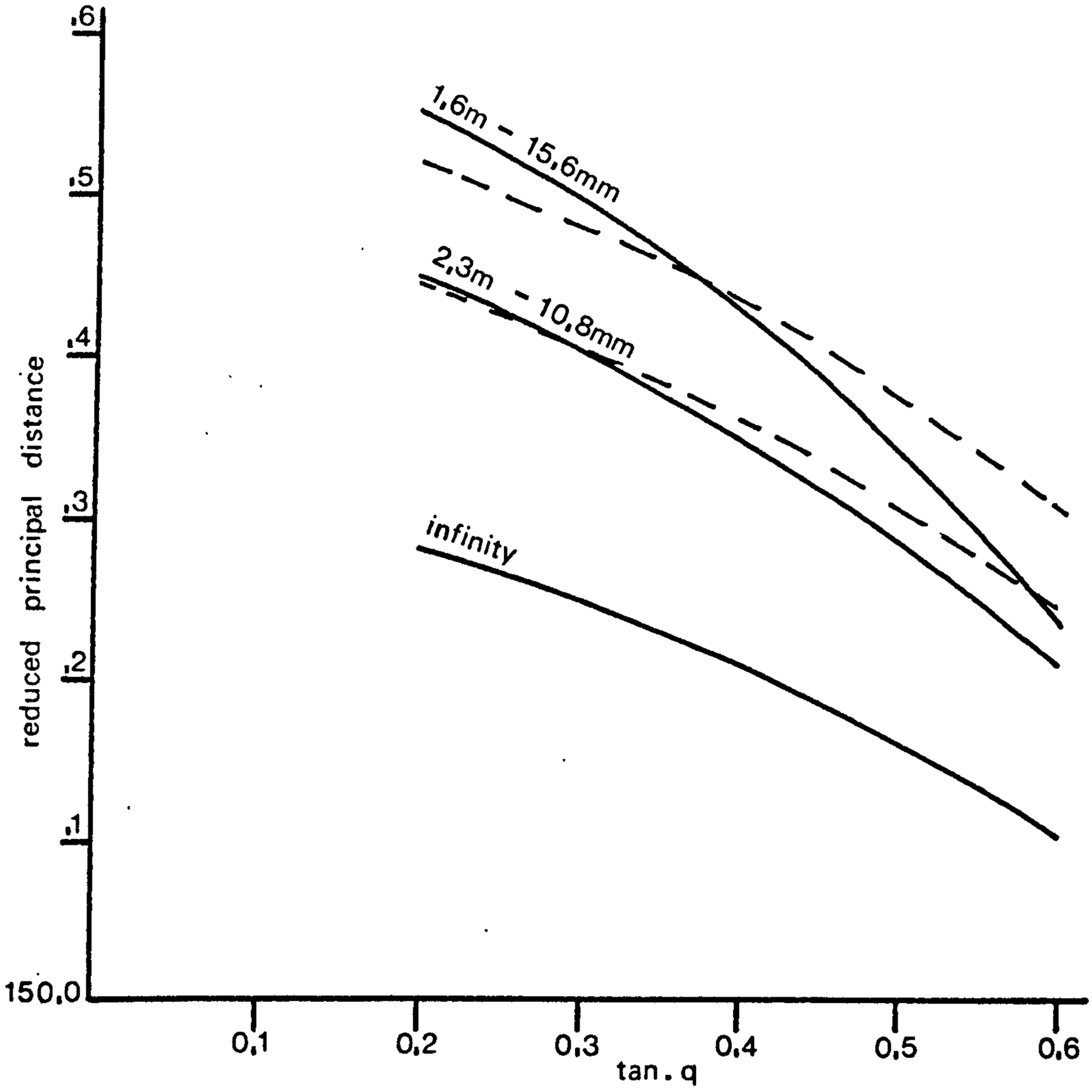
reduced principal distance
6
5
4
3
2
1
150,0
0,1
0,2
0,3
0,4
0,5
0,6
tan . q
1,6m - 15,6mm
2,3m - 10,8mm
infinity

Fig . 20 113 d

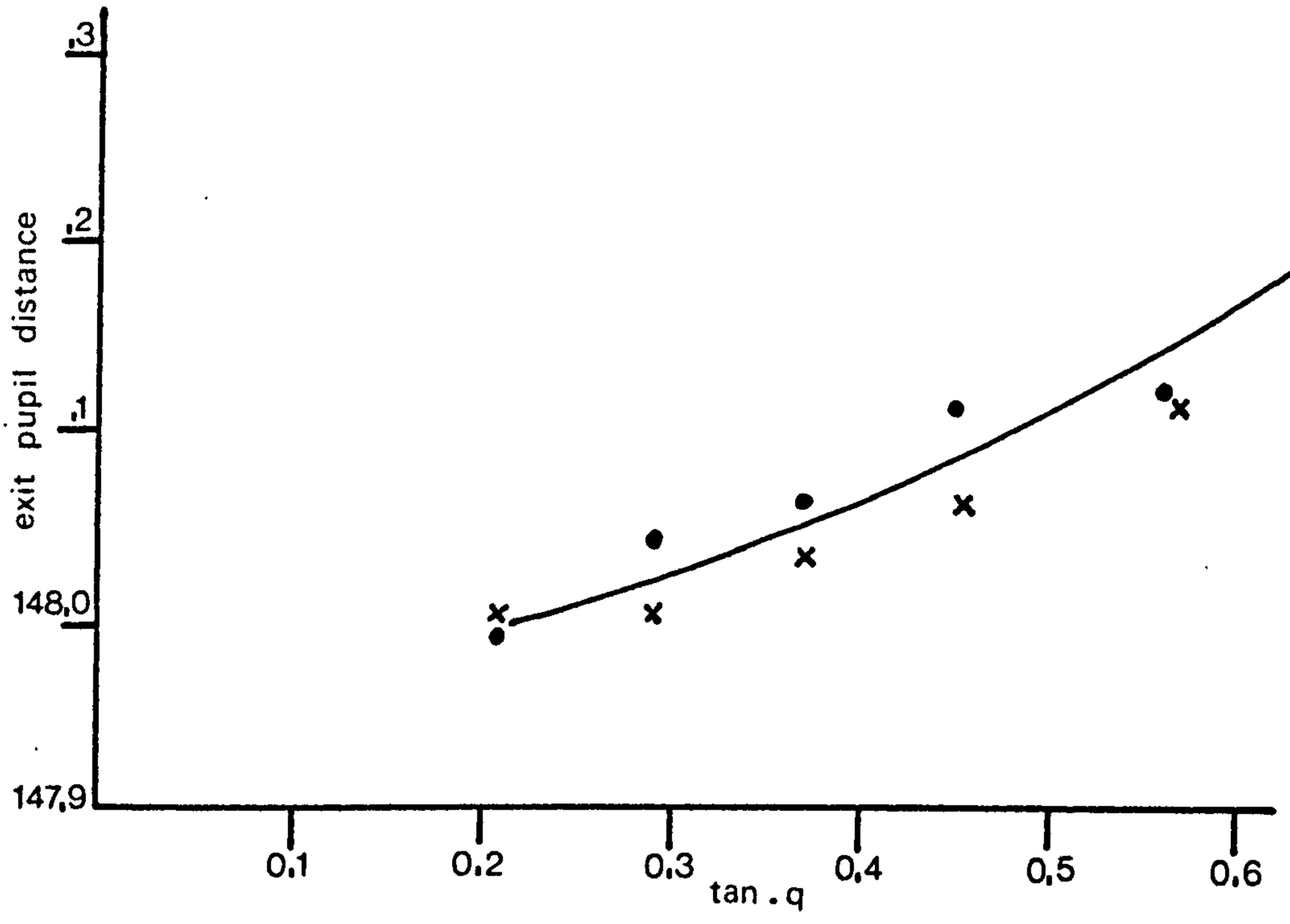
exit pupil distance
3
2
1
148,0
147,9
0,1
0,2
0,3
0,4
0,5
0,6
tan . q

Fig . 21

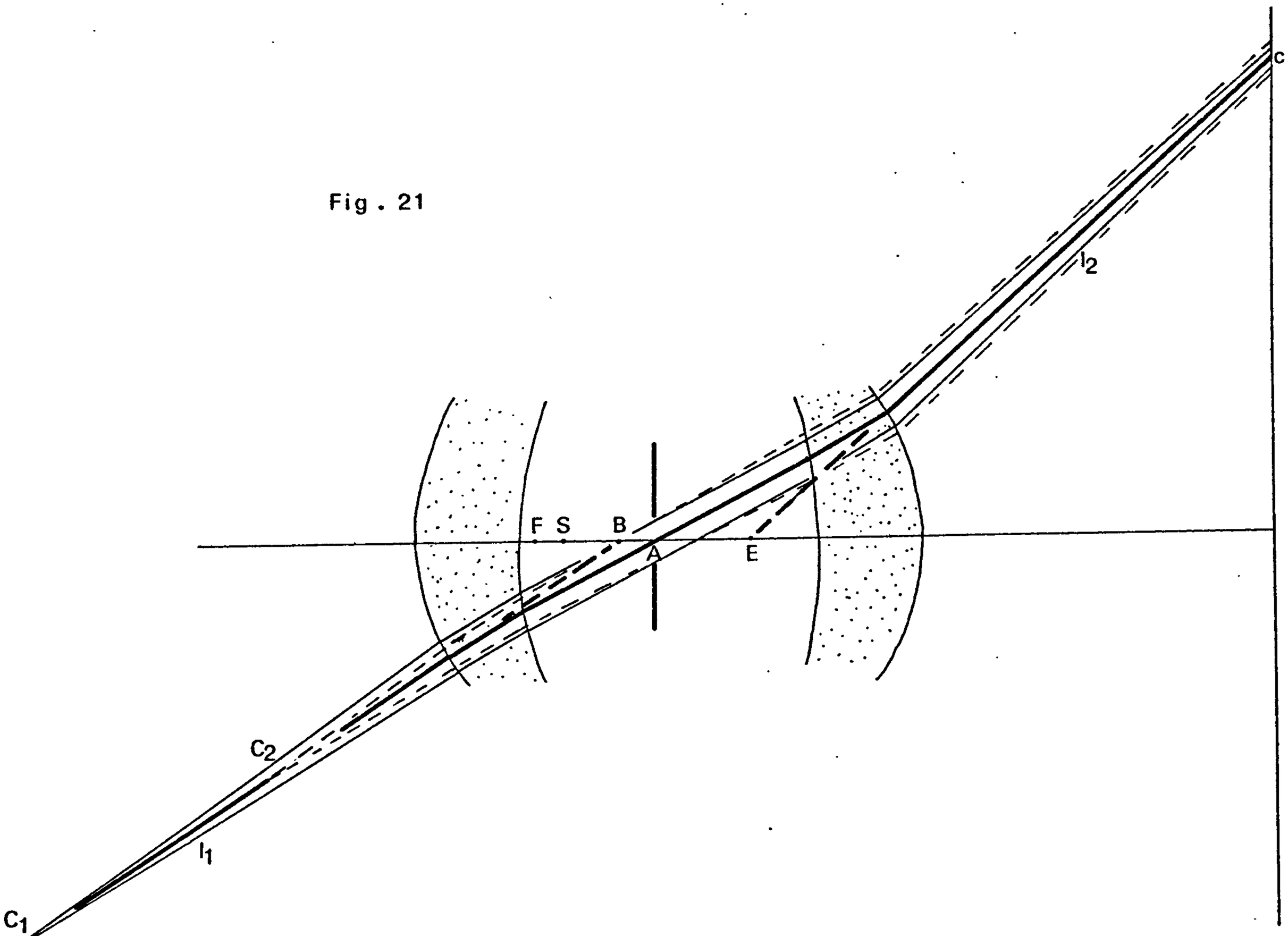

Fig. 22

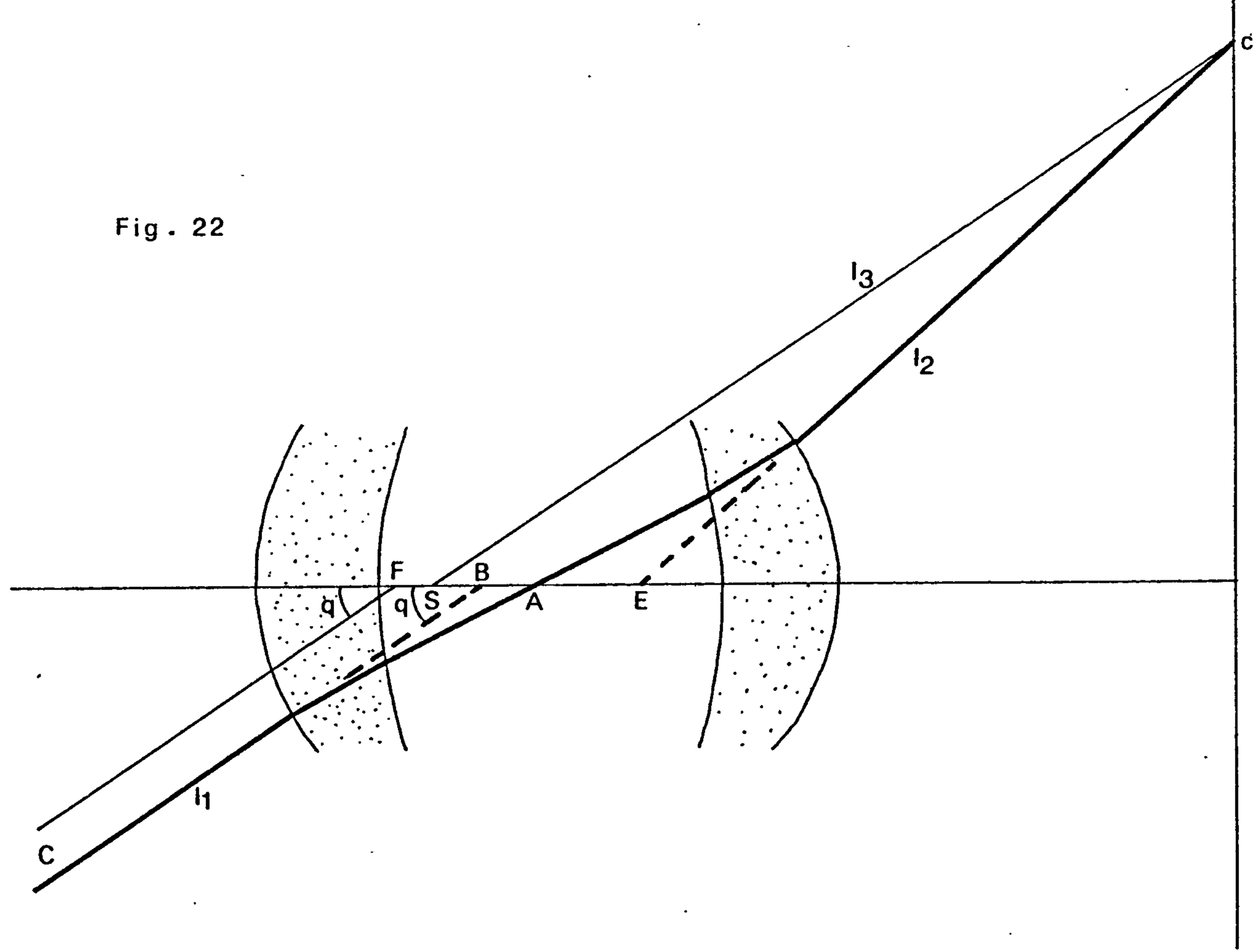

Fig. 23

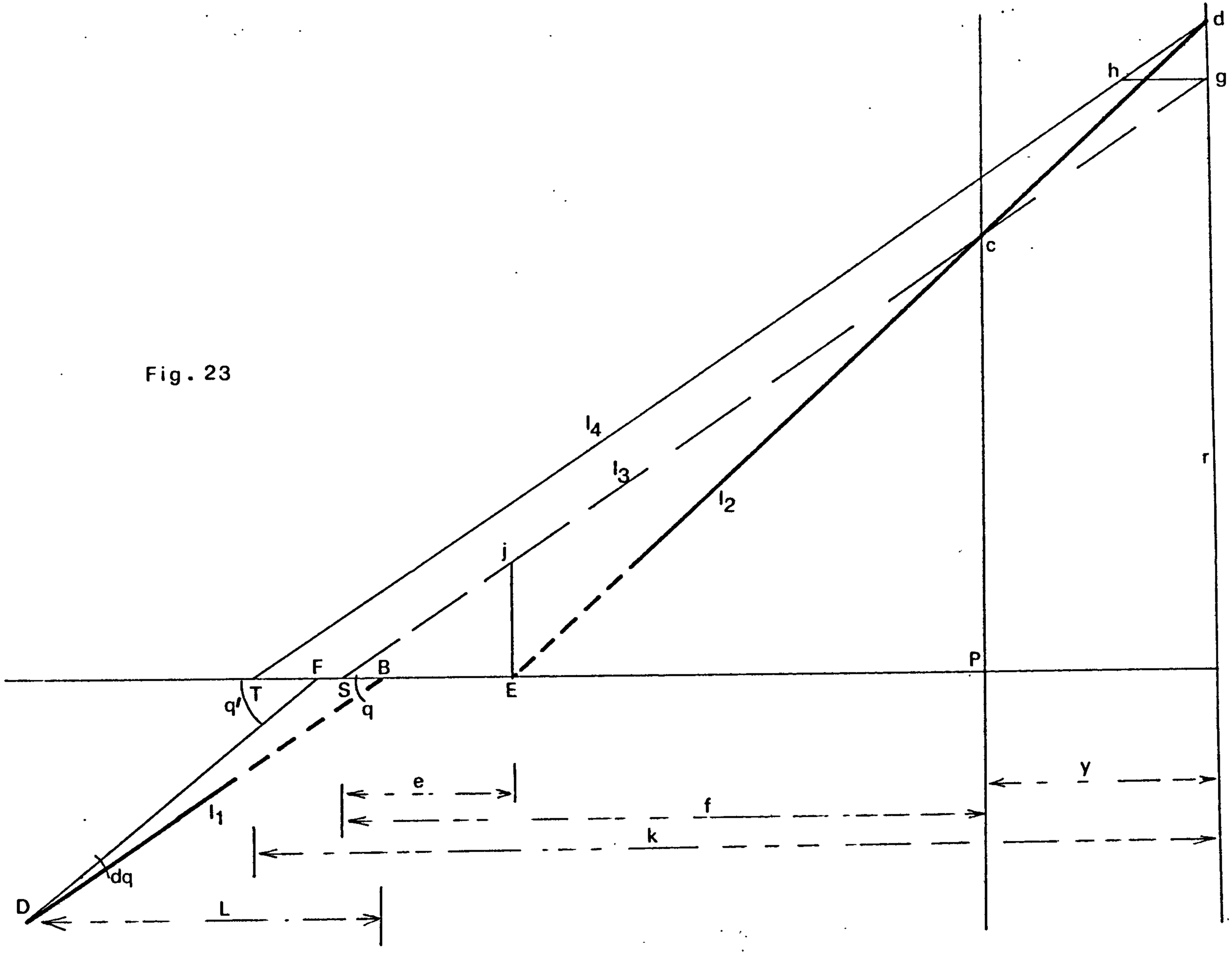

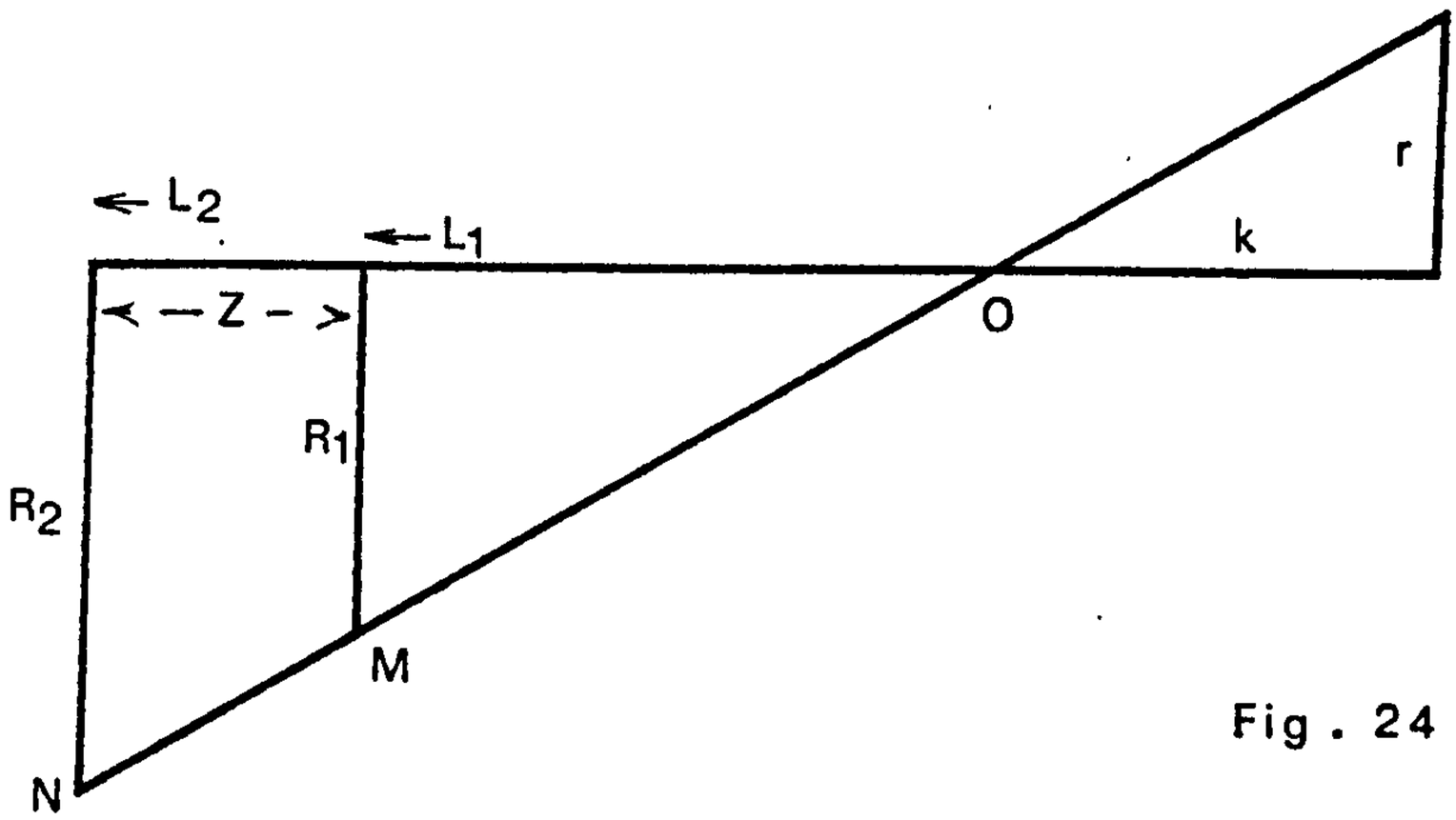


Fig . 24

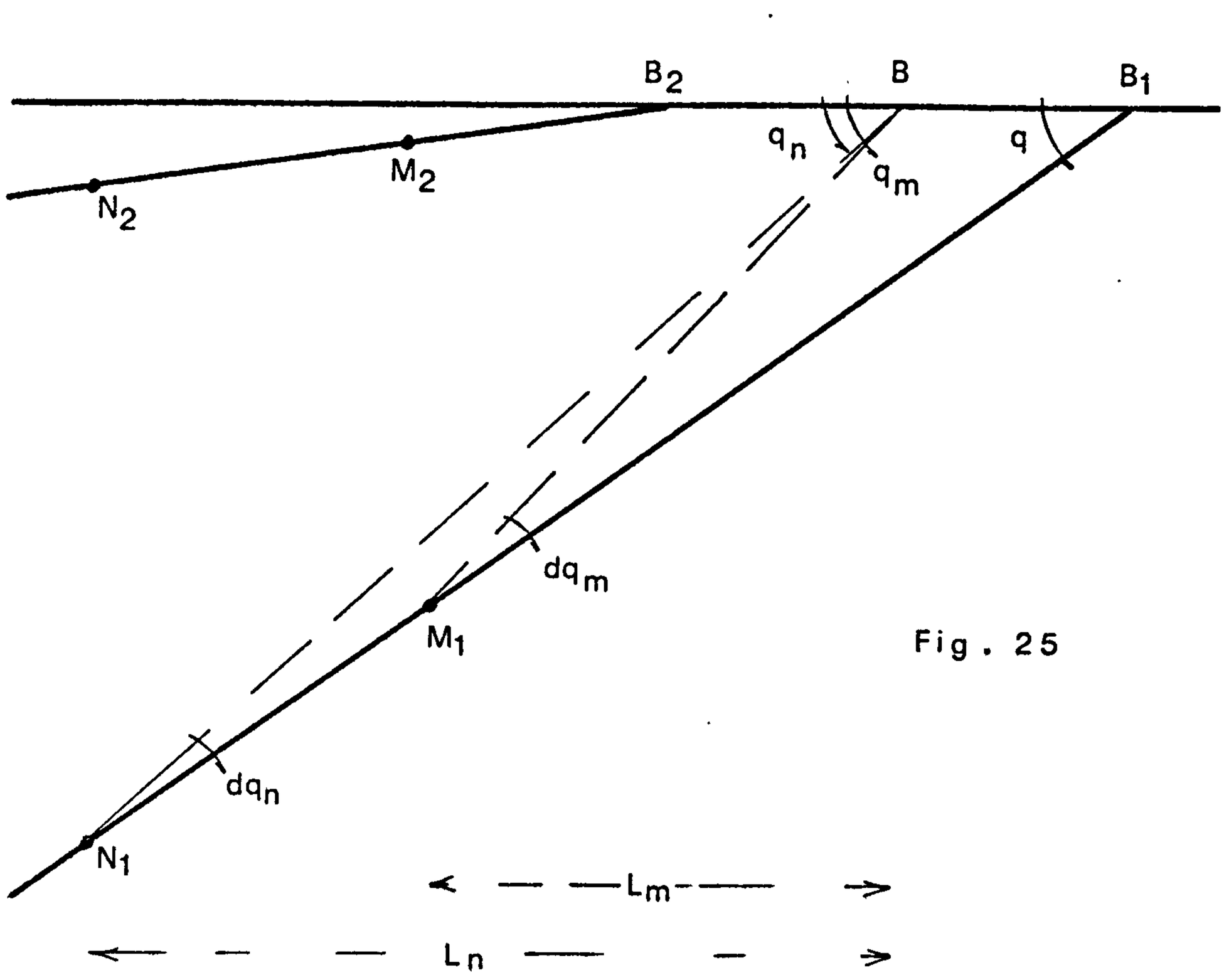


Fig . 25

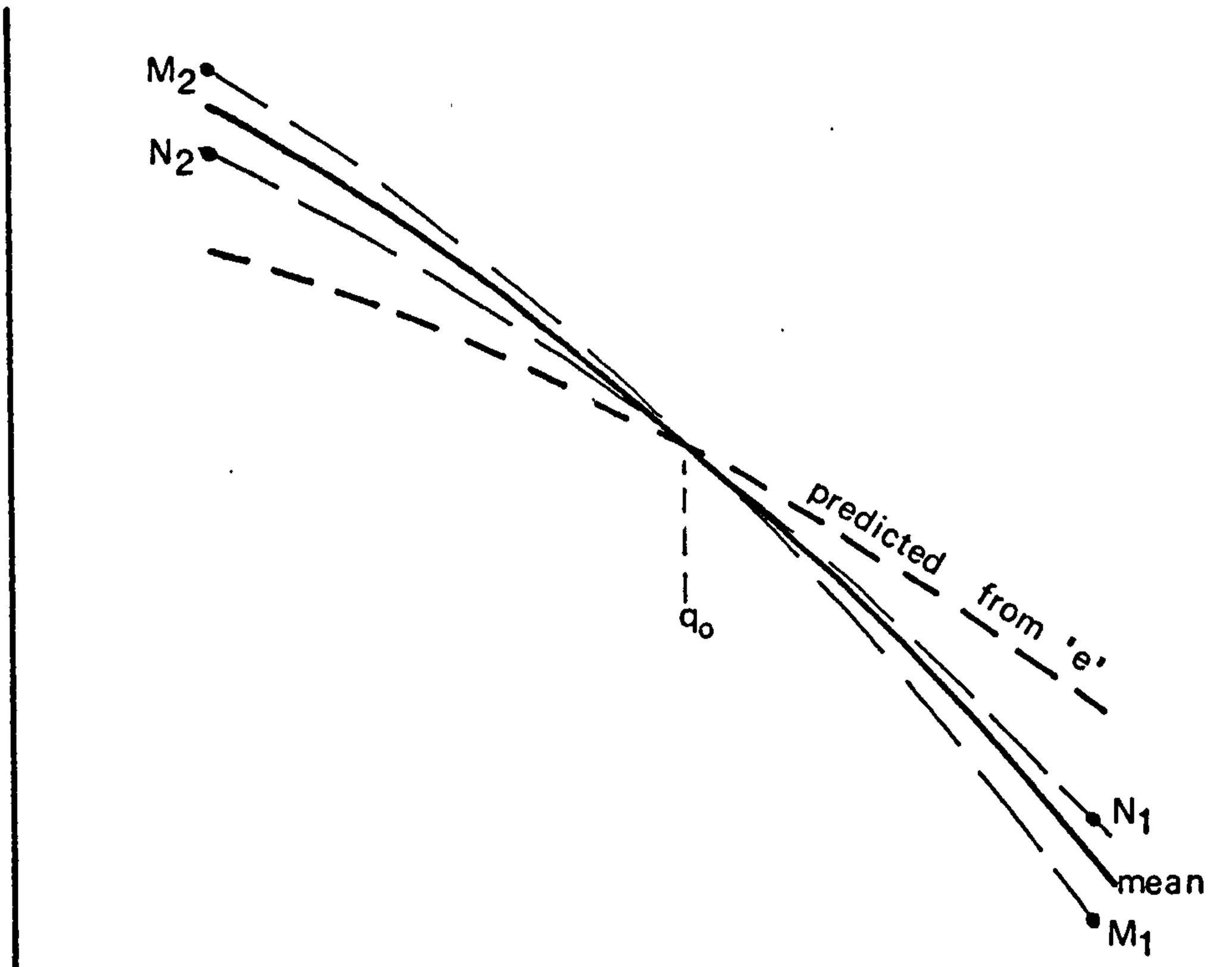


Fig . 26

# Chapter 7.

## The pupils in perspective.

### Introduction.

The three calibrations of each camera are compared. The difference in principal distance between the three is found to contain an increment which depends on the position of the exit pupil. The importance of the pupil in close range photogrammetry is examined, and an expression for the increment developed. Subsequently variation of entrance pupil position with incident angle is shown to produce a change in the infinite focus principal distance distortion pattern at close focus.

### Increase of principal distance at close focus.

It will be recalled that the distance from lens to picture plane at infinite focus was increased by inserting a 10,8mm spacer to achieve sharp focus at 2,3m object distance. If the principal distance distortion curve at this focal setting were reduced by 10,8mm, one might therefore expect that the curve would coincide with the infinite focus pattern. Figures 19 and 20 show these reduced curves for 113s and 113d respectively, as well as the 1,6m focus curves similarly reduced by 15,6mm. Obviously the lack of coincidence is too large to be ignored. It implies that the perspective centre assumes a different position within the lens for each new focal setting. The disparity can largely be attributed to the relative positions of exit pupil and rear node. The significance of this relationship is not widely understood, and is explained below.

It will also be noticed from the figures that the slope of the infinite focus curve has increased progressively for the close focus curves. This increase is shown to be a result of the variation in position of the entrance pupil.

Definition of terms.

The theoretical thin lens has a centre through which all rays pass without deviation. In practice this point must be divided into a front and a rear node. An incident ray which, when produced, meets the axis at the front node, emerges from the lens along a line from the rear node, parallel to its original direction. No other ray which enters the lens has this property. Now since we force the camera to obey the central projection model, two other points in the lens must be defined. The perspective centre of the central projection must be divided into an object space point and an image space point, which we shall call the outer and inner perspective centre respectively. These points do not necessarily coincide with the nodes and, to demonstrate this, we must introduce the pupils.

The camera lens generally consists of a front and a rear element, with an aperture stop between them. The stop is necessary for the obvious reasons of light control and maintenance of sharp focus within a required depth of field. It is positioned where it will produce the least vignetting effect on off-axis rays. Thus the images of the stop seen from the object space and image space, known as the entrance pupil and exit pupil respectively, do not necessarily coincide with the nodes.

The lens process.

We now concern ourselves with a camera lens in which the nodes and pupils are not coincident, as in figure 21. Thus the front and rear nodes F and S are separated from the centres of the entrance and exit pupils B and E.

A bundle of rays, emanating from a point object C1, traverses the lens, passing through the aperture stop, and emerging to form a photographic image in the picture plane. The principal ray I1 which by definition passes through the centre A of the stop, will emerge along I2.

We locate the centres of the entrance and exit pupils B and E by producing I1 and I2 to the axis.

The photographic image is not a point, but a finite spot generally in the shape of an ellipse. The ray I2 meets the picture plane at c, which is to all intents and purposes the centre of the image, and the point we wish to observe. Extending the same reasoning to a second object C2 which creates another elliptical image centred on c, it is clear that C2 must lie on the principal ray I1 from C1. The only way that the central projection model can be fitted is for the two objects, the image and the perspective centre to be collinear. We are thus led to the conclusion that the outer perspective centre is not at the front node, but at the centre of the entrance pupil B, where the line C1-C2 meets the axis.

Now the inner perspective centre is located by producing a ray back from c parallel to the incident ray. When the object is so far away that the incident beam is parallel, as in figure 22, then the incident angle q is the same at F and B and, purely by coincidence, the ray I1 from c to the inner perspective centre is parallel to the ray incident at the front node. Thus the inner perspective centre coincides with the rear node <u>at infinite focus.</u> It is easy to see how a fairly common misconception arises that the outer perspective centre coincides with the front node, and in fact the misconception does not affect us while the camera remains focussed at infinity.

<u>The effect of the exit pupil.</u>

If the camera is now focussed on a close object, the separation of lens and focal plane is increased by an amount y in figure 23. The object D subtending the same angle q as before at the outer perspective centre B will now form an image at d on I2 and not at g on I3 as might have been supposed by the central projection. Tracing a new ray I4 back from d parallel to I1 as before, the new

perspective centre T is fcund, and the principal distance has increased by (y + ST) and not y as might have been imaqined. The inner perspective centre has thus moved away from the rear node because the rear node did not coincide with the exit pupil, and thus I2 was not collinear with I3.

It is worth notinq that the finite object distance L creates a different anqle of incidence q' at the front node, and that I4 is thus not parallel to the ray incident at the front node when the camera is focussed at close ranqe. The incident ray with which the central projection is concerned is DB, since B is the outer perspective centre.

We may develop an expression for the increment ST from fiqure 23. Construct a perpendicular to the picture plane at g meetinq I4 at h, and another to the camera axis at E meetinq I3 at j.

$$\text{Now} \quad ST = gh$$

$$= gd \,.\, \cot q$$

and from similar trianqles Ecj and dcg

$$gd \,.\, \cot q = \frac{Ej \,.\, y \,.\, \cot q}{EP}$$

$$= \frac{e \,.\, y}{EP}$$

where e is the distance ES, positive away from P.

$$\text{or} \quad ST = \frac{e \,.\, y}{f - e} \qquad (1)$$

where f is the principal distance at infinite focus.

Neglecting the increment ST.

It may seem facile to consider the effect of ignoring ST. In many close ranqe cameras, however, focussinq is achieved by advancinq the lens throuqh precisely measured steps y, and the user may well be excused for assuming that the new principal distance is simply the infinite focus value f increased by y.

There is one interesting way of showing the result of this assumption which bears consideration, as it goes some way towards dispelling a myth which concerns the phenomenon of variation of principal distance with object distance. At least one author (Brown, 1971) has written of its existence. A camera is shown to have different radial distortion curves for each object distance at a given focal setting. The text implies, however, that the method of calibration used was to assume that the principal distance was just the infinite focus value increased by the lens movement, and this is no calibration at all. A calibration may not assume anything, but all three inner orientation parameters must be derived from it.

The simplified central projection in figure 24 shows two coordinated targets M and N which create the same image. O is the perspective centre, and k = f + y + ST is the true principal distance. Let the object distance be evaluated from point M, using the erroneous principal distance k - ST. Then, instead of L1, we obtain

$$L1' = \frac{R1}{r}(k - ST)$$

Now if the photograph is to be made to fit N as well, then

$$k2 = \frac{r}{R2}(L1' + Z)$$

where k2 is the principal distance necessary to keep L1' unchanged, and Z = (L2 - L1)

$$\text{Since } Z = (R2 - R1)\frac{k}{r}$$

by substitution we find that

$$k2 = k - \frac{R1}{R2} ST$$

$$\text{or} \quad k2 = k - \frac{L1}{L2} ST \qquad (2)$$

Clearly, k2 is greater than k - ST, the principal distance used for the L1 plane. The effect would thus be seen as a change of principal distance with the object

distance. We note that since we assumed the principal distance, we did not calibrate the camera. The assumed value was used to evaluate O, and we therefore obtained the wrong object distance L1'. The variation in principal distance expressed in (2) can thus be avoided by taking ST into account.

If we return to Brown (1971) , we may obtain some figures to demonstrate equation (2) . From the graph of radial distortion (p.863) we may scale the values at a radial distance of r = 70mm for dr(4,3) and dr(4,6) which are the distortions for the camera focussed on 4m, and objects at distances of 3m and 6m respectively. These can then be converted to principal distance distortions using the relationship dk = dr . k/r. k is quoted as c4 = 5,950 inches, or 151,13mm.

dr(4,3) = -0,235mm i.e. dk(4,3) = -0,507mm

dr(4,6) = -0,252mm i.e. dk(4,6) = -0,544mm

The values of k obtained for object distances of 3m and 6m respectively at r = 70mm can thus be deduced: k(3) = (151,13 - 0,507) = 150,623mm and similarly k(6) = 150,586mm. We now construct a hypothetical target field as in figure 24, to fit the values L1 = 3m, L2 = 6m, k - ST = 150,623mm, k2 = 150,586mm and r = 70mm.

Since R = L . r/k' where k' is the value of the principal distance for the particular value of L,

$$R1 = \frac{3 \cdot 70}{150,623} = 1,39421m$$

$$\text{and } R2 = \frac{6 \cdot 70}{150,586} = 2,78910m$$

If we substitute in our equation (2) above, using k = (150,623 + ST) we can calculate ST:

$$150,586 = (150,623 + ST) - \frac{3}{6} ST$$

from which ST = -0,074mm

k can now be deduced:

$$k = (k - ST) + ST$$
$$= 150,623 - 0,074$$
$$= 150,549mm$$

The claim in (2) is that the value k will fit both objects. We may test this by evaluating L1 and L2 in the hypothetical field calculated above, and deducing Z which should be 6 - 3 = 3m.

$$L1 = 1,39421 \cdot 150,549 = 2,99853$$
$$\text{and } L2 = 2,78910 \cdot 150,549 = 5,99853m$$
$$\text{from which } Z = 3,00000m$$

Thus it is possible to obtain a single value of k which will fit all the control points, and the use of a different value for the different object distances is unnecessary.

For the sake of completeness we may re-express equation (1) to calculate e:

$$e = \frac{f \cdot ST}{y + ST}$$

f is quoted as 5,300 inches or 134,62mm and y is thus 151,13 - 134,62 = 16,51mm. From the equation we thus have e = -0,6mm. It is an interesting thought that if the above process were used over the full range of r in the diagram from the article, we would obtain the values of k across the field and hence the distortion graph of the principal distance. This graph is not likely to agree exactly with one obtained from a calibration, and the deduced value of e will not be the same as that observed in the lens, as we are working from a mathematically produced graph. The accuracy of the restitution using the new value 150,549mm will, however, be equal to that using the old values varying between 150,623mm and 150,586mm and of course the restitution is very much simpler using the single value.

It is my personal opinion that the effect in (2) is the one which has drawn so much attention to the concept of variation in principal distance with object distance, and that the true effect which is the consequence of a variation in the position of the entrance pupil is too small to affect most projects. This effect is described later.

It was now decided to substantiate the theory expressed in (1) by locating the exit pupil and, by comparison with the infinite focus principal distance, evaluating e across the field. By substitution in (1) ST could be calculated, and principal distances for the y spacings of 10,8mm and 15,6mm could then be predicted from the form

$$k = f + y + ST$$

These could then be compared with the calibration curves.

Evaluation of the separation SE.

The exit pupil is not necessarily a fixed point, and it usually varies with the angle of incidence. Its position and variation were thus determined by intersection from a measured base on the focal plane side of the lens. The base subtended equal and opposite angles at E with the lens axis. The procedure was repeated over a range of angles covering the field of the lens across the diagonal of the picture plane. The second diagonal was also observed.

High accuracy was required in the measurement of the various bases. The measuring theodolite was thus mounted on the horizontal slide of the goniometer as shown in plate 11. Two reading microscopes 200mm apart were attached to the slide, passing over a finely divided 300mm glass scale. They allowed base distances of up to 420mm (the limit of travel of the slide) to be traversed with an uncertainty of about 0,01mm. A converging lens was attached to the theodolite telescope, allowing it to focus down to 350mm. Directional stability of the slide was

monitored from the autocollimating theodolite, mounted at the end of the slide's travel and observing onto a mirror attached to the slide.

The direction to E was obtained at each base station by observing to each side of the pupil and bisecting the angle. Similar pointings were made to a mark on the metal lens mount. The distance from this mark to the focal plane was later measured, and the distance of E from the focal plane could then be deduced. The graphs in figures 19 and 20 show the mean position of E obtained from the two picture plane diagonals of each camera. By comparison with the infinite focus graphs, we see that the distance e on 113s varies from 2,5mm to 2,0mm between the centre and the edge of the format, and from 2,3mm to 1,8mm on 113d.

Comparison of predicted and calibrated curves.

Predicted curves, shown as broken lines in figures 19 and 20, were obtained using the form k = f + y + ST as described above. They agree with the position of the calibrated curves to a high degree of accuracy, which proves the theory of the importance of the pupil. The predicted curves are, however, shallower in all cases than those obtained by calibration, particularly in the case of the 1,6m curves. This can be explained as follows.

It is reasonable to assume that the entrance pupil, or outer perspective centre, will vary approximately in the same pattern as the exit pupil. Thus in figure 25, the line between targets M1 and N1 which create a single image define a position B1 for the pupil, and M2 and N2 a position B2. The central projection requires a single position for the outer perspective centre. If B is chosen, the incident angles of M1 and N1 will be calculated as qm and qn respectively instead of q as shown. We may assess the effect of the change in incident angle on the resulting value of k by differentiating the fundamental expression:

$$k = r \cdot \cot q$$

$$\text{thus, } dk = -r \cdot \operatorname{cosec}^2 q \cdot dq$$

Now, for M1, from the figure,

$$dqm = \frac{BB1 \cdot \sin q}{Lm \cdot \sec q}$$

$$\text{Thus by substitution, } dkm = \frac{-k \cdot BB1}{Lm}$$

$$\text{and similarly for N1, } dkn = \frac{-k \cdot BB1}{Ln}$$

Obviously dk varies with the object distance L, but even more importantly the effect is cf the opposite sign for M2 and N2 because B2 is on the other side of B. An infinite focus distortion curve will thus change shape continously throughout the depth of field when the camera is focussed at close range. In particular, the disposition of points in the figure together with the infinite focus distortion curve for the Santoni camera gives rise to two new shapes as shown in figure 26. If B has been chosen sensibly, there will be at least one incident angle qo for which the defined front node agrees with B.

It must be pointed out as well that if the variation in B is not great the difference in dk between M and N will be difficult to detect. Thus for most reasonable metric cameras the change in principal distance with object distance will not be blatantly obvious in a calibration. A single curve fitted to all points would, however, show a definite change of slope from the infinite focus pattern, as shown by the broken line in figure 26.

No attempt has been made to measure the variation of the entrance pupil because the amount of work necessary to modify the goniometer was not justified by the expected gain. The point is made that the calibrated curve is obtained from a single chosen B and it therefore fits the central projection model better than the predicted curve does.

## Conclusion

The error made by assuming that ST does not exist is in this case totally unacceptable. Unless it can be shown that the rear node and exit pupil are nearly coincident in a metric camera, the principal distance may not be assumed to increase simply by the amount of the lens shift, and the camera must be recalibrated.

Location of E is difficult and requires special equipment. Prediction is therefore not suggested as a serious alternative to calibration. It has served here only to illustrate a theory.

## Reference.

Brown, D.C., 1971. Close-range camera calibration. Photogrammetric Engineering 37(8) : 855-866.

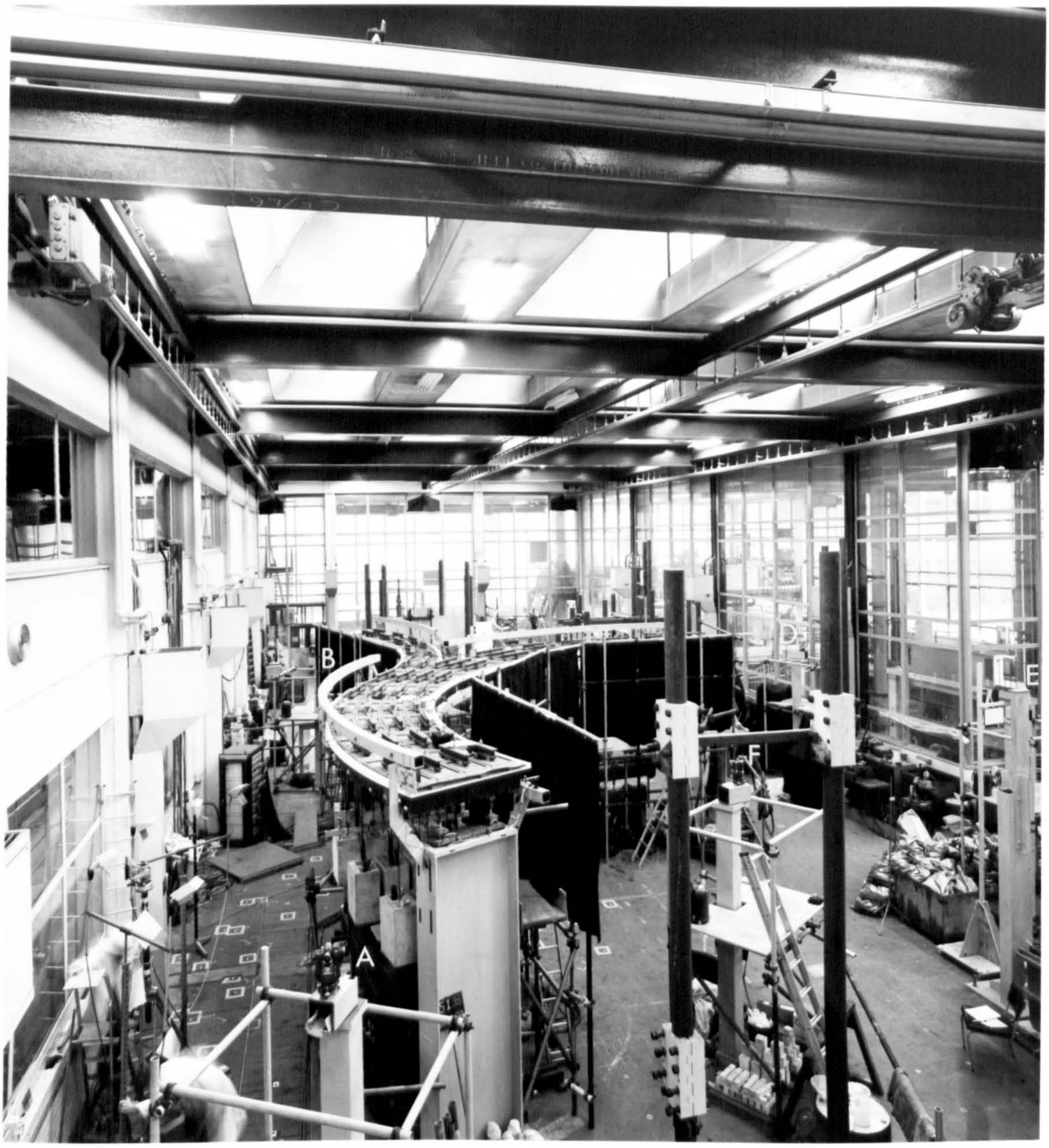


Plate 11. The bifurcated bridge, showing the disposition of the theodolite pillars. The two columns in the foreground support a beam from which the five calibration plumbwires were hung.

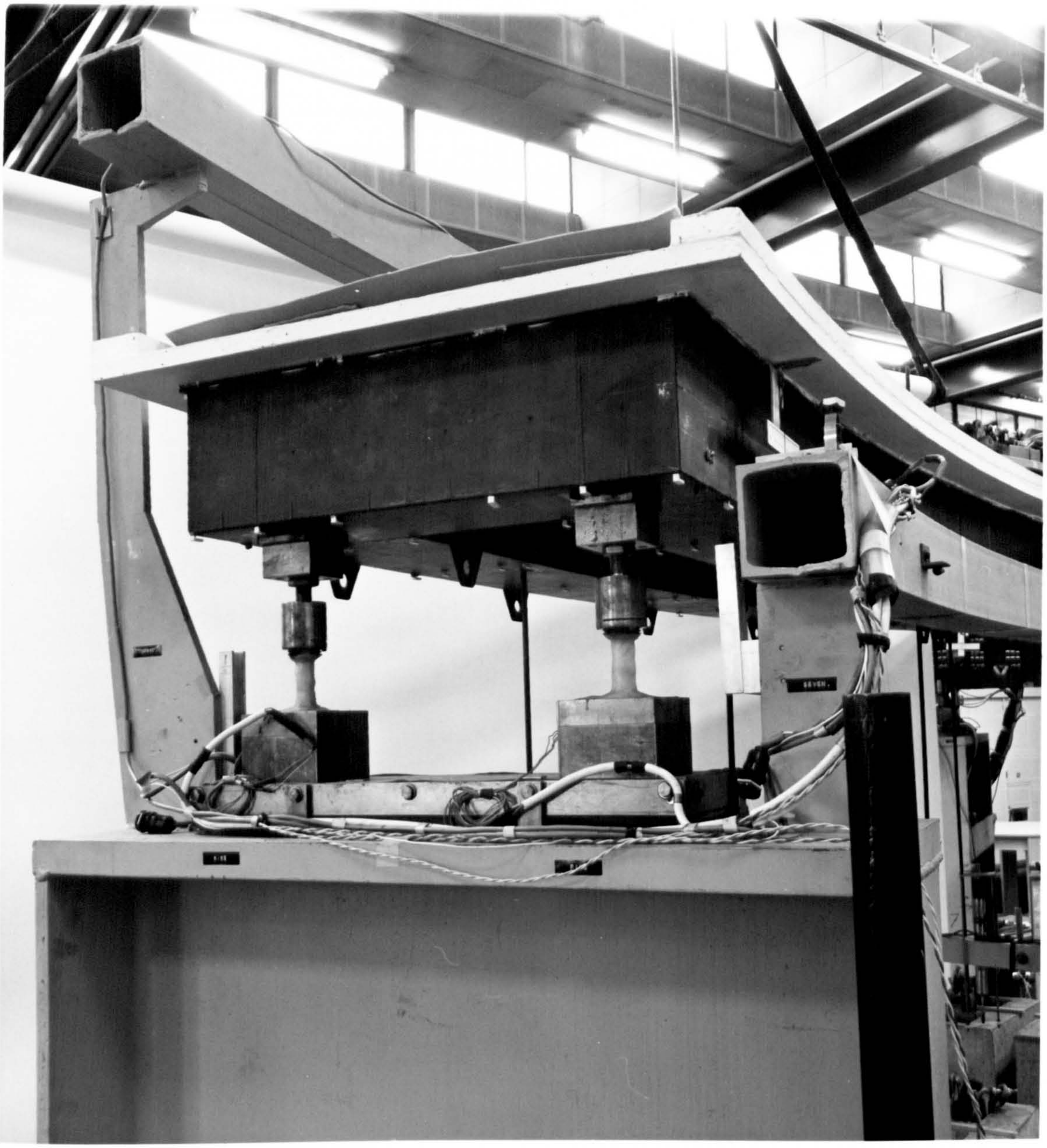

Plate 12. One of the bridge support columns with the longitudinal deflection beams. A right-angled plumbwire support bracket can be seen on the right-hand beam.


Plate 13. Observing at one of the theodolite pillars. The bolt which goes through to the strong floor can be seen just below the theodolite.

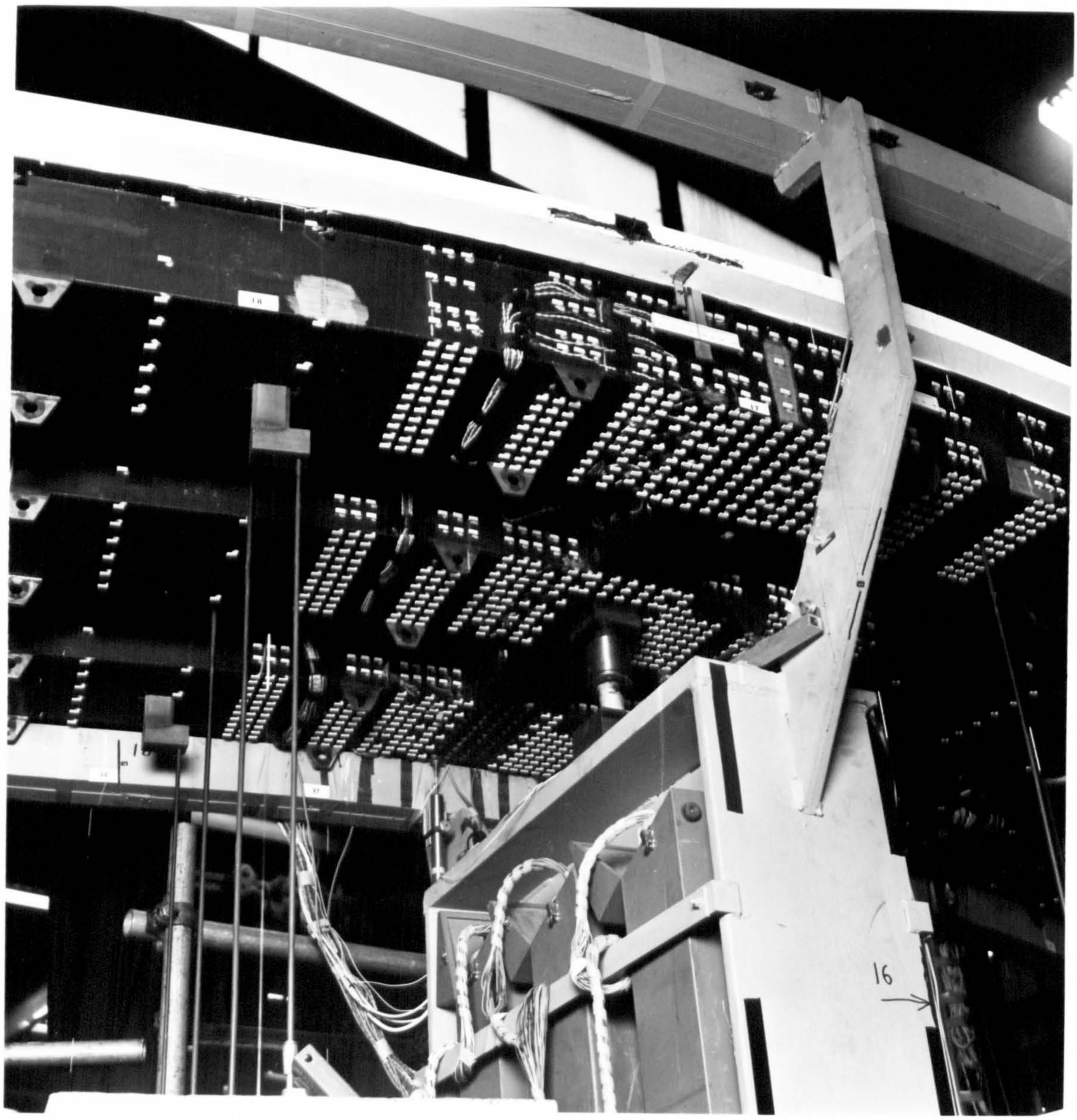


Plate 14. A dense area of premarked targets at the widest part of the model. Several control marks can be seen on their plumbwires.

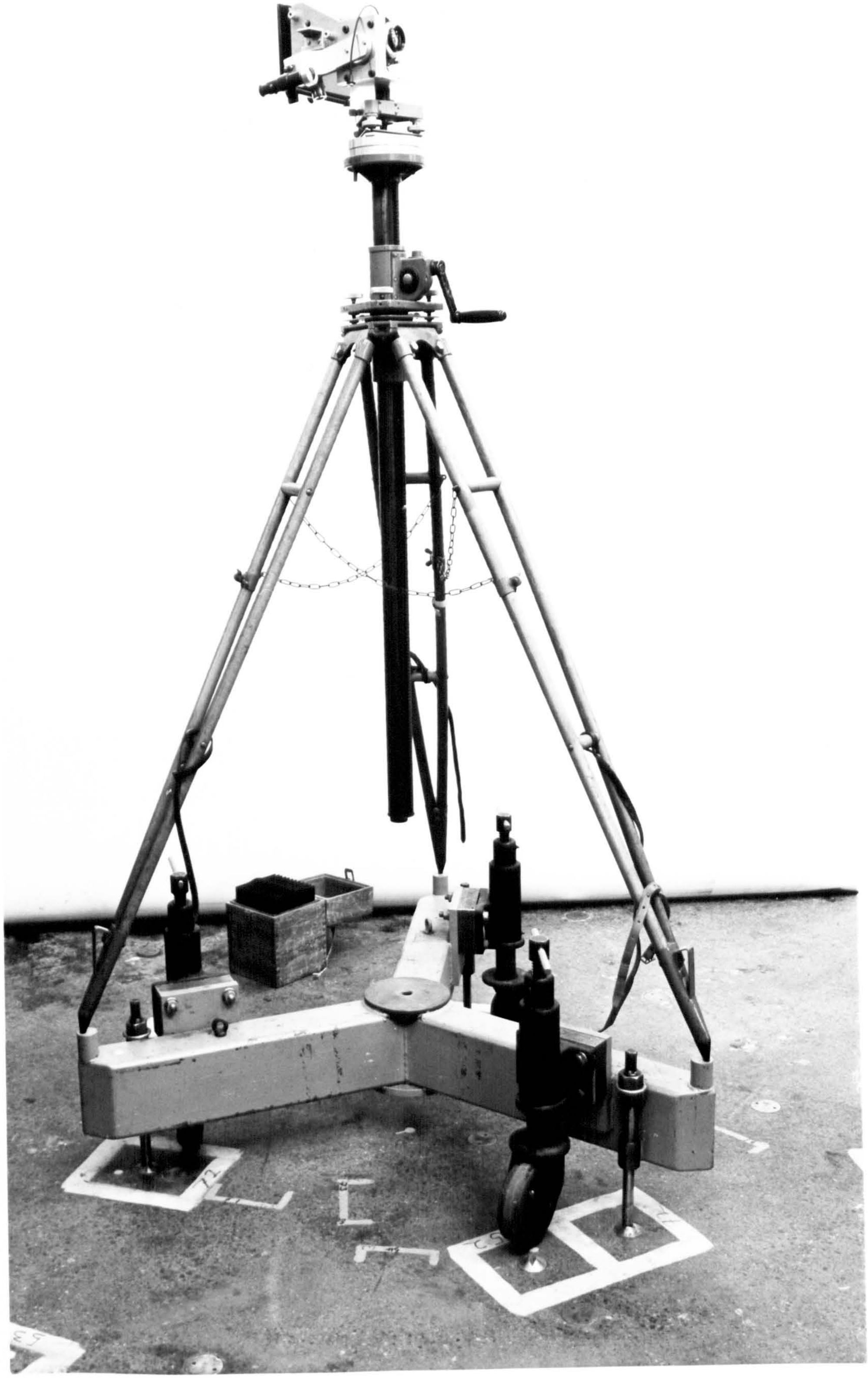

Plate 15. The camera mount and telescope on the racking tripod which stands on the trolley. Two of the pointed feet can be seen located in the grooves. The wheels have been wound up.

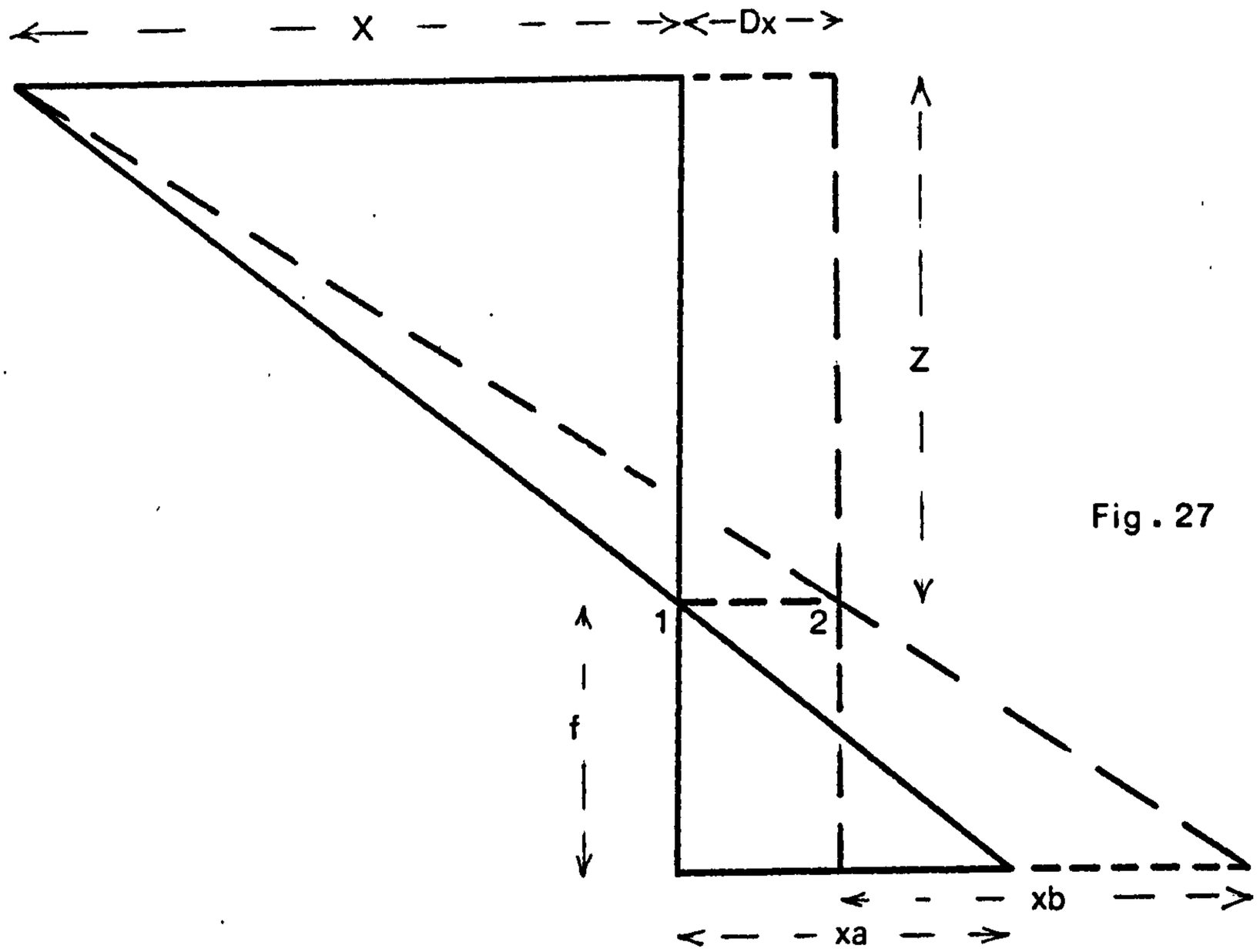


Fig. 27

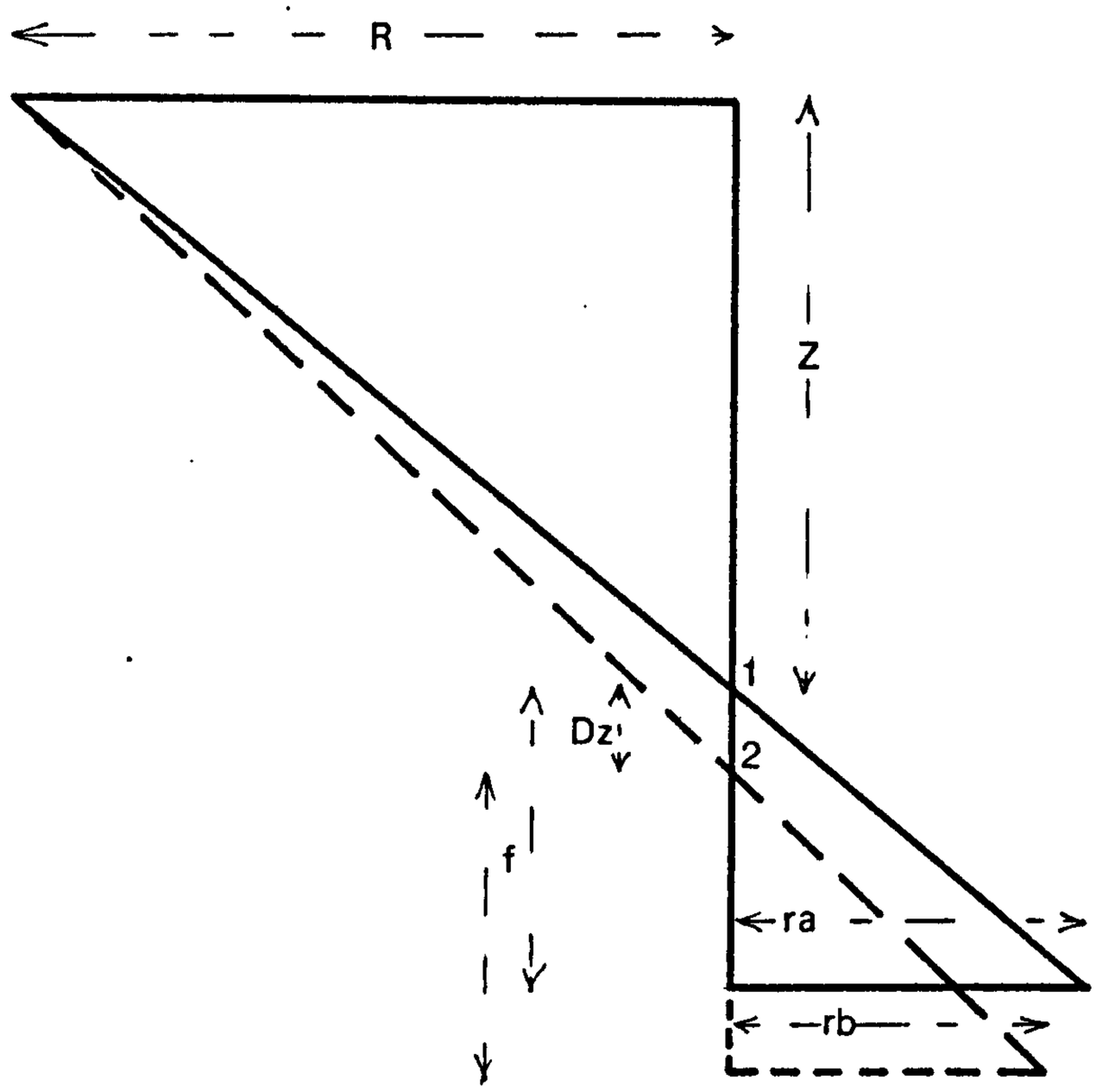


Fig. 28

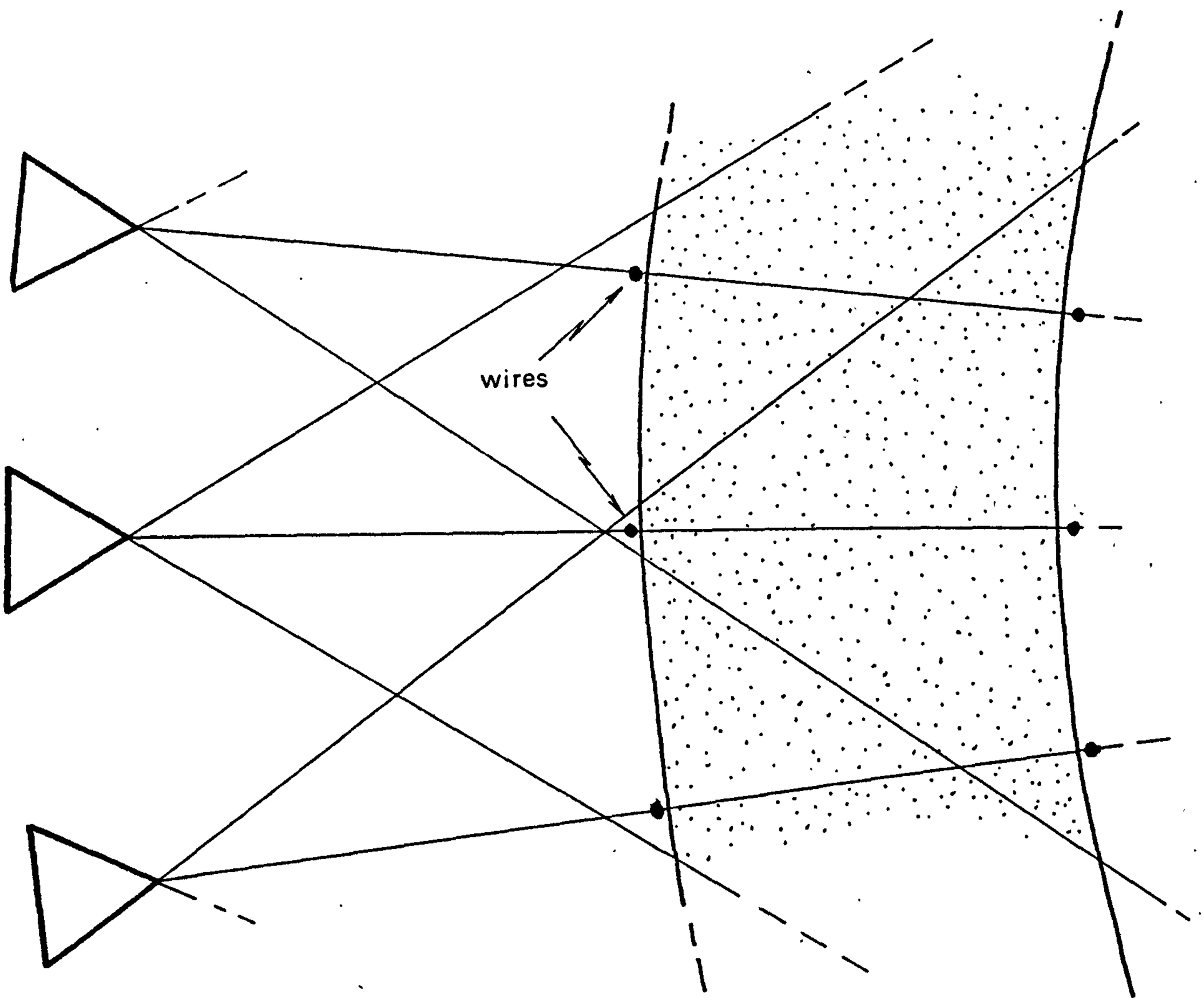


Fig. 29a Plan

Fig. 29b Section

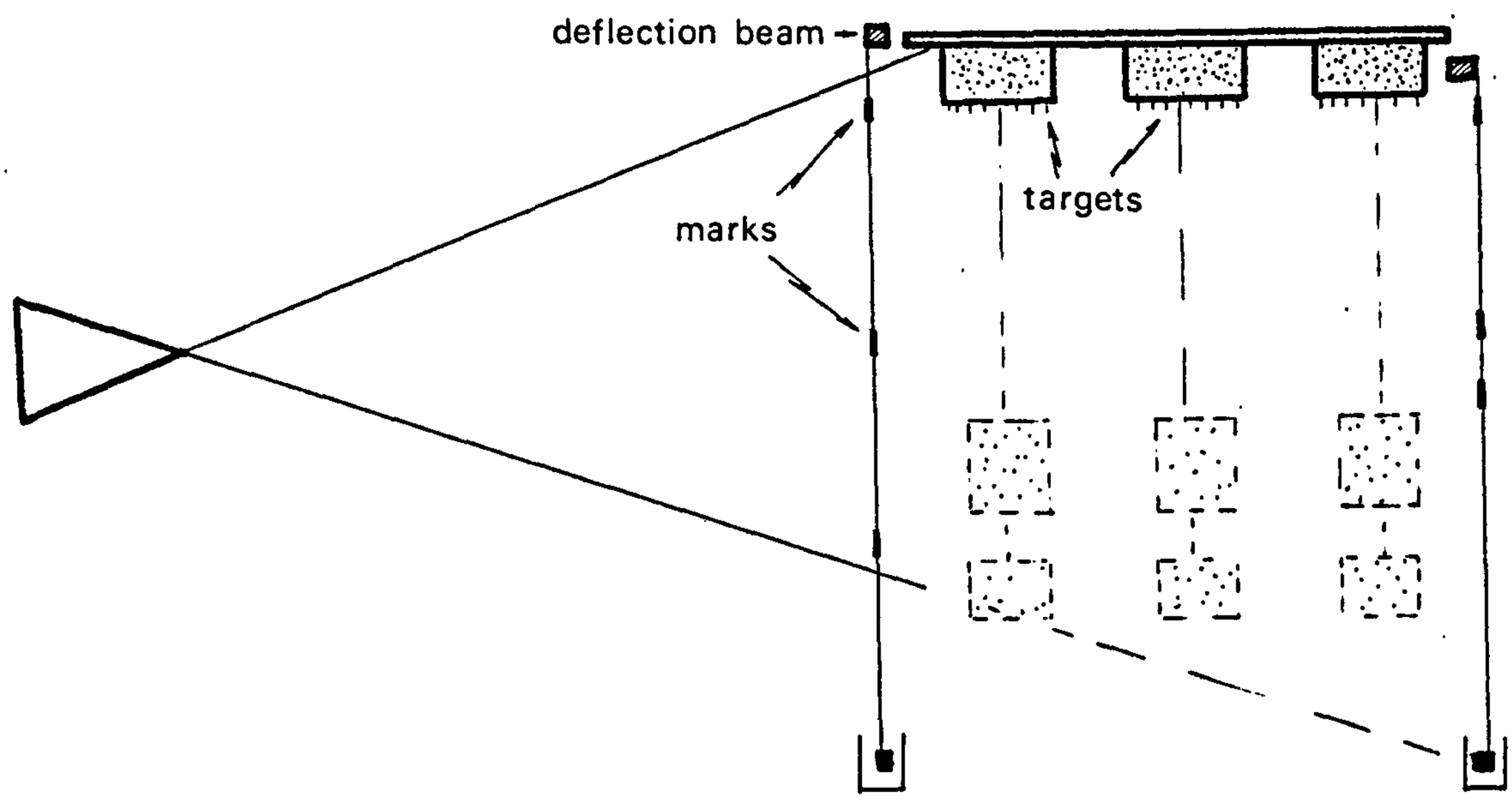

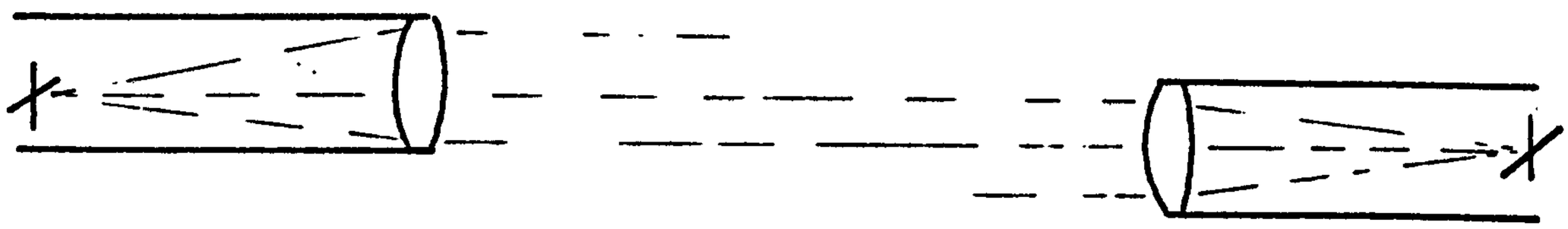

Fig . 30 a

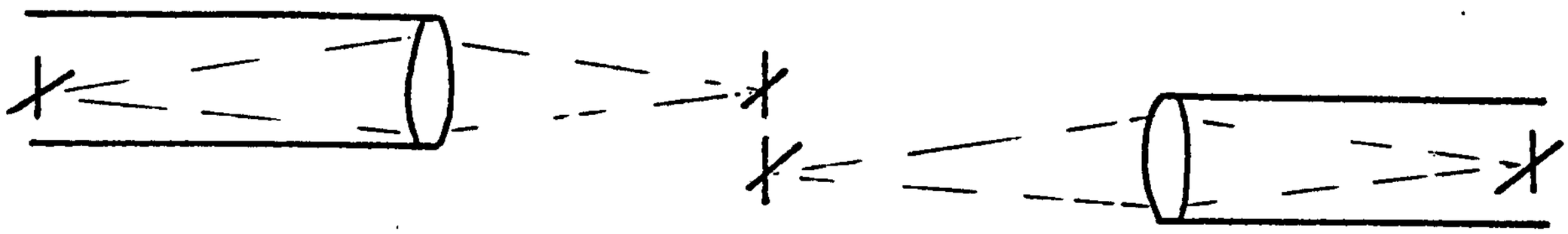

Fig . 30 b

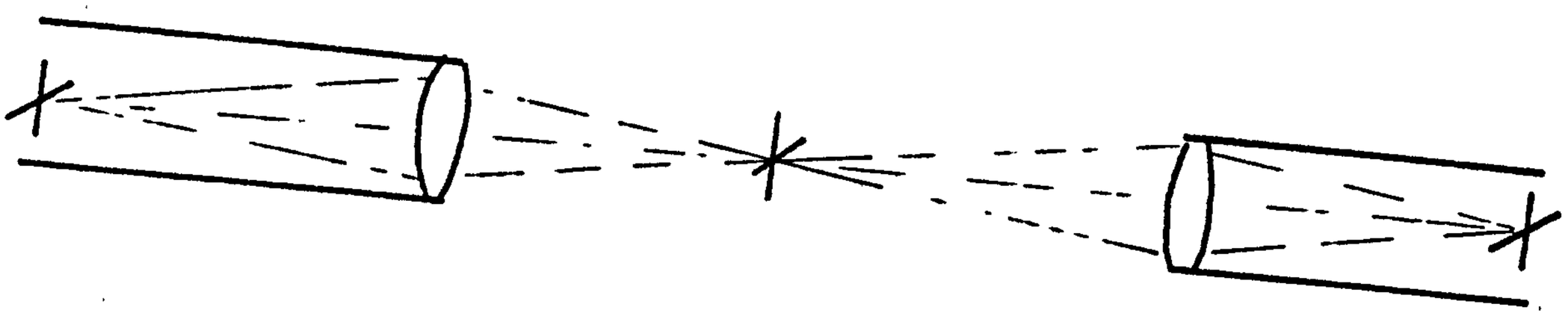

Fig . 30 c

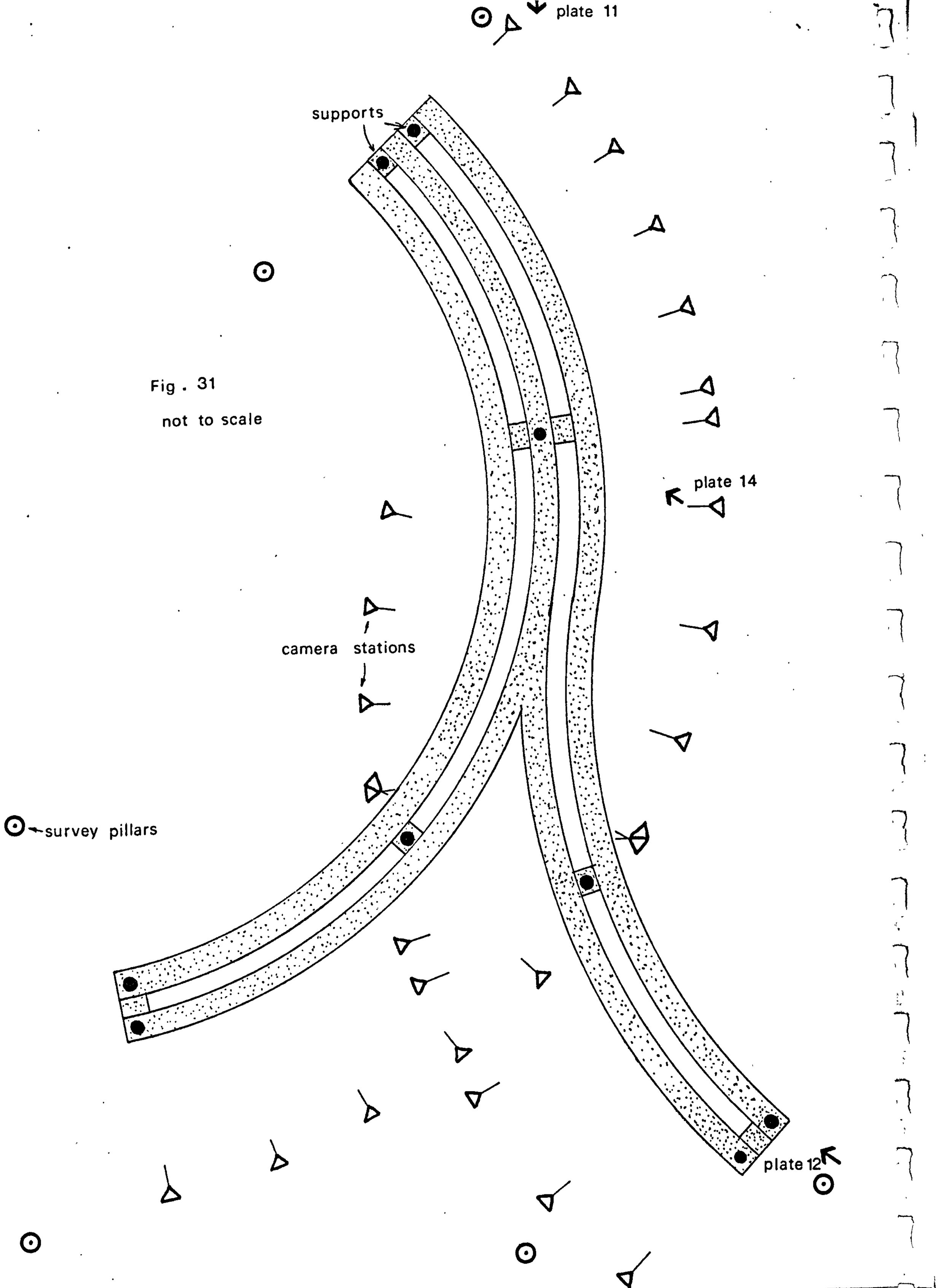


Fig . 31

not to scale

# Chapter 8.

## The box girder bridge project.

### Introduction.

A brief explanation of the box girder bridge test has been supplied by the civil engineer controlling the project, and is presented here. The photogrammetric methods are then described, and their accuracy examined using the results of a laboratory test where a typical stereoscopic overlap was simulated.

### The composite box girder bridge project.

I am indebted to Mr. G. H. Owens for the report below. Mr. Owens is the lecturer from the Department cf Civil Engineering, Imperial College of Science and Technology, who has managed the project through its difficult six year long programme. Plate 11 and figure 31 give the general layout of the bridge and should be studied in conjunction with the report:

"It was once estimated that at 1969 prices, £1000 million would be spent on elevated motorways, to provide a basic network of such roadways in our major cities. Mindful of the particular problems of such structures, the Department of the Environment instituted a programme of experimental research to provide data to validate existing methods of analysis. The programme was divided into two sections, and the first portion was entirely concerned with linear elastic studies. This box girder bridge is the first model in the second section where representative non-linearities of the full scale structure are reproduced and the loading is extended through the working load range to unserviceability levels and collapse.

"While changing environmental considerations and a deteriorating economic situation make the original

estimated requirements for such structures now seem unrealistically high, it is likely that, in the long term at least, a proportion of such motorways will prove essential. Even if this were not so, these studies will enable engineers to develop their ideas on global analysis, observe the effects of the attainment of the serviceability limit state and finally have a rare opportunity to study the ultimate load behaviour of an entire structure. Limit state design philosophy requires greater knowledge in all these fields if it is to develop into a rational design approach.

"The special features of urban motorways relate to the need for complete flexibility of layout. Planning may dictate horizontal curves of small radii, and require a branch or bifurcation at any given point in the layout. Constraints of existing structures and subterranean services may only allow supports at positions other than the structurally ideal and, on occasion, only permit one column leading to torsion spans of substantial length. The chosen model layout incorporates all these features. It simulates a typical multi-box girder bridge of medium span, the steel acting compositely with the reinforced concrete deck. It is obviously necessary to be able to use representative materials, these being, in this model, a micro-concrete with similar properties to a full scale mix, and steel sheet with the same characteristics as structural plate. The scale must be such that imperfections are realistic. In steel, both the residual stresses and the geometric initial imperfection should have values close to those of the prototype and, in the concrete, the tolerances on the slab thickness and the placing of the reinforcement must be realistic.

"From such considerations, it is clear that, the larger the scale, the better will be the model. However, constrictions of laboratory space, the difficulty of applying loading to a large structure, and financial considerations, led to the choice of a scale of 1:12.

This is a smaller scale than has been realistically attempted before."

The choice of photogrammetry for measurement.

The procedure in previous projects of this type has been to measure the area of failure after it occurred. There is, however, great advantage to be gained by obtaining deformation measurements at successive load stages before failure occurs. For reasons best known to the engineers, only the underside of each box was of interest, and its deformation would obviously be confined in the first order to the vertical direction only. The standard engineering method of measuring the movement is by transducer, where a wire attached to the underside of the bridge is pulled into or out of a cylinder, altering the length of a resistance wire inside. The change in resistance is converted to a shift with a claimed accuracy of 0,1mm. These transducers are bulky and, in an area where many points must be measured, they would be difficult to mount. The density of photogrammetric measurement on the other hand is limited only by the size of the premarked target required, and these targets are very cheap. Perhaps the greatest advantage of photogrammetry, however, is in the fact that a large number of targets can be recorded, and only those in the area of failure need be measured when that area is known.

Selection of the Santoni camera.

The Santoni camera described earlier was the most obvious choice in the beginning because it was available in the Department. The stated accuracy requirement of 0,1mm in the relative shift of targets in an area, however, made it necessary to consider other types. Mr. Owens was prepared to buy or hire a more suitable camera if required. The Zeiss (Jena) UMK was very much in vogue at the time and it was suggested. As will be described later, the largest depth of field required on

the photography of the bridge was 1,4m. The Zeiss camera with its minimum aperture of f/36 could accommodate this at a focal setting of 2,9m or 2,4m from the front of the bridge and 3,8m from the back. The scale of the photograph, with the principal distance of 104mm, would thus vary between 1:23 and 1:37. The Santoni camera, on the other hand, with its smallest aperture of f/50, could accommodate the depth of field at 2,3m focal setting or 1,8m from the front and 3,2m from the back. With its principal distance of 160mm, therefore, the scale would vary between 1:11 and 1:20, a decided advantage over the Zeiss camera. It was not known at that time that the Santoni had such poor distortion characteristics but the point must be made that after calibration, and distortion removal, the Santoni's results have the 2:1 scale advantage, and the knowledge should not have affected the decision.

We note that the Zeiss has the advantage, in relative orientation, of being a wide angle camera but, as is explained below, accuracy was required in the comparison between two plates taken from one station and not in absolute coordination. For this type of measurement the angle of the camera is immaterial.

The method of false parallax.

Since the expected deformations were confined to the vertical direction, it was decided to use false parallax measurements to determine the shifts of the premarked targets. The method is well known, but is described here.

If the camera is positioned so that the picture plane is parallel to the shift of an object, comparison of two photographs from the same point before and after deformation will reveal parallax only on points which have shifted. The parallax can be converted, using the ratio of object distance to principal distance, to the shift at true scale. On the bridge photography, however, 27 camera stations were required and there was no guarantee that the

camera could be returned to each one in exactly the same position and attitude for every new load stage. By a method described later, the camera was returned as closely as possible, but the small residual rotations and translations between the photographs had to be determined using expressions for the x and y parallax introduced by them on the control point images. The expressions are developed here.

If (xa, ya, f) are the coordinates of an image on the first photograph and (xb, yb, f) are those of the corresponding image on the second photograph, taken by a camera in the same position but in a different attitude, the second can be transformed onto the first using the standard form of the matrix of small rotations;

$$\begin{pmatrix} xa \\ ya \\ f \end{pmatrix} = \frac{f}{f'} \begin{pmatrix} 1 & -n & m \\ n & 1 & -l \\ -m & l & 1 \end{pmatrix} \begin{pmatrix} xb \\ yb \\ f \end{pmatrix}$$

where l, m and n are the rotations about the x, y and z axes respectively, and f' is the principal distance of the second photograph transformed onto the first. Thus f' = -m.xb + l.yb + f. The matrix is not truly orthogonal, but does yield linear equations in the three unknowns; ignoring second order terms,

$$xa - xb = -l\frac{xb.yb}{f} + m\frac{(f^2 + xb^2)}{f} - n.yb$$

$$ya - yb = -l\frac{(f^2 + yb^2)}{f} + m.\frac{xb.yb}{f} + n.xb$$

For the effect of a small translation, we may consider figure 27 where a translation Dx has been introduced prior to the second photograph: in the first picture,

$$xa = \frac{f.X}{Z}$$

and in the second,

$$xb = \frac{f.(X + Dx)}{Z}$$

Thus $xa - xb = \frac{-f.Dx}{Z}$

and $ya - yb = \frac{-f.Dy}{Z}$

The effect of a small translation Dz along the camera's principal axis can be seen in figure 28. In the first photograph an object a distance R from the axis creates an image of radial distance ra:

$$ra = \frac{f.R}{Z}$$

In the second photograph, $rb = \frac{f.R}{Z + Dz}$

and by substituting for R, $rb = \frac{Z \quad .ra}{Z + Dz}$

Thus $$ra - rb = \frac{Dz \quad .ra}{Z + Dz}$$

This is not linear and, as with the rotations, an approximate form is used:

$$ra - rb = \frac{ra.Dz}{Z}$$

The linear equations now become:

$$xa - xb = -l.\frac{xb.yb}{f} + m\frac{(f^2 + xb^2)}{f} - n.yb \frac{-f.Dx}{Z} + \frac{xb.Dx}{Z}$$

$$ya - yb = -l\frac{(f^2 + yb^2)}{f} + m.\frac{xb.yb}{f} + n.xb \frac{-f.Dy}{Z} + \frac{yb.Dx}{Z}$$

Now if the object distance of each control point is known, the pair of equations can be set up for all points and values of l, m, n, Dx, Dy and Dz obtained. An orthogonal matrix P can be formed in the normal way from l, m and n and the second photograph's images transformed using the rigorous form:

$$\begin{pmatrix} xa \\ ya \\ f \end{pmatrix} = \frac{f}{f'} .P \begin{pmatrix} xb \\ yb \\ f \end{pmatrix} - \frac{\dot{f}}{Z} \begin{pmatrix} Dx \\ Dy \\ 0 \end{pmatrix} + \frac{Dz}{Z+Dz} \begin{pmatrix} xb \\ yb \\ 0 \end{pmatrix}$$

The solution must then be reiterated to convergence. Coordinates of the premarked shift targets on the second photograph can now be transformed onto the first

photograph system using the same form and any residual parallax assumed to be due to the deformation. If the object distance of the premarked target is known, the parallax is easily converted into the shift.

Since the object distance of all control points and deformation targets must be known, much preliminary work is necessary. All control points must be surveyed, and the targets coordinated by normal relative and absolute orientation. The perspective centre coordinates (Xs, Ys, Zs) of the first photograph and the rotation matrix R of its axes on the control system must then be obtained, so that the object distance Z of any point (Xp, Yp, Zp) can be calculated from the normal relationship:

$$Z = R3* \begin{pmatrix} Xp - Xs \\ Yp - Ys \\ Zp - Zs \end{pmatrix}$$

where R3* is the third row of R.

Xs, Ys, Zs and R are easiest obtained from a space resection.

The control point system.

Marks in the same form as those used in the close range calibration were used as control points throughout. The bridge was supported on six massive steel columns. A deflection beam either side of the bridge joined the columns, as shown in plate 12. Nowhere did the bridge touch these beams and the plumbwires were thus attached to them.

A wire was hung directly in front of each camera station at the front of the bridge and another at the back, as shown in figures 29a and b. On the front wire, three marks were placed at the top, middle and bottom of the visible section while on the back wire the three marks had to be closer together to avoid being obscured by the bridge itself or the concrete blocks used as a dead load.

A minimum of four wires appeared on each stereoscopic overlap, qiving 12 points for relative and absolute orientation. All wires were cocrdinated by survey, and not by photoqrammetric trianqulation, because it was expected that some wires would be lost during the test.

For the resection, as well as the false parallax orientation, a minimum of six wires, or 18 points could be seen.

Survey of the control points.

Six pillars similar to that in plate 13 were distributed around the bridqe as indicated in figure 31. They were bolted to the strong floor on which the bridge stood. Each pillar had its own Hilger and Watts single second theodolite. The height cf collimation of these was the same as that of the thin bridqe supports on the top of the steel columns seen in plate 12, and consequently it was possible to position the pillars such that all were intervisible.

The scale of the fiqure was determined by Dr. A. L. Allan usinq a Tellurometer MA 100, and triangulated usinq a method devised by Dr. I. A. Harley of the University of Queensland. The method is shown in figure 30, and is explained below.

In figure 30a, the two theodolites are focussed on infinity and autocollimated against each other so that their lines of collimation are parallel, although not necessarily collinear. The theodolites are now focussed on a piece of paper half way between them, as in figure 30b, thus projecting their cross hairs to the midway plane. When the paper is removed, any non-coincidence is half removed by the first theodolite and half by the second, as in fiqure 30c. Now if the theodolites are refocussed on infinity, the crosshairs should remain in coincidence. It is, of course, necessary to use successive approximation.

The full figure was observed at the beginning of the load test and again towards the end. The second set of observations showed better results than the first set, and the largest misclosure among the twenty triangles was 11", as opposed to 17" for the first. The second set was thus accepted for the final coordination. The stations were coordinated using T. K. Rylance's program for adjustment by variation of coordinates. The largest error ellipse at any of the points had a semi-major axis of 0,11mm, which was extremely satisfactory as the longest line measured 16m.

A great advantage of the method is that the vertical angles are measured simultaneously with the horizontal observations. Height differences between the stations could thus be calculated, and the net was adjusted using Mr. D. P. Mason's least squares adjustment program. One line required a correction of 0,29mm while the next largest correction was less than 0,1mm, a reasonable justification for the rejection of the former, but there was little point since the required accuracy of the coordinates was 0,1mm, and the removal would not have changed the result significantly.

Each of the 43 plumbwires was now intersected from at least three of the pillars, and the height of each mark was determined by vertical angles from two pillars. Plan coordinates were chosen by simple error figure and heights by weighted mean. In the event, only 30 of the surveyed wires had to be coordinated. During the test, several local resurveys were necessary because of suspected movement of wires, and after failure all 43 were re-intersected and vertical angles were re-observed. Three significant movements were located during these checks.

Premarked deformation targets.

Plate 14 shows the most dense area of targets. They were made of plastic, and the mark was a cross with arms 0,2mm wide, identified by a four digit number. Some 4000

targets were attached to the bridge but less than 1000 had to be coordinated by photogrammetry. Failure occurred more or less simultaneously at the three inner support columns, where the density of the targets was highest as the bridge had been expected to fail there.

Photography.

The camera was mounted on a racking tripod which in turn was carried on a trolley shown in plate 15. The principal axis was horizontal, as required for false parallax, and normal to the longitudinal section of the bridge as shown in figure 29b. The plan of the 27 camera stations is shown in figure 31.

The camera trolley had three pointed feet which were located above three corresponding v-grooves in metal plates on the floor. Each station was defined by three such plates. The wheels were then wound up allowing the trolley to reposition itself very precisely. Since the footscrews of the tripod were never moved during the test, the camera returned approximately to the same position for each new load stage. The original attitude was regained by levelling the camera's tribrach and rotating the mount about its vertical axis until a sighting mark on the bridge was seen through the mount's telescope.

It required just over two hours to occupy all 27 stations. Dark room processing then required one hour, using the bulk processing rack in plate 4. Twenty sets of photographs were taken during the twelve days of continuous testing between 24th January and 4th February, 1977.

Camera calibration during the test.

Throughout the test, the inner orientation of the camera was never disturbed. After the last load stage had been photographed, the camera was calibrated by the plumbwire method described in Chapter 5. No significant

change in the curve was found, but the origin of symmetry had moved about 0,1mm. The results from this calibration were used throughout the box girder processing.

Coordination and analysis of the photographs.

Stereoscopic overlaps were observed in the Hilger and Watts stereocomparator, and all points in the areas of failure were coordinated. Because of the large depth of field, targets toward the back of the bridge could be coordinated from two or even three overlaps.

The first load stage photograph was now compared with the last, or twentieth, using stereoscopic observation procedures on the comparator. The computer program for false parallax thus showed immediately which of the targets had moved at all during the test. This greatly reduced the number of points to be observed in subsequent load stage comparisons.

Photographs from load stages 19 and 18 were now observed, and each in turn compared against photograph 1 for false parallax. Photographs 17 and 16 followed until no shift could be detected anywhere in the area. This report is being written before the completion of the calculations and no idea can be formed about the extent of the observation required.

A test on accuracy.

A typical section of the widest part of the bridge was simulated in the laboratory to test the accuracy of the method. Figure 29 shows the disposition of control points and camera stations. In the object space, six pairs of deformation targets were placed in representative positions. All control points and deformation targets were now coordinated by intersection from two theodolites. Two photographs were taken from each of the three camera stations with shifts and rotations being introduced to the camera mount between exposures.

The first plates from each station were used to form two stereoscopic overlaps, and all twelve deformatien targets were coordinated in the normal way. Each pair of plates from a station was now observed for false parallax by treating the pairs of deformation targets as a single target before and after load. Each target pair could thus be measured two ways, giving 12 horizontal and 12 vertical shifts. Four of the six pairs of targets were visible on all three plates, giving three measurements of the shifts which were meaned. The other two pairs only appeared on two plates. Residuals between these mean photogrammetric shifts and the relatively error free surveyed values are grouped as follows: 10 shifts had residuals of ±0,0mm, 7 had residuals of ±0,1mm and the remaining 5 had residuals of ±0,2mm. The root mean square residual is thus ±0,11mm which just satisfies the specification for the box girder.

A test was now carried out on the same simulation to find the increase of accuracy after calibration. It is perhaps worth noting that because expected target shifts on the box girder were less than 1mm at photograph scale, radial distance would not change significantly enough to affect the radial distortion. No increase in false parallax accuracy is therefore expected from calibration. The accuracy of absolute coordination was tested by processing the stereoscopic overlaps in three ways:

A. Coordinates were modified using the calibration values d and e and the shifts C-F1 and C-F2 developed in chapter 6.

B. The increment ST in chapter 7 was ignored and the principal distance at infinite focus assumed to have increased by y = 10,8mm. The origin of symmetry was that determined in the infinite focus calibration.

C. The maker's claim that the camera was nearly distortion free (Ferri - Gelli 1972) was accepted and the values of d, e, C-F1 and C-F2 assumed to be zero.

The table belcw compares the accuracy of the three methcds at various staqes of calculation.

| | A | B | C |
|---|---|---|---|
| root mean square parallax at orientation points. | | | |
| Model 1 | 0,008mm | 0,009mm | 0,016mm |
| Model 2 | 0,009mm | 0,009mm | 0,012mm |
| root mean square residual at control points on absolute orientaticn. | | | |
| Model 1 | 1,3mm | 2,1mm | 5,6mm |
| Model 2 | 0,9mm | 1,5mm | 4,6mm |
| root mean square residual at deformation targets on absolute orientation. | | | |
| Model 1 | 1,0mm | 1,8mm | 4,9mm |
| Model 2 | 0,8mm | 1,2mm | 3,9mm |

While the improvement from B to A (taking the increment ST into account) is nct as dramatic as that from C to A, it is obviously highly significant.

## Conclusions.

This project has shown that photogrammetric methods have qreat potential fcr deformation measurement if the false parallax principle can be used. The large residuals of 1,0mm and 0,8mm at the deformation targets indicate that comparison of two absolute coordinations at successive load staqes will certainly not produce the accuracy required of the shift measurement.

It is difficult to assess the saving to the engineers cf not mountinq 4000 transducers, but during the actual

test photogrammetry slowed the loading process considerably. In this particular case, the extra time taken during the 12 day test was negligible compared with the 6 years that the whole project lasted, but it may be significant in tests where the structure is unstable and testing must be carried out in the minimum time.

The great amount of work involved in photography and processing is not to be undertaken lightly. If the measurement were done commercially it might prove prohibitively expensive. The cost of transducers and the logging system and computer to accompany them may very well be less. The advantages of photogrammetry have been mentioned earlier, and in this project they outweighed the disadvantages, but a careful study of a project is essential before a decision is made.

There is no doubt at all that the subsidiary research into camera calibration described in this project has been of great benefit.

## Reference.

Ferri,W.S. and Gelli,G., 1972. Mechanical and optical problems in the design and construction of close-range photogrammetric plate cameras. International Archives of Photogrammetry Vol.XIX, part 5. 19 pages.

CAMERA 113S DIAGONAL 500-100 OBJECT DISTANCE 2,3M

PLATE -32 NOMINAL P.D. 161.33 APPROX. DIST. TO 1ST WIRE 1.790

DEFINED P.P. 193.730 200.971 SELECTED P.P. 193.754

PLATE Y COORD. OF IMAGE LINES 200.163 200.084 199.953 199.887 199.798

PRINCIPAL POINT ON WIRES 3.52306 3.51736 3.51108 3.50256 3.49194
RESIDUALS OF FITTED LINE 0.04 -0.04 -0.01 -0.02 0.03 STD. DEVIATION 0.03 SLOPE -0.020883

| POINTS | CONSTANTS OF UPPER AND LOWER RADIAL LINES M' | M" | N' | N" | COORDINATES OF S L | H | RESIDUALS OF LINE HEIGHTS | | | | | STD.DEV. |
|---|---|---|---|---|---|---|---|---|---|---|---|---|
| 1 13 | 0.607429 | 4.64802 | -0.608161 | 2.47180 | -1.79026 | 3.56057 | -0.03 | 0.10 | -0.09 | 0.01 | 0.01 | 0.07 |
| | | | | | | | -0.07 | 0.07 | 0.05 | -0.04 | -0.00 | 0.06 |
| 2 12 | 0.558909 | 4.56137 | -0.560104 | 2.55794 | -1.79035 | 3.56073 | 0.04 | -0.04 | -0.01 | 0.02 | 0.00 | 0.03 |
| | | | | | | | -0.01 | 0.07 | -0.06 | -0.04 | 0.03 | 0.05 |
| 3 11 | 0.495464 | 4.44759 | -0.496480 | 2.67182 | -1.79019 | 3.56061 | 0.05 | 0.02 | -0.05 | -0.10 | 0.08 | 0.08 |
| | | | | | | | -0.09 | 0.03 | 0.05 | 0.08 | -0.08 | 0.08 |
| 4 10 | 0.403995 | 4.28378 | -0.405024 | 2.83586 | -1.78972 | 3.56074 | -0.06 | 0.09 | -0.01 | -0.02 | -0.00 | 0.05 |
| | | | | | | | 0.06 | -0.05 | -0.03 | 0.01 | 0.02 | 0.04 |
| 5 9 | 0.309648 | 4.11503 | -0.310864 | 3.00413 | -1.79030 | 3.56066 | -0.05 | 0.04 | 0.02 | 0.01 | -0.02 | 0.04 |
| | | | | | | | -0.06 | 0.04 | 0.01 | 0.05 | -0.05 | 0.05 |
| 6 8 | 0.186630 | 3.89444 | -0.187842 | 3.22433 | -1.78947 | 3.56047 | -0.06 | 0.09 | 0.01 | -0.07 | 0.02 | 0.06 |
| | | | | | | | -0.04 | 0.03 | -0.01 | 0.06 | -0.04 | 0.04 |

WEIGHTED MEAN COORDINATES OF S -1.79013 3.56064 SLOPE OF AXIS -4306.9 SECONDS
INCREMENTS -0.00013 3.56064 ITERATION 1
HT. BY EXTENSION OF AXIS EQUATION 3.55049

PRINCIPAL POINT ON WIRES 3.52306 3.51735 3.51108 3.50256 3.49194
RESIDUALS OF FITTED LINE 0.04 -0.04 -0.01 -0.02 0.03 STD. DEVIATION 0.03 SLOPE -0.020883

| POINTS | CONSTANTS OF UPPER AND LOWER RADIAL LINES M' | M" | N' | N" | COORDINATES OF S L | H | RESIDUALS OF LINE HEIGHTS | | | | | STD.DEV. |
|---|---|---|---|---|---|---|---|---|---|---|---|---|
| 1 13 | 0.607429 | 4.64802 | -0.608161 | 2.47180 | -1.79026 | 3.56057 | -0.03 | 0.10 | -0.09 | 0.01 | 0.01 | 0.07 |
| | | | | | | | -0.07 | 0.07 | 0.05 | -0.04 | -0.00 | 0.06 |
| 2 12 | 0.558909 | 4.56137 | -0.560104 | 2.55794 | -1.79035 | 3.56073 | 0.04 | -0.04 | -0.01 | 0.02 | 0.00 | 0.03 |
| | | | | | | | -0.01 | 0.07 | -0.06 | -0.04 | 0.03 | 0.05 |
| 3 11 | 0.495464 | 4.44759 | -0.496480 | 2.67182 | -1.79019 | 3.56061 | 0.05 | 0.02 | -0.05 | -0.10 | 0.08 | 0.08 |
| | | | | | | | -0.09 | 0.03 | 0.05 | 0.08 | -0.08 | 0.08 |
| 4 10 | 0.403996 | 4.28378 | -0.405024 | 2.83586 | -1.78971 | 3.56074 | -0.06 | 0.09 | -0.01 | -0.02 | -0.00 | 0.05 |
| | | | | | | | 0.06 | -0.05 | -0.03 | 0.01 | 0.02 | 0.04 |
| 5 9 | 0.309648 | 4.11503 | -0.310864 | 3.00413 | -1.79030 | 3.56066 | -0.05 | 0.04 | 0.02 | 0.01 | -0.02 | 0.04 |
| | | | | | | | -0.06 | 0.04 | 0.01 | 0.05 | -0.05 | 0.05 |
| 6 8 | 0.186630 | 3.89444 | -0.187842 | 3.22433 | -1.78947 | 3.56047 | -0.06 | 0.09 | 0.01 | -0.07 | 0.02 | 0.06 |
| | | | | | | | -0.04 | 0.03 | -0.01 | 0.06 | -0.04 | 0.04 |

WEIGHTED MEAN COORDINATES OF S -1.79013 3.56064 SLOPE OF AXIS -4306.9 SECONDS
INCREMENTS 0.00000 0.00000 ITERATION 2
HT. BY EXTENSION OF AXIS EQUATION 3.56049
SEC.SQD.W = 1.000436 TAN.W = -0.020883

CURVE CONSTANTS R*R*-0.3766 + R* 0.0002 + 166.394 = P.D.
SHIFT TO ORIGIN OF SYMMETRY -0.000

| CALCED F | TAN.Q RADIAL | DH(MM) | CALCED F | TAN.Q RADIAL | DH(MM) | CALCED F | TAN.Q RADIAL | DH(MM) | CALCED F | TAN.Q RADIAL | DH(MM) | CALCED F | TAN.Q RADIAL | DH(MM) |
|---|---|---|---|---|---|---|---|---|---|---|---|---|---|---|
| 166.023 | 0.581 | 0.08 | 166.002 | 0.580 | 0.20 | 166.035 | 0.577 | 0.06 | 166.022 | 0.576 | 0.17 | 166.043 | 0.576 | 0.04 |
| | 96.556 | | | 96.447 | | | 95.963 | | | 95.815 | | | 95.669 | |
| 166.068 | 0.533 | 0.11 | 166.122 | 0.532 | -0.09 | 166.131 | 0.530 | -0.14 | 166.092 | 0.530 | 0.06 | 166.099 | 0.529 | 0.02 |
| | 88.656 | | | 88.358 | | | 88.121 | | | 88.169 | | | 87.994 | |
| 166.145 | 0.476 | 0.05 | 166.177 | 0.475 | -0.07 | 166.191 | 0.473 | -0.13 | 166.161 | 0.472 | 0.01 | 166.157 | 0.471 | 0.03 |
| | 79.174 | | | 78.974 | | | 78.607 | | | 78.388 | | | 78.317 | |
| 166.215 | 0.386 | 0.07 | 166.250 | 0.385 | -0.03 | 166.260 | 0.383 | -0.06 | 166.253 | 0.382 | -0.05 | 166.219 | 0.381 | 0.12 |
| | 64.086 | | | 63.983 | | | 63.614 | | | 63.532 | | | 63.388 | |
| 166.341 | 0.294 | -0.08 | 166.345 | 0.292 | -0.09 | 166.340 | 0.293 | -0.10 | 166.280 | 0.292 | 0.08 | 166.277 | 0.292 | 0.11 |
| | 48.841 | | | 48.591 | | | 48.636 | | | 48.458 | | | 48.544 | |
| 166.391 | 0.175 | -0.04 | 166.444 | 0.172 | -0.11 | 166.408 | 0.173 | -0.07 | 166.382 | 0.173 | -0.04 | 166.355 | 0.173 | 0.02 |
| | 29.016 | | | 28.589 | | | 28.718 | | | 28.751 | | | 28.712 | |
| 166.348 | -0.190 | -0.01 | 166.331 | -0.191 | -0.04 | 166.340 | -0.191 | -0.03 | 166.348 | -0.191 | -0.02 | 166.321 | -0.190 | -0.09 |
| | -31.578 | | | -31.801 | | | -31.777 | | | -31.685 | | | -31.525 | |
| 166.291 | -0.309 | -0.01 | 166.263 | -0.310 | -0.08 | 166.262 | -0.310 | -0.09 | 166.257 | -0.310 | -0.13 | 166.259 | -0.309 | -0.14 |
| | -51.304 | | | -51.506 | | | -51.579 | | | -51.470 | | | -51.438 | |
| 166.231 | -0.403 | 0.02 | 166.204 | -0.406 | -0.06 | 166.211 | -0.403 | -0.05 | 166.180 | -0.401 | -0.21 | 166.193 | -0.400 | -0.18 |
| | -67.019 | | | -67.409 | | | -66.916 | | | -66.633 | | | -66.469 | |
| 166.192 | -0.492 | 0.17 | 166.124 | -0.495 | -0.06 | 166.157 | -0.493 | 0.07 | 166.142 | -0.492 | -0.00 | 166.177 | -0.492 | 0.22 |
| | -81.785 | | | -82.264 | | | -81.945 | | | -81.766 | | | -81.744 | |
| 166.097 | -0.554 | 0.09 | 166.088 | -0.553 | 0.05 | 166.087 | -0.553 | 0.06 | 166.102 | -0.551 | 0.15 | 166.113 | -0.551 | 0.25 |
| | -92.082 | | | -91.931 | | | -91.874 | | | -91.594 | | | -91.575 | |
| 165.995 | -0.602 | -0.09 | 165.999 | -0.601 | -0.09 | 166.025 | -0.600 | 0.03 | 166.029 | -0.598 | 0.05 | 166.047 | -0.598 | 0.20 |
| | -100.034 | | | -99.864 | | | -99.750 | | | -99.425 | | | -99.422 | |

STD. DEVIATION OF CURVE ACROSS ONE DIAGONAL 0.10 MM.

CURVE VALUES , INTERPOLATED LINE POINTS AND TARGET HEIGHTS

| P.D. | TAN.Q | LINE | TARGET | LINE | TARGET | LINE | TARGET | LINE | TARGET | LINE | TARGET |
|---|---|---|---|---|---|---|---|---|---|---|---|
| 166.046 | 0.579 | 3.79028 | 3.7936 | 3.87903 | 3.8819 | 3.99928 | 3.9981 | 4.17395 | 4.1709 | 4.35585 | 4.3504 |
| 166.101 | 0.531 | 3.73428 | 3.7371 | 3.81551 | 3.8163 | 3.92609 | 3.9248 | 4.08670 | 4.0857 | 4.25394 | 4.2505 |
| 166.161 | 0.474 | 3.66587 | 3.6693 | 3.73844 | 3.7407 | 3.83709 | 3.8363 | 3.98036 | 3.9770 | 4.12965 | 4.1248 |
| 166.241 | 0.383 | 3.55920 | 3.5618 | 3.61810 | 3.6202 | 3.69819 | 3.6972 | 3.81438 | 3.8123 | 3.93570 | 3.9314 |
| 166.305 | 0.292 | 3.45169 | 3.4533 | 3.49683 | 3.4967 | 3.55830 | 3.5585 | 3.64752 | 3.6458 | 3.74040 | 3.7395 |
| 166.363 | 0.173 | 3.31097 | 3.3128 | 3.33804 | 3.3367 | 3.37496 | 3.3746 | 3.42847 | 3.4284 | 3.48428 | 3.4837 |
| 166.356 | -0.190 | 2.88443 | 2.8851 | 2.85582 | 2.8558 | 2.81935 | 2.8184 | 2.76503 | 2.7649 | 2.70830 | 2.7102 |
| 166.294 | -0.309 | 2.74511 | 2.7462 | 2.69957 | 2.6992 | 2.63780 | 2.6367 | 2.54822 | 2.5481 | 2.45483 | 2.4551 |
| 166.225 | -0.402 | 2.63651 | 2.6356 | 2.57702 | 2.5729 | 2.49635 | 2.4961 | 2.37920 | 2.3820 | 2.25723 | 2.2626 |
| 166.141 | -0.493 | 2.53099 | 2.5318 | 2.45773 | 2.4549 | 2.35880 | 2.3584 | 2.21503 | 2.2165 | 2.06540 | 2.0674 |
| 166.076 | -0.553 | 2.46110 | 2.4592 | 2.37915 | 2.3782 | 2.26787 | 2.2673 | 2.10663 | 2.1090 | 1.93849 | 1.9415 |
| 166.019 | -0.601 | 2.40535 | 2.4030 | 2.31630 | 2.3150 | 2.19547 | 2.1950 | 2.02011 | 2.0231 | 1.83737 | 1.8409 |

COMPOSITE CURVE CONSTANTS R*R*-0.3630 + 166.389 = P.D.

CURVE VALUES FOR PLOTTING

| | | | | | | |
|---|---|---|---|---|---|---|
| 0.05 166.386 | 0.10 166.379 | 0.15 166.366 | 0.20 166.349 | 0.25 166.326 | 0.30 166.298 | 0.35 166.266 |
| 0.40 166.228 | 0.45 166.186 | 0.50 166.138 | 0.55 166.085 | 0.60 166.028 | 0.65 165.965 | 0.70 165.897 |

STD. DEVIATION OF COMPOSITE CURVE 0.10 MM. HEIGHT AT THE WIRES

Location of principal points:

P.1 = point of autocollimation

C = centre of fiducial marks

V = chosen origin of symmetry

P.2, V' = second calibration

Scale 1mm = 1 μm.

Camera 113.s

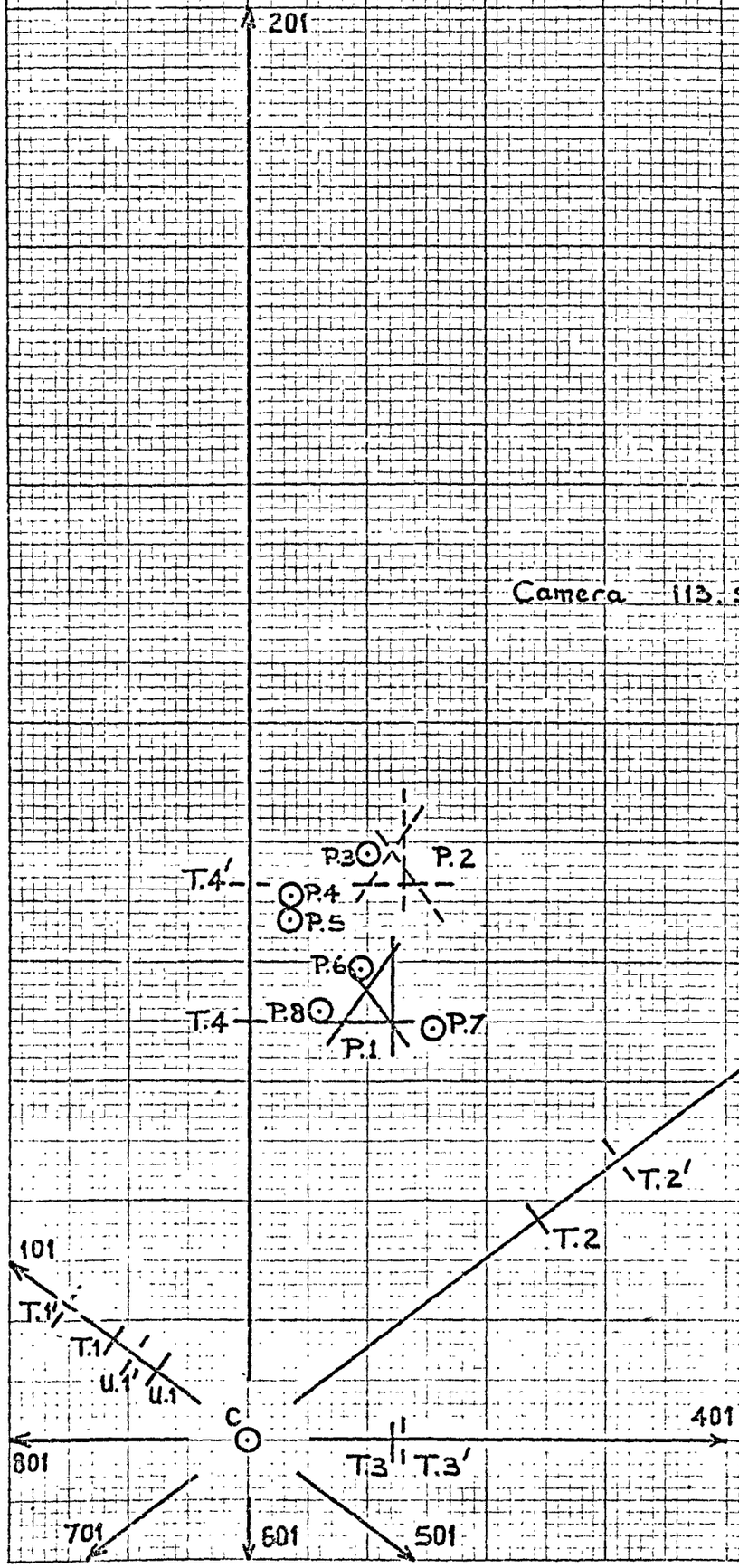


Camera 113.d

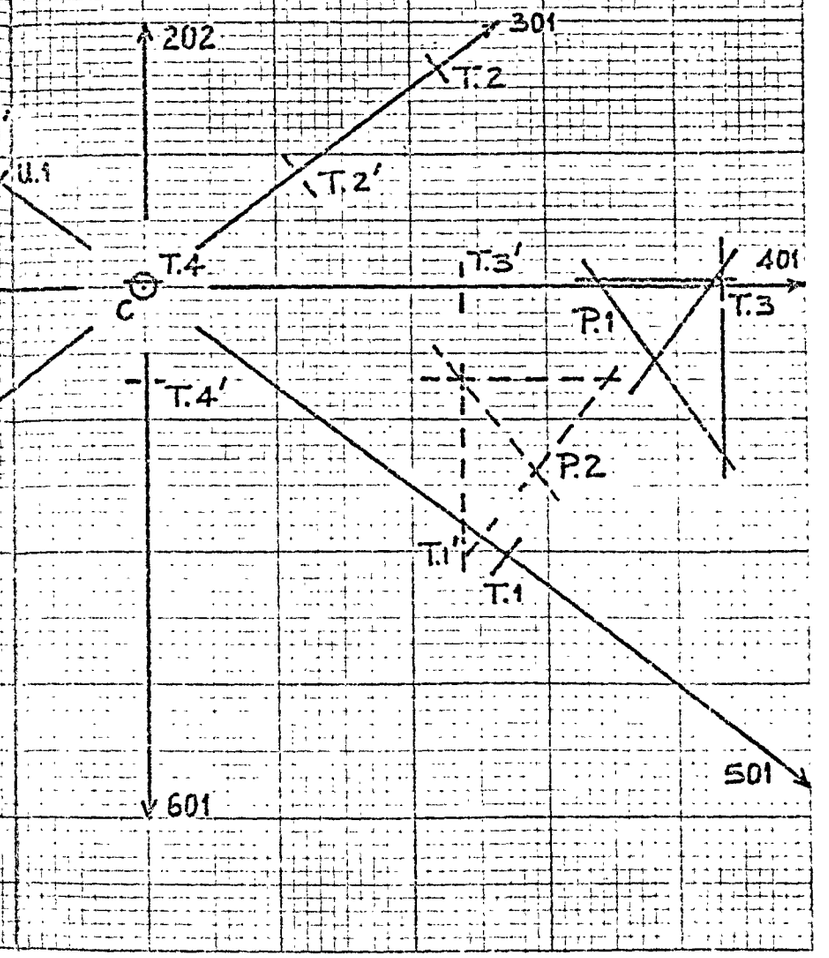

APPENDIX A3.

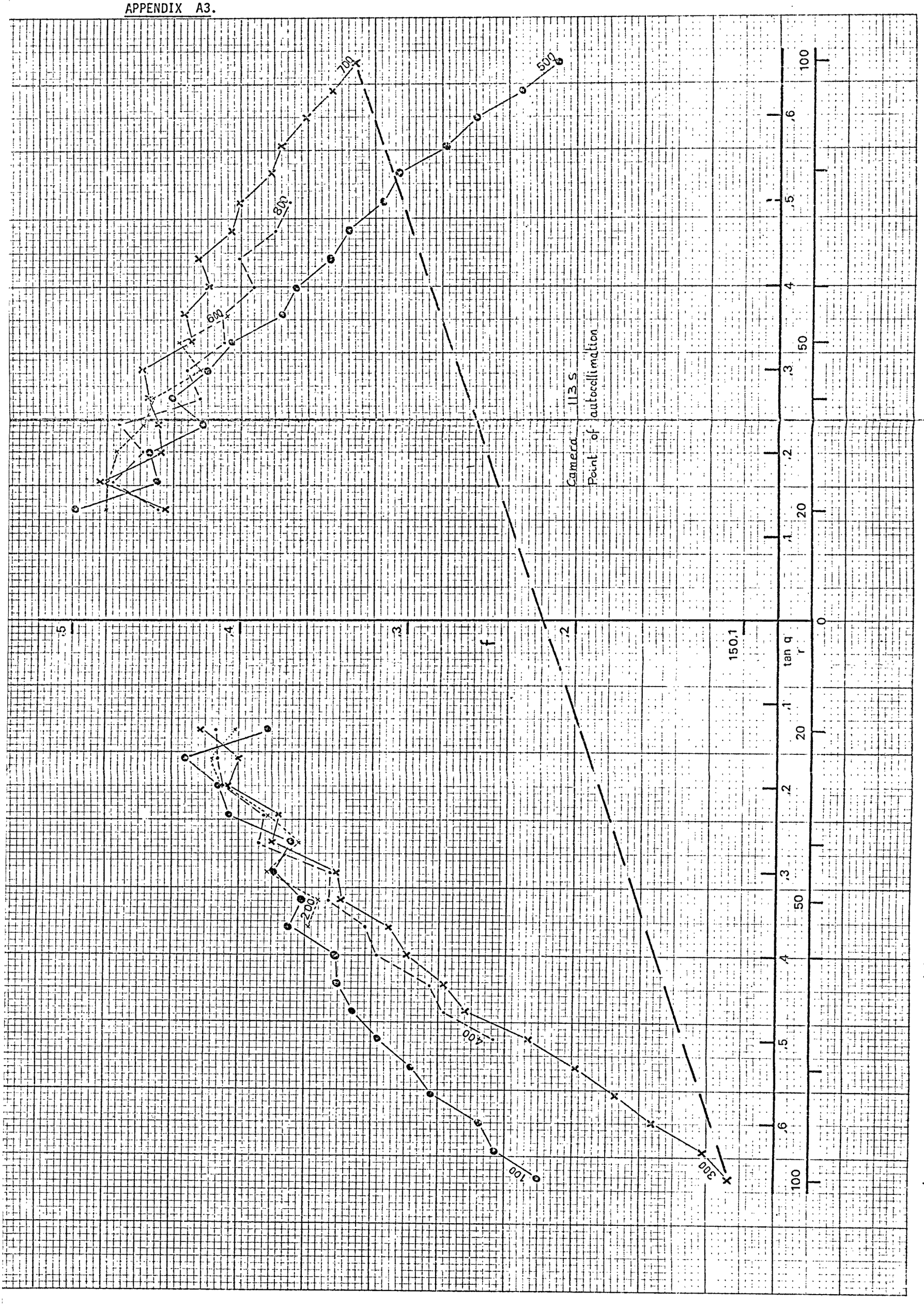
500
700
800
600
200
400
100
300
f
tan q
r
150,1
Camera
Point of autocollimation
113 S
0
20
50
100
.1
.2
.3
.4
.5
.6

APPENDIX A4.

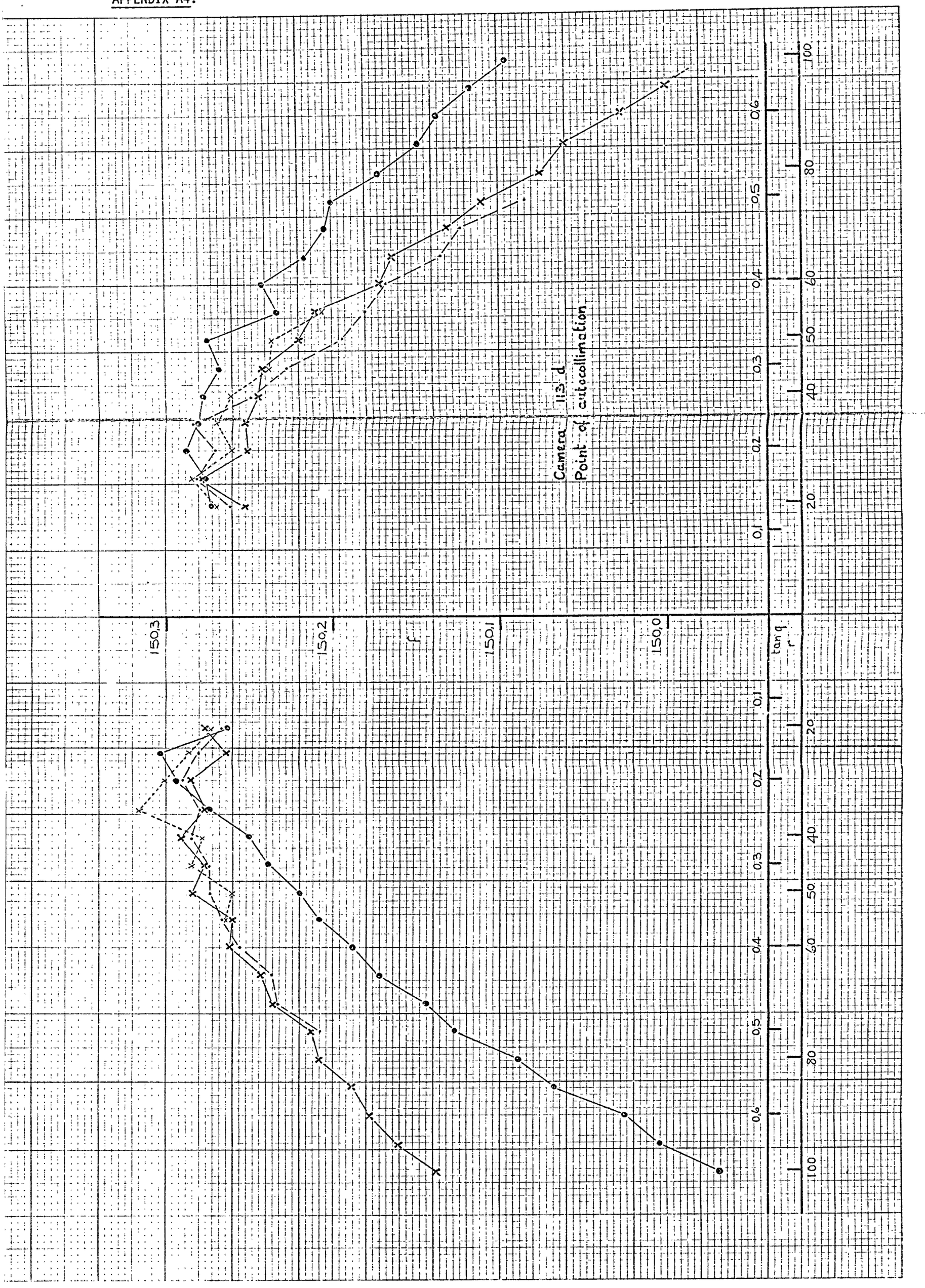
Camera 113 d
Point of autocollimation
f
150,3
150,2
150,1
150,0
tan q
0,1
0,2
0,3
0,4
0,5
0,6
20
40
50
60
80
100

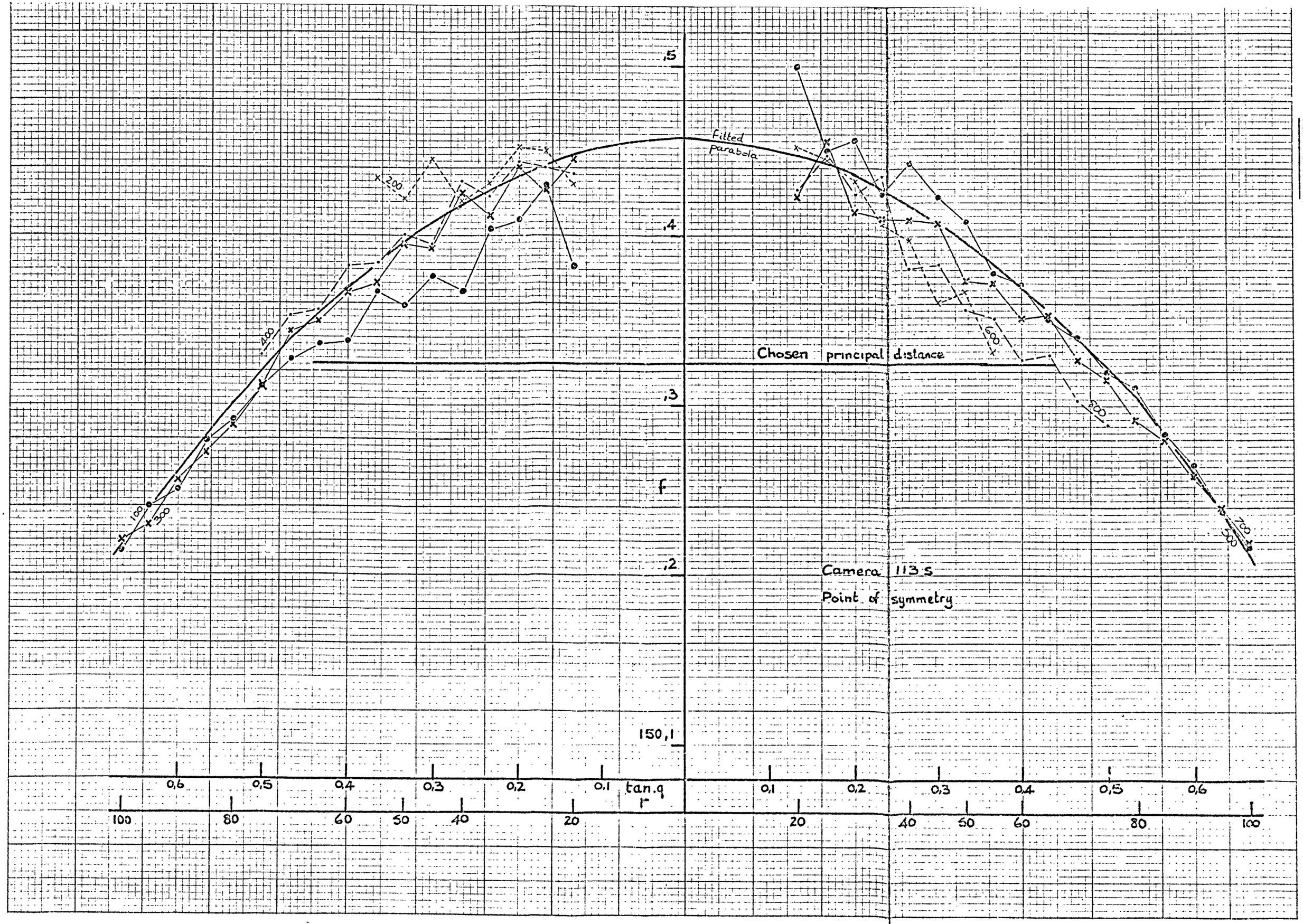
,5
,4
,3
,2
f
150,1
Fitted parabola
Chosen principal distance
Camera 113 s
Point of symmetry
100
200
300
400
500
600
700
800
0,6
0,5
0,4
0,3
0,2
0,1
tan.q
100
80
60
50
40
20
0,1
0,2
0,3
0,4
0,5
0,6
20
40
50
60
80
100

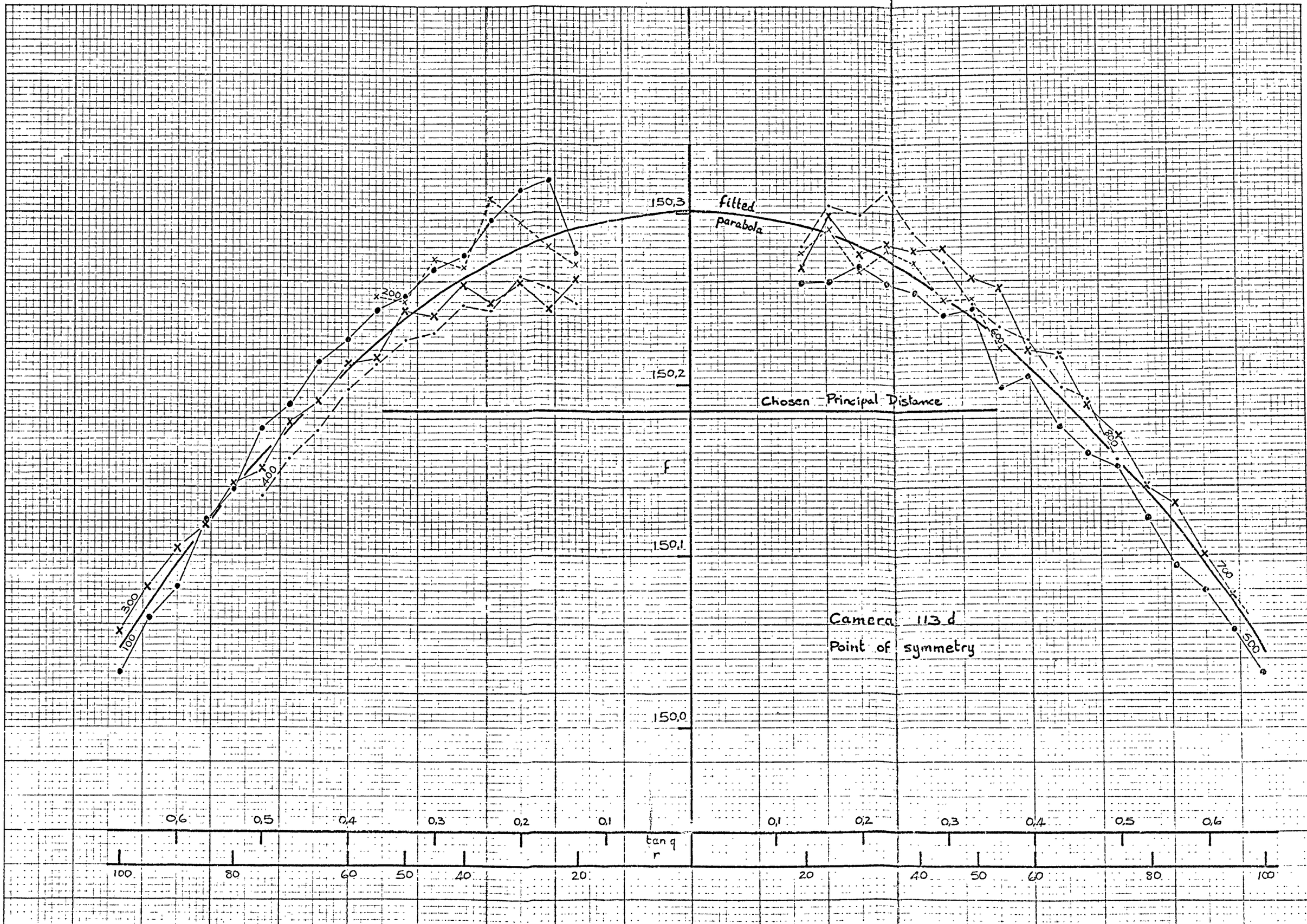
150,3
150,2
150,1
150,0
f
fitted
parabola
Chosen Principal Distance
Camera 113 d
Point of symmetry
200
300
400
600
700
800
500
0,6
0,5
0,4
0,3
0,2
0,1
tan q
r
100
80
60
50
40
20

CAMERA 113S  DIAGONAL 300-700  OBJECT DISTANCE 1,6M

PLATE -14 NOMINAL P.D. 166.23 APPROX. DIST. TO 1ST WIRE 1.175

DEFINED P.P. 200.499 200.185  SELECTED P.P. 200.727

PLATE Y COORD. OF IMAGE LINES  200.576  200.371  200.187  200.061  199.789

PRINCIPAL POINT ON WIRES  3.10776  3.10884  3.11023  3.11236  3.11458
RESIDUALS OF FITTED LINE  -0.01  -0.03  0.04  0.01  -0.02  STD. DEVIATION  0.03  SLOPE  0.007082

| POINTS | CONSTANTS OF UPPER AND LOWER RADIAL LINES M' | M" | N' | N" | COORDINATES OF S L | H | RESIDUALS OF LINE HEIGHTS | STD.DEV. |
|---|---|---|---|---|---|---|---|---|
| 1 13 | 0.588088 | 3.79033 | -0.590600 | 2.40533 | -1.17503 | 3.09931 | 0.05 -0.08 0.06 -0.07 0.04<br>-0.01 0.03 -0.03 0.03 -0.01 | 0.07<br>0.03 |
| 2 12 | 0.540478 | 3.73414 | -0.543406 | 2.46105 | -1.17456 | 3.09932 | -0.14 0.08 0.14 -0.06 -0.02<br>-0.05 0.01 0.05 0.01 -0.03 | 0.11<br>0.04 |
| 3 11 | 0.482311 | 3.66578 | -0.484081 | 2.53085 | -1.17440 | 3.09936 | -0.09 0.03 0.11 -0.02 -0.03<br>-0.14 0.12 0.00 0.10 -0.09 | 0.07<br>0.11 |
| 4 10 | 0.391498 | 3.55912 | -0.394398 | 2.63649 | -1.17399 | 3.09950 | -0.08 0.02 0.07 0.07 -0.08<br>-0.03 0.03 -0.03 0.06 -0.04 | 0.08<br>0.04 |
| 5 9 | 0.300257 | 3.45165 | -0.301826 | 2.74508 | -1.17355 | 3.09928 | -0.04 0.01 0.06 -0.04 0.00<br>-0.03 0.02 0.01 0.01 -0.01 | 0.04<br>0.02 |
| 6 8 | 0.180248 | 3.31092 | -0.183121 | 2.88443 | -1.17371 | 3.09936 | -0.05 0.04 0.02 0.01 -0.02<br>0.00 0.02 -0.01 -0.03 0.02 | 0.03<br>0.02 |

WEIGHTED MEAN COORDINATES OF S  -1.17437  3.09935  SLOPE OF AXIS  1460.7 SECONDS
INCREMENTS  0.00063  3.09935  ITERATION 1
HT. BY EXTENSION OF AXIS EQUATION  3.09943

PRINCIPAL POINT ON WIRES  3.10775  3.10884  3.11022  3.11235  3.11457
RESIDUALS OF FITTED LINE  -0.01  -0.03  0.04  0.01  -0.02  STD. DEVIATION  0.03  SLOPE  0.007082

| POINTS | CONSTANTS OF UPPER AND LOWER RADIAL LINES M' | M" | N' | N" | COORDINATES OF S L | H | RESIDUALS OF LINE HEIGHTS | STD.DEV. |
|---|---|---|---|---|---|---|---|---|
| 1 13 | 0.588085 | 3.79033 | -0.590597 | 2.40533 | -1.17504 | 3.09931 | 0.05 -0.08 0.06 -0.07 0.04<br>-0.01 0.03 -0.03 0.03 -0.01 | 0.07<br>0.03 |
| 2 12 | 0.540476 | 3.73414 | -0.543404 | 2.46105 | -1.17457 | 3.09932 | -0.14 0.08 0.14 -0.06 -0.02<br>-0.05 0.01 0.05 0.01 -0.03 | 0.11<br>0.04 |
| 3 11 | 0.482308 | 3.66578 | -0.484080 | 2.53085 | -1.17441 | 3.09936 | -0.09 0.03 0.11 -0.02 -0.03<br>-0.14 0.12 0.00 0.10 -0.09 | 0.07<br>0.12 |
| 4 10 | 0.391496 | 3.55912 | -0.394395 | 2.63649 | -1.17400 | 3.09950 | -0.08 0.02 0.07 0.07 -0.08<br>-0.03 0.03 -0.03 0.06 -0.04 | 0.08<br>0.04 |
| 5 9 | 0.300256 | 3.45165 | -0.301826 | 2.74508 | -1.17355 | 3.09928 | -0.04 0.01 0.06 -0.04 0.00<br>-0.03 0.02 0.01 0.01 -0.02 | 0.04<br>0.02 |
| 6 8 | 0.180247 | 3.31092 | -0.183121 | 2.88443 | -1.17372 | 3.09936 | -0.05 0.04 0.02 0.01 -0.02<br>-0.00 0.02 -0.01 -0.03 0.02 | 0.03<br>0.02 |

WEIGHTED MEAN COORDINATES OF S  -1.17437  3.09935  SLOPE OF AXIS  1460.8 SECONDS
INCREMENTS  -0.00001  0.00000  ITERATION 2
HT. BY EXTENSION OF AXIS EQUATION  3.09943
SEC.SQD.W = 1.000050  TAN.W = 0.007082

CAMERA 113S  DIAGONAL 300-700  OBJECT DISTANCE 2,3M

PLATE 31 NOMINAL P.D. 161.33 APPROX. DIST. TO 1ST WIRE 1.790

DEFINED P.P. 199.514 199.126  SELECTED P.P. 199.799

PLATE Y COORD. OF IMAGE LINES 200.166 200.078 199.939 199.860 199.764

PRINCIPAL POINT ON WIRES 3.55668 3.55564 3.55455 3.55308 3.55106
RESIDUALS OF FITTED LINE 0.02 0.02 -0.01 -0.07 0.05 STD. DEVIATION 0.04 SLOPE -0.003747

| POINTS | CONSTANTS OF UPPER AND LOWER RADIAL LINES M' | M" | N' | N" | COORDINATES OF S L | H | RESIDUALS OF LINE HEIGHTS | STD.DEV. |
|---|---|---|---|---|---|---|---|---|
| 1 13 | 0.606294 | 4.64866 | -0.609142 | 2.47235 | -1.79056 | 3.56305 | 0.03 0.06 -0.15 0.04 0.02 | 0.08 |
| | | | | | | | -0.05 0.00 0.04 0.06 -0.06 | 0.05 |
| 2 12 | 0.557948 | 4.56190 | -0.561302 | 2.55861 | -1.78985 | 3.56326 | 0.04 -0.07 -0.01 0.07 -0.03 | 0.06 |
| | | | | | | | -0.04 0.11 -0.07 -0.03 0.03 | 0.07 |
| 3 11 | 0.494370 | 4.44820 | -0.497604 | 2.67245 | -1.79011 | 3.56322 | 0.01 0.02 0.02 -0.10 0.06 | 0.06 |
| | | | | | | | -0.06 -0.00 0.08 0.04 -0.06 | 0.06 |
| 4 10 | 0.402913 | 4.28438 | -0.406085 | 2.83645 | -1.78978 | 3.56325 | -0.07 0.10 -0.01 -0.02 -0.00 | 0.06 |
| | | | | | | | 0.01 -0.05 0.03 0.04 -0.03 | 0.04 |
| 5 9 | 0.308573 | 4.11563 | -0.312052 | 3.00479 | -1.78987 | 3.56332 | -0.03 0.02 0.07 -0.07 0.02 | 0.05 |
| | | | | | | | -0.01 0.03 -0.02 -0.00 0.00 | 0.02 |
| 6 8 | 0.185447 | 3.89510 | -0.189052 | 3.22500 | -1.78930 | 3.56328 | -0.04 0.06 0.03 -0.07 0.03 | 0.06 |
| | | | | | | | -0.06 0.04 0.02 0.05 -0.05 | 0.05 |

WEIGHTED MEAN COORDINATES OF S -1.79002 3.56321  SLOPE OF AXIS -772.9 SECONDS
INCREMENTS -0.00002 3.55321  ITERATION 1
HT. BY EXTENSION OF AXIS EQUATION 3.56341

PRINCIPAL POINT ON WIRES 3.55668 3.55564 3.55455 3.55308 3.55106
RESIDUALS OF FITTED LINE 0.02 0.02 -0.01 -0.07 0.05 STD. DEVIATION 0.04 SLOPE -0.003747

| POINTS | CONSTANTS OF UPPER AND LOWER RADIAL LINES M' | M" | N' | N" | COORDINATES OF S L | H | RESIDUALS OF LINE HEIGHTS | STD.DEV. |
|---|---|---|---|---|---|---|---|---|
| 1 13 | 0.606294 | 4.64866 | -0.609142 | 2.47235 | -1.79056 | 3.56305 | 0.03 0.06 -0.15 0.04 0.02 | 0.08 |
| | | | | | | | -0.05 0.00 0.04 0.06 -0.06 | 0.05 |
| 2 12 | 0.557948 | 4.56190 | -0.561302 | 2.55861 | -1.78985 | 3.56326 | 0.04 -0.07 -0.01 0.07 -0.03 | 0.06 |
| | | | | | | | -0.04 0.11 -0.07 -0.03 0.03 | 0.07 |
| 3 11 | 0.494370 | 4.44820 | -0.497604 | 2.67245 | -1.79011 | 3.56322 | 0.01 0.02 0.02 -0.10 0.06 | 0.06 |
| | | | | | | | -0.06 -0.00 0.08 0.04 -0.06 | 0.06 |
| 4 10 | 0.402913 | 4.28438 | -0.406085 | 2.83645 | -1.78978 | 3.56325 | -0.07 0.10 -0.01 -0.02 -0.00 | 0.06 |
| | | | | | | | 0.01 -0.05 0.03 0.04 -0.03 | 0.04 |
| 5 9 | 0.308573 | 4.11563 | -0.312052 | 3.00479 | -1.78987 | 3.56332 | -0.03 0.02 0.07 -0.07 0.02 | 0.05 |
| | | | | | | | -0.01 0.03 -0.02 -0.00 0.00 | 0.02 |
| 6 8 | 0.185447 | 3.89510 | -0.189052 | 3.22500 | -1.78930 | 3.56328 | -0.04 0.06 0.03 -0.07 0.03 | 0.06 |
| | | | | | | | -0.06 0.04 0.02 0.05 -0.05 | 0.05 |

WEIGHTED MEAN COORDINATES OF S -1.79002 3.56321  SLOPE OF AXIS -772.9 SECONDS
INCREMENTS 0.00000 0.00000  ITERATION 2
HT. BY EXTENSION OF AXIS EQUATION 3.56341
SEC.SQD.W = 1.000014  TAN.W = -0.003747

CAMERA 113S  DIAGONAL 500-100  OBJECT DISTANCE 1,6M

PLATE 13 NOMINAL P.D. 166.23 APPROX. DIST. TO 1ST WIRE 1.181

DEFINED P.P. 200.810 201.254  SELECTED P.P. 200.773

PLATE Y COORD. OF IMAGE LINES 200.465 200.310 200.184 200.094 199.878

PRINCIPAL POINT ON WIRES 3.10179 3.10244 3.10327 3.10467 3.10607
RESIDUALS OF FITTED LINE -0.03 -0.01 0.07 -0.01 -0.02 STD. DEVIATION 0.04 SLOPE 0.004464

| POINTS | CONSTANTS OF UPPER AND LOWER RADIAL LINES M' | M" | N' | N" | COORDINATES OF S L | H | RESIDUALS OF LINE HEIGHTS | STD.DEV. |
|---|---|---|---|---|---|---|---|---|
| 1 13 | 0.587323 | 3.79059 | -0.586298 | 2.40382 | -1.18162 | 3.09660 | 0.01 -0.06 0.10 -0.06 0.01 | 0.07 |
| 2 12 | 0.540109 | 3.73427 | -0.539127 | 2.45955 | -1.18113 | 3.09633 | -0.05 0.03 -0.02 0.11 -0.07 | 0.07 |
| 3 11 | 0.482090 | 3.66586 | -0.480116 | 2.52945 | -1.18104 | 3.09649 | -0.12 0.06 0.14 -0.05 -0.03 | 0.10 |
| 4 10 | 0.391660 | 3.55906 | -0.390801 | 2.63522 | -1.18069 | 3.09663 | -0.03 -0.01 0.08 -0.04 -0.00 | 0.05 |
| 5 9 | 0.300781 | 3.45146 | -0.298635 | 2.74395 | -1.18034 | 3.09644 | -0.08 0.05 0.08 -0.04 -0.01 | 0.06 |
| 6 8 | 0.181255 | 3.31056 | -0.180458 | 2.88349 | -1.18069 | 3.09656 | -0.14 0.12 0.01 0.08 -0.08 | 0.11 |
| | | | | | | | -0.05 0.03 0.04 0.02 -0.03 | 0.04 |
| | | | | | | | -0.04 0.04 -0.02 0.07 -0.05 | 0.05 |
| | | | | | | | -0.07 0.03 0.08 -0.04 -0.01 | 0.06 |
| | | | | | | | -0.04 0.01 0.04 0.01 -0.02 | 0.03 |
| | | | | | | | -0.04 -0.01 0.07 0.00 -0.03 | 0.04 |
| | | | | | | | 0.01 0.04 -0.03 -0.07 0.05 | 0.05 |

WEIGHTED MEAN COORDINATES OF S -1.18103 3.09650  SLOPE OF AXIS 920.8 SECONDS
INCREMENTS -0.00003 3.09650  ITERATION 1
HT. BY EXTENSION OF AXIS EQUATION 3.09648

PRINCIPAL POINT ON WIRES 3.10179 3.10244 3.10327 3.10467 3.10607
RESIDUALS OF FITTED LINE -0.03 -0.01 0.07 -0.01 -0.02 STD. DEVIATION 0.04 SLOPE 0.004464

| POINTS | CONSTANTS OF UPPER AND LOWER RADIAL LINES M' | M" | N' | N" | COORDINATES OF S L | H | RESIDUALS OF LINE HEIGHTS | STD.DEV. |
|---|---|---|---|---|---|---|---|---|
| 1 13 | 0.587323 | 3.79059 | -0.586298 | 2.40382 | -1.18162 | 3.09660 | 0.01 -0.06 0.10 -0.06 0.01 | 0.07 |
| 2 12 | 0.540109 | 3.73427 | -0.539127 | 2.45955 | -1.18113 | 3.09633 | -0.05 0.03 -0.02 0.11 -0.07 | 0.07 |
| 3 11 | 0.482091 | 3.66586 | -0.480116 | 2.52945 | -1.18104 | 3.09649 | -0.12 0.06 0.14 -0.05 -0.03 | 0.10 |
| 4 10 | 0.391660 | 3.55906 | -0.390801 | 2.63522 | -1.18069 | 3.09663 | -0.03 -0.01 0.08 -0.04 -0.00 | 0.05 |
| 5 9 | 0.300781 | 3.45146 | -0.298634 | 2.74395 | -1.18034 | 3.09644 | -0.08 0.05 0.08 -0.04 -0.01 | 0.06 |
| 6 8 | 0.181255 | 3.31056 | -0.180458 | 2.88349 | -1.18069 | 3.09656 | -0.14 0.12 0.01 0.08 -0.08 | 0.11 |
| | | | | | | | -0.05 0.03 0.04 0.02 -0.03 | 0.04 |
| | | | | | | | -0.04 0.04 -0.02 0.07 -0.05 | 0.05 |
| | | | | | | | -0.07 0.03 0.08 -0.04 -0.01 | 0.06 |
| | | | | | | | -0.04 0.01 0.04 0.01 -0.02 | 0.03 |
| | | | | | | | -0.04 -0.01 0.07 0.00 -0.03 | 0.04 |
| | | | | | | | 0.01 0.04 -0.03 -0.07 0.05 | 0.05 |

WEIGHTED MEAN COORDINATES OF S -1.18103 3.09650  SLOPE OF AXIS 920.8 SECONDS
INCREMENTS 0.00000 -0.00000  ITERATION 2
HT. BY EXTENSION OF AXIS EQUATION 3.09648
SEC.SQD.W = 1.000020  TAN.W = 0.004464

CURVE CONSTANTS R*R*-0.3646 + R*-0.0004 + 166.192 = P.D.
SHIFT TO ORIGIN OF SYMMETRY 0.001

| CALCED F | TAN.Q RADIAL | DH(MM) | CALCED F | TAN.Q RADIAL | DH(MM) | CALCED F | TAN.Q RADIAL | DH(MM) | CALCED F | TAN.Q RADIAL | DH(MM) | CALCED F | TAN.Q RADIAL | DH(MM) |
|---|---|---|---|---|---|---|---|---|---|---|---|---|---|---|
| 165.795 | 0.592 | 0.19 | 165.798 | 0.591 | 0.20 | 165.852 | 0.588 | -0.04 | 165.848 | 0.587 | -0.02 | 165.875 | 0.587 | -0.22 |
| | 98.281 | | | 98.177 | | | 97.693 | | | 97.540 | | | 97.390 | |
| 165.884 | 0.544 | 0.04 | 165.936 | 0.542 | -0.17 | 165.943 | 0.541 | -0.22 | 165.907 | 0.541 | -0.05 | 165.926 | 0.540 | -0.19 |
| | 90.351 | | | 90.041 | | | 89.792 | | | 89.832 | | | 89.655 | |
| 165.938 | 0.487 | 0.05 | 165.974 | 0.485 | -0.07 | 165.977 | 0.483 | -0.09 | 165.962 | 0.482 | -0.02 | 165.962 | 0.481 | -0.01 |
| | 80.799 | | | 80.590 | | | 80.205 | | | 79.981 | | | 79.903 | |
| 166.007 | 0.395 | 0.08 | 166.025 | 0.395 | 0.03 | 166.043 | 0.392 | -0.02 | 166.031 | 0.392 | 0.03 | 166.007 | 0.391 | 0.16 |
| | 65.636 | | | 65.515 | | | 65.136 | | | 65.039 | | | 64.889 | |
| 166.083 | 0.303 | 0.04 | 166.098 | 0.302 | 0.01 | 166.103 | 0.302 | -0.01 | 166.069 | 0.301 | 0.11 | 166.069 | 0.301 | 0.12 |
| | 50.324 | | | 50.064 | | | 50.099 | | | 49.914 | | | 49.991 | |
| 166.193 | 0.184 | -0.04 | 166.175 | 0.181 | -0.02 | 166.184 | 0.182 | -0.04 | 166.148 | 0.182 | 0.02 | 166.137 | 0.181 | 0.05 |
| | 30.481 | | | 30.027 | | | 30.149 | | | 30.164 | | | 30.116 | |
| 166.217 | -0.181 | 0.07 | 166.162 | -0.182 | 0.00 | 166.151 | -0.182 | -0.01 | 166.142 | -0.182 | -0.04 | 166.136 | -0.181 | -0.06 |
| | -30.002 | | | -30.237 | | | -30.230 | | | -30.157 | | | -30.018 | |
| 166.143 | -0.299 | 0.08 | 166.099 | -0.300 | -0.01 | 166.078 | -0.301 | -0.06 | 166.082 | -0.300 | -0.07 | 166.078 | -0.300 | -0.09 |
| | -49.615 | | | -49.833 | | | -49.922 | | | -49.840 | | | -49.824 | |
| 166.085 | -0.393 | 0.13 | 166.032 | -0.395 | -0.01 | 166.053 | -0.392 | 0.05 | 166.020 | -0.391 | -0.08 | 166.025 | -0.390 | -0.07 |
| | -65.217 | | | -65.617 | | | -65.157 | | | -64.901 | | | -64.754 | |
| 166.026 | -0.481 | 0.23 | 165.943 | -0.484 | -0.05 | 165.974 | -0.482 | 0.07 | 165.960 | -0.481 | 0.00 | 165.971 | -0.481 | 0.07 |
| | -79.845 | | | -80.337 | | | -80.045 | | | -79.895 | | | -79.881 | |
| 165.910 | -0.542 | 0.05 | 165.905 | -0.542 | 0.03 | 165.896 | -0.541 | -0.01 | 165.904 | -0.540 | 0.03 | 165.903 | -0.540 | 0.02 |
| | -90.028 | | | -89.906 | | | -89.871 | | | -89.618 | | | -89.613 | |
| 165.827 | -0.590 | -0.07 | 165.807 | -0.589 | -0.18 | 165.818 | -0.588 | -0.14 | 165.829 | -0.586 | -0.11 | 165.851 | -0.587 | 0.03 |
| | -97.904 | | | -97.747 | | | -97.653 | | | -97.364 | | | -97.384 | |

STD. DEVIATION OF CURVE ACROSS ONE DIAGONAL 0.10 MM.

CURVE VALUES , INTERPOLATED LINE POINTS AND TARGET HEIGHTS

| P.D. | TAN.Q | LINE | TARGET | LINE | TARGET | LINE | TARGET | LINE | TARGET | LINE | TARGET |
|---|---|---|---|---|---|---|---|---|---|---|---|
| 165.843 | 0.590 | 3.79031 | 3.7936 | 3.87902 | 3.8819 | 3.99923 | 3.9981 | 4.17394 | 4.1709 | 4.35588 | 4.3504 |
| 165.897 | 0.542 | 3.73415 | 3.7371 | 3.81545 | 3.8163 | 3.92611 | 3.9248 | 4.08682 | 4.0857 | 4.25409 | 4.2505 |
| 165.957 | 0.484 | 3.66574 | 3.6693 | 3.73835 | 3.7407 | 3.83713 | 3.8363 | 3.98046 | 3.9770 | 4.12985 | 4.1248 |
| 166.037 | 0.393 | 3.55902 | 3.5618 | 3.61803 | 3.6202 | 3.69819 | 3.6972 | 3.81454 | 3.8123 | 3.93595 | 3.9314 |
| 166.101 | 0.301 | 3.45156 | 3.4533 | 3.49681 | 3.4967 | 3.55831 | 3.5585 | 3.64761 | 3.6458 | 3.74062 | 3.7395 |
| 166.159 | 0.182 | 3.31072 | 3.3128 | 3.33798 | 3.3367 | 3.37495 | 3.3746 | 3.42866 | 3.4284 | 3.48462 | 3.4837 |
| 166.159 | -0.181 | 2.88420 | 2.8851 | 2.85565 | 2.8558 | 2.81933 | 2.8184 | 2.76521 | 2.7649 | 2.70877 | 2.7102 |
| 166.102 | -0.300 | 2.74484 | 2.7462 | 2.69941 | 2.6992 | 2.63776 | 2.6367 | 2.54847 | 2.5481 | 2.45532 | 2.4551 |
| 166.038 | -0.392 | 2.63622 | 2.6356 | 2.57680 | 2.5729 | 2.49636 | 2.4961 | 2.37949 | 2.3820 | 2.25777 | 2.2626 |
| 165.959 | -0.482 | 2.53070 | 2.5318 | 2.45759 | 2.4549 | 2.35881 | 2.3584 | 2.21534 | 2.2165 | 2.06586 | 2.0674 |
| 165.899 | -0.541 | 2.46076 | 2.4592 | 2.37899 | 2.3782 | 2.26789 | 2.2673 | 2.10692 | 2.1090 | 1.93900 | 1.9415 |
| 165.845 | -0.589 | 2.40508 | 2.4030 | 2.31509 | 2.3150 | 2.19539 | 2.1950 | 2.02038 | 2.0231 | 1.83798 | 1.8409 |

COMPOSITE CURVE CONSTANTS R*R*-0.3583 + 166.187 = P.D.

CURVE VALUES FOR PLOTTING

| | | | | | | | | | | | |
|---|---|---|---|---|---|---|---|---|---|---|---|
| 0.05 | 166.185 | 0.10 | 166.177 | 0.15 | 166.165 | 0.20 | 166.148 | 0.25 | 166.125 | 0.30 | 166.098 | 0.35 | 166.066 |
| 0.40 | 166.029 | 0.45 | 165.987 | 0.50 | 165.940 | 0.55 | 165.888 | 0.60 | 165.832 | 0.65 | 165.770 | 0.70 | 165.703 |

STD. DEVIATION OF COMPOSITE CURVE 0.10 MM. HEIGHT AT THE WIRES

CURVE CONSTANTS R*R*-0.3521 + R*-0.0002 + 166.182 = P.D.
SHIFT TO ORIGIN OF SYMMETRY 0.000

| CALCED F | TAN.Q RADIAL | DH(MM) | CALCED F | TAN.Q RADIAL | DH(MM) | CALCED F | TAN.Q RADIAL | DH(MM) | CALCED F | TAN.Q RADIAL | DH(MM) | CALCED F | TAN.Q RADIAL | DH(MM) |
|---|---|---|---|---|---|---|---|---|---|---|---|---|---|---|
| 165.778 | 0.600 | 0.23 | 165.755 | 0.599 | 0.38 | 165.823 | 0.596 | 0.08 | 165.830 | 0.595 | 0.06 | 165.856 | 0.594 | -0.12 |
| | 99.616 | | | 99.451 | | | 98.926 | | | 98.730 | | | 98.542 | |
| 165.884 | 0.552 | 0.01 | 165.938 | 0.550 | -0.22 | 165.951 | 0.548 | -0.30 | 165.904 | 0.548 | -0.08 | 165.912 | 0.547 | -0.14 |
| | 91.631 | | | 91.279 | | | 90.988 | | | 90.977 | | | 90.759 | |
| 165.932 | 0.494 | 0.05 | 165.976 | 0.492 | -0.12 | 165.985 | 0.490 | -0.16 | 165.963 | 0.488 | -0.06 | 165.952 | 0.488 | -0.01 |
| | 82.002 | | | 81.758 | | | 81.334 | | | 81.064 | | | 80.950 | |
| 166.003 | 0.402 | 0.06 | 166.018 | 0.401 | 0.02 | 166.050 | 0.399 | -0.08 | 166.036 | 0.398 | -0.03 | 166.005 | 0.397 | 0.13 |
| | 66.733 | | | 66.578 | | | 66.169 | | | 66.036 | | | 65.856 | |
| 166.103 | 0.309 | -0.03 | 166.117 | 0.307 | -0.07 | 166.119 | 0.307 | -0.08 | 166.070 | 0.306 | 0.07 | 166.057 | 0.306 | 0.13 |
| | 51.332 | | | 51.044 | | | 51.051 | | | 50.832 | | | 50.884 | |
| 166.147 | 0.189 | 0.00 | 166.132 | 0.186 | 0.02 | 166.178 | 0.187 | -0.05 | 166.127 | 0.187 | 0.04 | 166.092 | 0.186 | 0.13 |
| | 31.367 | | | 30.893 | | | 31.003 | | | 30.995 | | | 30.927 | |
| 166.202 | -0.177 | 0.06 | 166.134 | -0.178 | -0.02 | 166.148 | -0.178 | -0.01 | 166.097 | -0.177 | -0.11 | 166.099 | -0.176 | -0.12 |
| | -29.307 | | | -29.536 | | | -29.529 | | | -29.444 | | | -29.303 | |
| 166.135 | -0.295 | 0.08 | 166.096 | -0.296 | -0.00 | 166.079 | -0.297 | -0.05 | 166.082 | -0.296 | -0.05 | 166.093 | -0.296 | -0.01 |
| | -48.946 | | | -49.154 | | | -49.232 | | | -49.137 | | | -49.116 | |
| 166.100 | -0.389 | 0.18 | 166.050 | -0.391 | 0.05 | 166.061 | -0.388 | 0.09 | 166.032 | -0.387 | -0.02 | 166.043 | -0.386 | 0.02 |
| | -64.562 | | | -64.946 | | | -64.464 | | | -64.191 | | | -64.032 | |
| 166.029 | -0.477 | 0.23 | 165.948 | -0.480 | -0.04 | 165.977 | -0.478 | 0.07 | 165.958 | -0.477 | -0.02 | 165.983 | -0.477 | 0.13 |
| | -79.180 | | | -79.650 | | | -79.333 | | | -79.156 | | | -79.130 | |
| 165.905 | -0.538 | 0.02 | 165.890 | -0.537 | -0.05 | 165.891 | -0.537 | -0.06 | 165.910 | -0.535 | 0.04 | 165.914 | -0.535 | 0.07 |
| | -89.349 | | | -89.195 | | | -89.138 | | | -88.862 | | | -88.838 | |
| 165.839 | -0.586 | -0.04 | 165.811 | -0.584 | -0.19 | 165.822 | -0.584 | -0.16 | 165.830 | -0.582 | -0.15 | 165.854 | -0.582 | -0.00 |
| | -97.223 | | | -97.032 | | | -96.907 | | | -96.585 | | | -96.582 | |

STD. DEVIATION OF CURVE ACROSS ONE DIAGONAL 0.11 MM.

CURVE VALUES , INTERPOLATED LINE POINTS AND TARGET HEIGHTS

| P.D. | TAN.Q | LINE | TARGET | LINE | TARGET | LINE | TARGET | LINE | TARGET | LINE | TARGET |
|---|---|---|---|---|---|---|---|---|---|---|---|
| 165.837 | 0.597 | 3.78965 | 3.7936 | 3.87875 | 3.8819 | 3.99926 | 3.9981 | 4.17443 | 4.1709 | 4.35693 | 4.3504 |
| 165.890 | 0.549 | 3.73356 | 3.7371 | 3.81509 | 3.8163 | 3.92607 | 3.9248 | 4.08734 | 4.0857 | 4.25520 | 4.2505 |
| 165.949 | 0.491 | 3.66523 | 3.6693 | 3.73803 | 3.7407 | 3.83710 | 3.8363 | 3.98091 | 3.9770 | 4.13083 | 4.1248 |
| 166.027 | 0.399 | 3.55858 | 3.5618 | 3.61779 | 3.6202 | 3.69817 | 3.6972 | 3.81491 | 3.8123 | 3.93675 | 3.9314 |
| 166.090 | 0.307 | 3.45117 | 3.4533 | 3.49658 | 3.4967 | 3.55829 | 3.5585 | 3.64795 | 3.6458 | 3.74135 | 3.7395 |
| 166.148 | 0.187 | 3.31048 | 3.3128 | 3.33784 | 3.3367 | 3.37491 | 3.3746 | 3.42886 | 3.4284 | 3.48511 | 3.4837 |
| 166.152 | -0.177 | 2.88427 | 2.8851 | 2.85670 | 2.8558 | 2.81937 | 2.8184 | 2.76512 | 2.7649 | 2.70865 | 2.7102 |
| 166.097 | -0.296 | 2.74499 | 2.7462 | 2.69953 | 2.6992 | 2.63776 | 2.6367 | 2.54832 | 2.5481 | 2.45509 | 2.4551 |
| 166.036 | -0.388 | 2.63647 | 2.6356 | 2.57695 | 2.5729 | 2.49633 | 2.4961 | 2.37927 | 2.3820 | 2.25735 | 2.2626 |
| 165.961 | -0.478 | 2.53102 | 2.5318 | 2.45778 | 2.4549 | 2.35880 | 2.3584 | 2.21502 | 2.2165 | 2.06534 | 2.0674 |
| 165.903 | -0.537 | 2.46113 | 2.4592 | 2.37915 | 2.3782 | 2.26787 | 2.2673 | 2.10663 | 2.1090 | 1.93842 | 1.9415 |
| 165.852 | -0.584 | 2.40554 | 2.4030 | 2.31633 | 2.3150 | 2.19538 | 2.1950 | 2.02000 | 2.0231 | 1.83723 | 1.8409 |

CURVE CONSTANTS R*R*-0.3490 + R*-0.0004 + 166.383 = P.D.
SHIFT TO ORIGIN OF SYMMETRY 0.001

| CALCED F | TAN.Q RADIAL | DH(MM) | CALCED F | TAN.Q RADIAL | DH(MM) | CALCED F | TAN.Q RADIAL | DH(MM) | CALCED F | TAN.Q RADIAL | DH(MM) | CALCED F | TAN.Q RADIAL | DH(MM) |
|---|---|---|---|---|---|---|---|---|---|---|---|---|---|---|
| 166.026 | 0.584 | 0.12 | 166.022 | 0.583 | 0.15 | 166.066 | 0.580 | -0.04 | 166.053 | 0.579 | 0.04 | 166.074 | 0.579 | -0.10 |
| | 97.002 | | | 96.919 | | | 96.458 | | | 96.327 | | | 96.193 | |
| 166.098 | 0.536 | 0.03 | 166.140 | 0.534 | -0.14 | 166.151 | 0.533 | -0.21 | 166.111 | 0.533 | -0.01 | 166.114 | 0.532 | -0.03 |
| | 89.138 | | | 88.845 | | | 88.620 | | | 88.679 | | | 88.510 | |
| 166.139 | 0.479 | 0.08 | 166.175 | 0.478 | -0.05 | 166.181 | 0.476 | -0.07 | 166.155 | 0.475 | 0.06 | 166.162 | 0.474 | 0.03 |
| | 79.666 | | | 79.473 | | | 79.107 | | | 78.895 | | | 78.832 | |
| 166.200 | 0.389 | 0.10 | 166.229 | 0.388 | 0.03 | 166.232 | 0.386 | 0.03 | 166.225 | 0.385 | 0.06 | 166.216 | 0.384 | 0.12 |
| | 64.626 | | | 64.516 | | | 64.140 | | | 64.052 | | | 63.913 | |
| 166.303 | 0.297 | -0.01 | 166.334 | 0.296 | -0.08 | 166.336 | 0.296 | -0.10 | 166.280 | 0.295 | 0.06 | 166.279 | 0.295 | 0.08 |
| | 49.435 | | | 49.179 | | | 49.210 | | | 49.017 | | | 49.091 | |
| 166.340 | 0.179 | 0.02 | 166.366 | 0.176 | -0.02 | 166.420 | 0.177 | -0.11 | 166.376 | 0.177 | -0.04 | 166.365 | 0.176 | -0.03 |
| | 29.700 | | | 29.243 | | | 29.358 | | | 29.357 | | | 29.298 | |
| 166.353 | -0.184 | 0.00 | 166.320 | -0.185 | -0.05 | 166.347 | -0.186 | -0.01 | 166.352 | -0.186 | 0.00 | 166.290 | -0.185 | -0.15 |
| | -30.541 | | | -30.826 | | | -30.875 | | | -30.856 | | | -30.745 | |
| 166.325 | -0.302 | 0.06 | 166.290 | -0.303 | -0.01 | 166.271 | -0.304 | -0.06 | 166.274 | -0.304 | -0.07 | 166.276 | -0.304 | -0.07 |
| | -50.139 | | | -50.417 | | | -50.567 | | | -50.548 | | | -50.581 | |
| 166.274 | -0.395 | 0.12 | 166.235 | -0.398 | 0.01 | 166.239 | -0.396 | 0.02 | 166.206 | -0.395 | -0.12 | 166.222 | -0.394 | -0.06 |
| | -65.743 | | | -66.215 | | | -65.817 | | | -65.633 | | | -65.544 | |
| 166.210 | -0.484 | 0.18 | 166.140 | -0.487 | -0.06 | 166.168 | -0.486 | 0.05 | 166.155 | -0.485 | -0.01 | 166.183 | -0.486 | 0.17 |
| | -80.383 | | | -80.956 | | | -80.740 | | | -80.672 | | | -80.727 | |
| 166.098 | -0.545 | 0.00 | 166.098 | -0.545 | 0.00 | 166.086 | -0.545 | -0.06 | 166.115 | -0.544 | 0.10 | 166.115 | -0.544 | 0.12 |
| | -90.586 | | | -90.546 | | | -90.593 | | | -90.438 | | | -90.499 | |
| 166.036 | -0.593 | -0.04 | 166.025 | -0.592 | -0.10 | 166.042 | -0.592 | -0.02 | 166.027 | -0.591 | -0.13 | 166.058 | -0.591 | 0.09 |
| | -98.493 | | | -98.425 | | | -98.422 | | | -98.209 | | | -98.304 | |

STD. DEVIATION OF CURVE ACROSS ONE DIAGONAL 0.08 MM.

CURVE VALUES , INTERPOLATED LINE POINTS AND TARGET HEIGHTS

| P.D. | TAN.Q | LINE | TARGET | LINE | TARGET | LINE | TARGET | LINE | TARGET | LINE | TARGET |
|---|---|---|---|---|---|---|---|---|---|---|---|
| 166.058 | 0.582 | 3.79058 | 3.7936 | 3.87917 | 3.8819 | 3.99923 | 3.9981 | 4.17370 | 4.1709 | 4.35541 | 4.3504 |
| 166.108 | 0.534 | 3.73439 | 3.7371 | 3.81560 | 3.8163 | 3.92609 | 3.9248 | 4.08658 | 4.0857 | 4.25372 | 4.2505 |
| 166.164 | 0.477 | 3.66594 | 3.6693 | 3.73845 | 3.7407 | 3.83711 | 3.8363 | 3.98032 | 3.9770 | 4.12949 | 4.1248 |
| 166.239 | 0.386 | 3.55911 | 3.5618 | 3.61806 | 3.6202 | 3.69821 | 3.6972 | 3.81448 | 3.8123 | 3.93575 | 3.9314 |
| 166.299 | 0.296 | 3.45153 | 3.4533 | 3.49675 | 3.4967 | 3.55828 | 3.5585 | 3.64767 | 3.6458 | 3.74073 | 3.7395 |
| 166.353 | 0.177 | 3.31060 | 3.3128 | 3.33789 | 3.3367 | 3.37491 | 3.3746 | 3.42878 | 3.4284 | 3.48490 | 3.4837 |
| 166.351 | -0.185 | 2.88349 | 2.8851 | 2.85525 | 2.8558 | 2.81938 | 2.8184 | 2.76586 | 2.7649 | 2.70990 | 2.7102 |
| 166.295 | -0.303 | 2.74399 | 2.7462 | 2.69893 | 2.6992 | 2.63777 | 2.6367 | 2.54917 | 2.5481 | 2.45678 | 2.4551 |
| 166.233 | -0.396 | 2.63526 | 2.6356 | 2.57629 | 2.5729 | 2.49634 | 2.4961 | 2.38027 | 2.3820 | 2.25943 | 2.2626 |
| 166.156 | -0.486 | 2.52959 | 2.5318 | 2.45693 | 2.4549 | 2.35881 | 2.3584 | 2.21624 | 2.2165 | 2.06780 | 2.0674 |
| 166.098 | -0.545 | 2.45958 | 2.4592 | 2.37831 | 2.3782 | 2.26786 | 2.2673 | 2.10796 | 2.1090 | 1.94107 | 1.9415 |
| 166.046 | -0.592 | 2.40387 | 2.4030 | 2.31543 | 2.3150 | 2.19547 | 2.1950 | 2.02133 | 2.0231 | 1.84005 | 1.8409 |

CURVE CONSTANTS R*R*-0.2982 + R*-0.0003 + 161.286 = P.D.
SHIFT TO ORIGIN OF SYMMETRY 0.000

| CALCED F | TAN.Q RADIAL | DH(MM) | CALCED F | TAN.Q RADIAL | DH(MM) | CALCED F | TAN.Q RADIAL | DH(MM) |
|---|---|---|---|---|---|---|---|---|
| 161.000 | 0.523 | -0.10 | 161.022 | 0.622 | -0.29 | 160.986 | 0.622 | 0.00 |
| | 100.374 | | | 100.282 | | | 100.186 | |
| 161.048 | 0.574 | -0.11 | 161.036 | 0.573 | -0.04 | 161.037 | 0.573 | -0.05 |
| | 92.511 | | | 92.391 | | | 92.296 | |
| 161.086 | 0.510 | -0.01 | 161.086 | 0.509 | -0.00 | 161.088 | 0.509 | -0.02 |
| | 82.117 | | | 82.012 | | | 82.034 | |
| 161.139 | 0.417 | 0.05 | 161.154 | 0.416 | -0.02 | 161.135 | 0.416 | 0.10 |
| | 67.260 | | | 67.102 | | | 67.084 | |
| 161.173 | 0.322 | 0.12 | 161.199 | 0.322 | 0.03 | 161.204 | 0.322 | 0.01 |
| | 51.855 | | | 51.864 | | | 51.847 | |
| 161.212 | 0.198 | 0.10 | 161.220 | 0.198 | 0.09 | 161.229 | 0.197 | 0.08 |
| | 31.927 | | | 31.881 | | | 31.814 | |
| 161.326 | -0.179 | 0.13 | 161.259 | -0.177 | -0.01 | 161.280 | -0.177 | 0.05 |
| | -28.766 | | | -28.570 | | | -28.541 | |
| 161.257 | -0.301 | 0.14 | 161.248 | -0.300 | 0.12 | 161.252 | -0.299 | 0.16 |
| | -48.526 | | | -48.335 | | | -48.246 | |
| 161.180 | -0.394 | 0.07 | 161.194 | -0.393 | 0.14 | 161.170 | -0.393 | 0.02 |
| | -63.520 | | | -63.359 | | | -63.272 | |
| 161.130 | -0.485 | 0.14 | 161.110 | -0.484 | 0.03 | 161.120 | -0.484 | 0.11 |
| | -78.134 | | | -77.973 | | | -77.924 | |
| 161.049 | -0.548 | -0.03 | 161.027 | -0.547 | -0.19 | 161.052 | -0.546 | -0.03 |
| | -88.268 | | | -88.158 | | | -87.976 | |
| 160.977 | -0.596 | -0.23 | 160.988 | -0.594 | -0.19 | 160.984 | -0.593 | -0.26 |
| | -95.970 | | | -95.687 | | | -95.583 | |

STD. DEVIATION OF CURVE ACROSS ONE DIAGONAL 0.12 MM.

| CALCED F | TAN.Q RADIAL | DH(MM) | CALCED F | TAN.Q RADIAL | DH(MM) |
|---|---|---|---|---|---|
| 161.004 | 0.621 | -0.19 | 161.005 | 0.620 | -0.22 |
| | 100.080 | | | 99.943 | |
| 161.040 | 0.572 | -0.08 | 161.039 | 0.571 | -0.07 |
| | 92.248 | | | 92.024 | |
| 161.085 | 0.508 | 0.01 | 161.082 | 0.507 | 0.05 |
| | 81.919 | | | 81.742 | |
| 161.136 | 0.416 | 0.11 | 161.148 | 0.416 | 0.03 |
| | 67.083 | | | 66.978 | |
| 161.184 | 0.321 | 0.12 | 161.207 | 0.321 | -0.01 |
| | 51.734 | | | 51.715 | |
| 161.192 | 0.197 | 0.22 | 161.230 | 0.197 | 0.10 |
| | 31.778 | | | 31.810 | |
| 161.256 | -0.176 | -0.02 | 161.283 | -0.176 | 0.07 |
| | -28.415 | | | -28.343 | |
| 161.246 | -0.299 | 0.15 | 161.232 | -0.298 | 0.09 |
| | -48.138 | | | -48.001 | |
| 161.166 | -0.392 | -0.00 | 161.181 | -0.391 | 0.11 |
| | -63.172 | | | -63.013 | |
| 161.112 | -0.482 | 0.05 | 161.117 | -0.481 | 0.10 |
| | -77.736 | | | -77.512 | |
| 161.038 | -0.545 | -0.17 | 161.039 | -0.543 | -0.20 |
| | -87.762 | | | -87.566 | |
| 160.990 | -0.592 | -0.26 | 161.003 | -0.591 | -0.16 |
| | -95.371 | | | -95.206 | |

CURVE VALUES , INTERPOLATED LINE POINTS AND TARGET HEIGHTS

| P.D. | TAN.Q | LINE | TARGET | LINE | TARGET | LINE | TARGET | LINE | TARGET | LINE | TARGET |
|---|---|---|---|---|---|---|---|---|---|---|---|
| 160.986 | 0.522 | 4.64830 | 4.6505 | 4.81632 | 4.8177 | 4.99811 | 4.9983 | 5.24608 | 5.2445 | 5.55332 | 5.5487 |
| 161.032 | 0.573 | 4.56152 | 4.5639 | 4.71637 | 4.7176 | 4.88337 | 4.8834 | 5.11168 | 5.1109 | 5.39443 | 5.3890 |
| 161.085 | 0.509 | 4.44783 | 4.4495 | 4.58500 | 4.5856 | 4.73300 | 4.7340 | 4.93538 | 4.9346 | 5.18599 | 5.1815 |
| 161.151 | 0.416 | 4.28405 | 4.2858 | 4.39579 | 4.3958 | 4.51655 | 4.5163 | 4.68151 | 4.6812 | 4.88569 | 4.8832 |
| 161.206 | 0.321 | 4.11533 | 4.1159 | 4.20092 | 4.2017 | 4.29336 | 4.2940 | 4.41988 | 4.4187 | 4.57628 | 4.5745 |
| 161.255 | 0.197 | 3.89476 | 3.8957 | 3.94630 | 3.9468 | 4.00191 | 4.0015 | 4.07810 | 4.0770 | 4.17215 | 4.1715 |
| 161.262 | -0.177 | 3.22467 | 3.2220 | 3.17235 | 3.1718 | 3.11611 | 3.1159 | 3.03906 | 3.0410 | 2.94384 | 2.9476 |
| 161.216 | -0.299 | 3.00440 | 3.0013 | 2.91811 | 2.9170 | 2.82505 | 2.8251 | 2.69777 | 2.6997 | 2.54011 | 2.5452 |
| 161.167 | -0.393 | 2.83603 | 2.8332 | 2.72379 | 2.7226 | 2.60247 | 2.6024 | 2.43675 | 2.4384 | 2.23168 | 2.2369 |
| 161.105 | -0.483 | 2.67212 | 2.6690 | 2.53432 | 2.5328 | 2.38581 | 2.3848 | 2.18261 | 2.1847 | 1.93112 | 1.9382 |
| 161.055 | -0.546 | 2.55822 | 2.5546 | 2.40275 | 2.4000 | 2.23535 | 2.2349 | 2.00609 | 2.0093 | 1.72237 | 1.7302 |
| 161.014 | -0.594 | 2.47198 | 2.4674 | 2.30341 | 2.3018 | 2.12139 | 2.1211 | 1.87264 | 1.8760 | 1.56473 | 1.5721 |

CURVE CONSTANTS R*R*-0.2832 + R* 0.0002 + 161.270 = P.D.
SHIFT TO ORIGIN OF SYMMETRY -0.000

| CALCED F | TAN.Q RADIAL | DH(MM) | CALCED F | TAN.Q RADIAL | DH(MM) | CALCED F | TAN.Q RADIAL | DH(MM) | CALCED F | TAN.Q RADIAL | DH(MM) | CALCED F | TAN.Q RADIAL | DH(MM) |
|---|---|---|---|---|---|---|---|---|---|---|---|---|---|---|
| 160.986 | 0.627 | -0.04 | 161.001 | 0.627 | -0.15 | 160.974 | 0.626 | 0.07 | 160.989 | 0.626 | -0.08 | 160.987 | 0.625 | -0.05 |
| | 101.076 | | | 100.989 | | | 100.907 | | | 100.807 | | | 100.675 | |
| 161.042 | 0.578 | -0.11 | 161.035 | 0.578 | -0.08 | 161.031 | 0.577 | -0.06 | 161.028 | 0.577 | -0.03 | 161.028 | 0.575 | -0.02 |
| | 93.185 | | | 93.078 | | | 92.988 | | | 92.945 | | | 92.728 | |
| 161.084 | 0.514 | -0.05 | 161.085 | 0.513 | -0.06 | 161.065 | 0.513 | 0.08 | 161.066 | 0.512 | 0.09 | 161.079 | 0.511 | -0.02 |
| | 82.754 | | | 82.660 | | | 82.679 | | | 82.574 | | | 82.412 | |
| 161.141 | 0.421 | -0.01 | 161.157 | 0.420 | -0.09 | 161.135 | 0.420 | 0.03 | 161.126 | 0.420 | 0.10 | 161.137 | 0.419 | 0.03 |
| | 67.851 | | | 67.703 | | | 67.692 | | | 67.695 | | | 67.597 | |
| 161.174 | 0.325 | 0.06 | 161.200 | 0.325 | -0.03 | 161.183 | 0.325 | 0.04 | 161.181 | 0.325 | 0.06 | 161.175 | 0.324 | 0.11 |
| | 52.406 | | | 52.425 | | | 52.409 | | | 52.310 | | | 52.289 | |
| 161.234 | 0.201 | 0.01 | 161.248 | 0.201 | -0.02 | 161.222 | 0.201 | 0.05 | 161.179 | 0.201 | 0.21 | 161.204 | 0.201 | 0.15 |
| | 32.446 | | | 32.411 | | | 32.345 | | | 32.316 | | | 32.353 | |
| 161.262 | -0.175 | 0.03 | 161.219 | -0.174 | -0.05 | 161.280 | -0.174 | 0.08 | 161.261 | -0.173 | 0.04 | 161.277 | -0.172 | 0.10 |
| | -28.243 | | | -28.042 | | | -28.012 | | | -27.879 | | | -27.798 | |
| 161.210 | -0.298 | 0.02 | 161.208 | -0.296 | 0.01 | 161.208 | -0.296 | 0.01 | 161.218 | -0.295 | 0.07 | 161.231 | -0.294 | 0.15 |
| | -47.967 | | | -47.769 | | | -47.671 | | | -47.560 | | | -47.424 | |
| 161.172 | -0.391 | 0.06 | 161.191 | -0.389 | 0.16 | 161.166 | -0.389 | 0.04 | 161.164 | -0.388 | 0.04 | 161.173 | -0.387 | 0.11 |
| | -62.935 | | | -62.767 | | | -62.672 | | | -62.565 | | | -62.397 | |
| 161.109 | -0.481 | 0.05 | 161.099 | -0.480 | -0.00 | 161.105 | -0.480 | 0.03 | 161.103 | -0.478 | 0.02 | 161.113 | -0.477 | 0.11 |
| | -77.497 | | | -77.332 | | | -77.273 | | | -77.081 | | | -76.853 | |
| 161.046 | -0.544 | -0.04 | 161.019 | -0.543 | -0.24 | 161.055 | -0.542 | 0.01 | 161.057 | -0.540 | 0.03 | 161.035 | -0.539 | -0.23 |
| | -87.603 | | | -87.481 | | | -87.298 | | | -87.086 | | | -86.871 | |
| 160.998 | -0.591 | -0.09 | 160.994 | -0.589 | -0.15 | 160.994 | -0.589 | -0.18 | 161.008 | -0.587 | -0.07 | 161.017 | -0.586 | 0.00 |
| | -95.288 | | | -94.988 | | | -94.879 | | | -94.665 | | | -94.491 | |

STD. DEVIATION OF CURVE ACROSS ONE DIAGONAL 0.09 MM.

CURVE VALUES , INTERPOLATED LINE POINTS AND TARGET HEIGHTS

| P.D. | TAN.Q | LINE | TARGET | LINE | TARGET | LINE | TARGET | LINE | TARGET | LINE | TARGET |
|---|---|---|---|---|---|---|---|---|---|---|---|
| 160.982 | 0.627 | 4.64848 | 4.6505 | 4.81645 | 4.8177 | 4.99807 | 4.9983 | 5.24592 | 5.2445 | 5.55302 | 5.5487 |
| 161.025 | 0.577 | 4.56171 | 4.5639 | 4.71642 | 4.7176 | 4.88335 | 4.8834 | 5.11157 | 5.1109 | 5.39414 | 5.3890 |
| 161.076 | 0.513 | 4.44799 | 4.4495 | 4.58504 | 4.5856 | 4.73309 | 4.7340 | 4.93531 | 4.9346 | 5.18559 | 5.1815 |
| 161.140 | 0.420 | 4.28423 | 4.2858 | 4.39585 | 4.3958 | 4.51653 | 4.5163 | 4.68141 | 4.6812 | 4.88543 | 4.8832 |
| 161.192 | 0.325 | 4.11548 | 4.1159 | 4.20097 | 4.2017 | 4.29340 | 4.2940 | 4.41969 | 4.4187 | 4.57609 | 4.5745 |
| 161.240 | 0.201 | 3.89491 | 3.8957 | 3.94633 | 3.9468 | 4.00193 | 4.0015 | 4.07800 | 4.0770 | 4.17193 | 4.1715 |
| 161.247 | -0.174 | 3.22477 | 3.2220 | 3.17241 | 3.1718 | 3.11615 | 3.1159 | 3.03900 | 3.0410 | 2.94357 | 2.9476 |
| 161.205 | -0.296 | 3.00454 | 3.0013 | 2.91813 | 2.9170 | 2.82499 | 2.8251 | 2.69765 | 2.6997 | 2.53998 | 2.5452 |
| 161.158 | -0.389 | 2.83621 | 2.8332 | 2.72390 | 2.7226 | 2.60247 | 2.6024 | 2.43662 | 2.4384 | 2.23133 | 2.2369 |
| 161.101 | -0.479 | 2.67227 | 2.6690 | 2.53442 | 2.5328 | 2.38578 | 2.3848 | 2.18250 | 2.1847 | 1.93088 | 1.9382 |
| 161.054 | -0.542 | 2.55838 | 2.5546 | 2.40273 | 2.4000 | 2.23535 | 2.2349 | 2.00612 | 2.0093 | 1.72199 | 1.7302 |
| 161.014 | -0.589 | 2.47221 | 2.4674 | 2.30344 | 2.3018 | 2.12135 | 2.1211 | 1.87254 | 1.8760 | 1.56441 | 1.5721 |

COMPOSITE CURVE CONSTANTS R*R*-0.2907 + 161.278 = P.D.

CURVE VALUES FOR PLOTTING

| | | | | | | | | | | | |
|---|---|---|---|---|---|---|---|---|---|---|---|
| 0.05 | 161.276 | 0.10 | 161.270 | 0.15 | 161.261 | 0.20 | 161.247 | 0.25 | 161.230 | 0.30 | 161.210 | 0.35 | 161.185 |
| 0.40 | 161.157 | 0.45 | 161.125 | 0.50 | 161.089 | 0.55 | 161.049 | 0.60 | 161.006 | 0.65 | 160.959 | 0.70 | 160.908 |

STD. DEVIATION OF COMPOSITE CURVE 0.11 MM. HEIGHT AT THE WIRES

CURVE CONSTANTS R*R*-0.2780 + R* 0.0001 + 161.455 = P.D.
SHIFT TO ORIGIN OF SYMMETRY -0.000

| CALCED F | TAN.Q RADIAL | DH(MM) | CALCED F | TAN.Q RADIAL | DH(MM) | CALCED F | TAN.Q RADIAL | DH(MM) | CALCED F | TAN.Q RADIAL | DH(MM) | CALCED F | TAN.Q RADIAL | DH(MM) |
|---|---|---|---|---|---|---|---|---|---|---|---|---|---|---|
| 161.187 | 0.612 | -0.02 | 161.191 | 0.611 | -0.05 | 161.166 | 0.611 | 0.18 | 161.185 | 0.610 | 0.01 | 161.183 | 0.610 | 0.05 |
| | 98.719 | | | 98.636 | | | 98.564 | | | 98.476 | | | 98.353 | |
| 161.248 | 0.564 | -0.14 | 161.226 | 0.563 | -0.00 | 161.231 | 0.562 | -0.04 | 161.235 | 0.562 | -0.08 | 161.221 | 0.561 | 0.03 |
| | 90.921 | | | 90.816 | | | 90.740 | | | 90.710 | | | 90.495 | |
| 161.283 | 0.500 | -0.05 | 161.281 | 0.499 | -0.04 | 161.278 | 0.499 | -0.02 | 161.260 | 0.499 | 0.13 | 161.275 | 0.498 | 0.01 |
| | 80.592 | | | 80.507 | | | 80.543 | | | 80.438 | | | 80.286 | |
| 161.336 | 0.408 | -0.01 | 161.363 | 0.407 | -0.15 | 161.337 | 0.407 | -0.01 | 161.328 | 0.407 | 0.05 | 161.326 | 0.407 | 0.08 |
| | 65.814 | | | 65.682 | | | 65.678 | | | 65.690 | | | 65.595 | |
| 161.392 | 0.313 | -0.03 | 161.400 | 0.313 | -0.06 | 161.406 | 0.313 | -0.10 | 161.374 | 0.312 | 0.06 | 161.387 | 0.312 | -0.01 |
| | 50.477 | | | 50.501 | | | 50.501 | | | 50.402 | | | 50.395 | |
| 161.411 | 0.190 | 0.04 | 161.441 | 0.189 | -0.03 | 161.413 | 0.189 | 0.05 | 161.366 | 0.189 | 0.21 | 161.382 | 0.189 | 0.18 |
| | 30.590 | | | 30.569 | | | 30.512 | | | 30.492 | | | 30.535 | |
| 161.491 | -0.187 | 0.13 | 161.446 | -0.186 | 0.04 | 161.455 | -0.185 | 0.07 | 161.447 | -0.185 | 0.05 | 161.475 | -0.184 | 0.17 |
| | -30.174 | | | -29.959 | | | -29.910 | | | -29.768 | | | -29.680 | |
| 161.372 | -0.310 | -0.05 | 161.364 | -0.309 | -0.09 | 161.377 | -0.308 | -0.04 | 161.374 | -0.307 | -0.07 | 161.374 | -0.306 | -0.08 |
| | -50.011 | | | -49.797 | | | -49.692 | | | -49.566 | | | -49.416 | |
| 161.319 | -0.404 | -0.08 | 161.333 | -0.402 | -0.03 | 161.319 | -0.402 | -0.11 | 161.319 | -0.401 | -0.14 | 161.330 | -0.400 | -0.07 |
| | -65.103 | | | -64.919 | | | -64.817 | | | -64.699 | | | -64.521 | |
| 161.297 | -0.495 | 0.10 | 161.291 | -0.494 | 0.08 | 161.285 | -0.493 | 0.04 | 161.296 | -0.492 | 0.14 | 161.310 | -0.491 | 0.29 |
| | -79.840 | | | -79.662 | | | -79.586 | | | -79.387 | | | -79.149 | |
| 161.233 | -0.558 | 0.02 | 161.212 | -0.557 | -0.13 | 161.237 | -0.556 | 0.05 | 161.233 | -0.555 | 0.00 | 161.228 | -0.553 | -0.06 |
| | -90.072 | | | -89.939 | | | -89.737 | | | -89.507 | | | -89.289 | |
| 161.170 | -0.607 | -0.13 | 161.176 | -0.605 | -0.11 | 161.183 | -0.604 | -0.07 | 161.192 | -0.602 | -0.01 | 161.213 | -0.601 | 0.24 |
| | -97.854 | | | -97.542 | | | -97.425 | | | -97.194 | | | -97.015 | |

STD. DEVIATION OF CURVE ACROSS ONE DIAGONAL 0.10 MM.

CURVE VALUES , INTERPOLATED LINE POINTS AND TARGET HEIGHTS

| P.D. | TAN.Q | LINE | TARGET | LINE | TARGET | LINE | TARGET | LINE | TARGET | LINE | TARGET |
|---|---|---|---|---|---|---|---|---|---|---|---|
| 161.185 | 0.611 | 4.64863 | 4.6505 | 4.81560 | 4.8177 | 4.99809 | 4.9983 | 5.24576 | 5.2445 | 5.55268 | 5.5487 |
| 161.226 | 0.563 | 4.56186 | 4.5639 | 4.71658 | 4.7176 | 4.88335 | 4.8834 | 5.11135 | 5.1109 | 5.39389 | 5.3890 |
| 161.275 | 0.499 | 4.44819 | 4.4495 | 4.58517 | 4.5856 | 4.73298 | 4.7340 | 4.93520 | 4.9346 | 5.18529 | 5.1815 |
| 161.335 | 0.407 | 4.28445 | 4.2858 | 4.39593 | 4.3958 | 4.51650 | 4.5163 | 4.68123 | 4.6812 | 4.88516 | 4.8832 |
| 161.384 | 0.313 | 4.11566 | 4.1159 | 4.20111 | 4.2017 | 4.29333 | 4.2940 | 4.41961 | 4.4187 | 4.57572 | 4.5745 |
| 161.429 | 0.189 | 3.89514 | 3.8957 | 3.94642 | 3.9468 | 4.00190 | 4.0015 | 4.07782 | 4.0770 | 4.17159 | 4.1715 |
| 161.430 | -0.185 | 3.22506 | 3.2220 | 3.17253 | 3.1718 | 3.11607 | 3.1159 | 3.03876 | 3.0410 | 2.94316 | 2.9476 |
| 161.386 | -0.308 | 3.00480 | 3.0013 | 2.91829 | 2.9170 | 2.82504 | 2.8251 | 2.69745 | 2.6997 | 2.53948 | 2.5452 |
| 161.338 | -0.402 | 2.83644 | 2.8332 | 2.72393 | 2.7226 | 2.60248 | 2.6024 | 2.43645 | 2.4384 | 2.23097 | 2.2369 |
| 161.279 | -0.493 | 2.67251 | 2.6690 | 2.53455 | 2.5328 | 2.38570 | 2.3848 | 2.18232 | 2.1847 | 1.93053 | 1.9382 |
| 161.231 | -0.556 | 2.55865 | 2.5546 | 2.40296 | 2.4000 | 2.23532 | 2.2349 | 2.00581 | 2.0093 | 1.72163 | 1.7302 |
| 161.191 | -0.604 | 2.47239 | 2.4674 | 2.30355 | 2.3018 | 2.12138 | 2.1211 | 1.87234 | 1.8760 | 1.56411 | 1.5721 |

CURVE CONSTANTS R*R*-0.2597 + R*-0.0001 + 161.448 = P.D.
SHIFT TO ORIGIN OF SYMMETRY 0.000

| CALCED F | TAN.Q RADIAL | DH(MM) | CALCED F | TAN.Q RADIAL | DH(MM) | CALCED F | TAN.Q RADIAL | DH(MM) | CALCED F | TAN.Q RADIAL | DH(MM) | CALCED F | TAN.Q RADIAL | DH(MM) |
|---|---|---|---|---|---|---|---|---|---|---|---|---|---|---|
| 161.175 | 0.637 | -0.01 | 161.195 | 0.637 | -0.17 | 161.175 | 0.636 | 0.00 | 161.188 | 0.635 | -0.13 | 161.190 | 0.634 | -0.18 |
| | 102.813 | | | 102.704 | | | 102.604 | | | 102.481 | | | 102.332 | |
| 161.211 | 0.588 | 0.02 | 161.207 | 0.587 | 0.06 | 161.217 | 0.586 | -0.01 | 161.227 | 0.586 | -0.11 | 161.231 | 0.585 | -0.16 |
| | 94.840 | | | 94.708 | | | 94.605 | | | 94.548 | | | 94.313 | |
| 161.267 | 0.523 | -0.02 | 161.266 | 0.522 | -0.02 | 161.259 | 0.522 | 0.04 | 161.257 | 0.521 | 0.07 | 161.279 | 0.520 | -0.15 |
| | 84.331 | | | 84.210 | | | 84.215 | | | 84.087 | | | 83.910 | |
| 161.315 | 0.430 | 0.04 | 161.347 | 0.429 | -0.12 | 161.330 | 0.428 | -0.04 | 161.332 | 0.428 | -0.06 | 161.336 | 0.428 | -0.10 |
| | 69.316 | | | 69.149 | | | 69.120 | | | 69.107 | | | 68.987 | |
| 161.322 | 0.333 | 0.19 | 161.355 | 0.333 | 0.08 | 161.357 | 0.333 | 0.08 | 161.361 | 0.332 | 0.07 | 161.362 | 0.332 | 0.09 |
| | 53.770 | | | 53.767 | | | 53.737 | | | 53.619 | | | 53.582 | |
| 161.382 | 0.209 | 0.08 | 161.431 | 0.209 | -0.03 | 161.396 | 0.208 | 0.07 | 161.365 | 0.208 | 0.19 | 161.385 | 0.208 | 0.14 |
| | 33.722 | | | 33.670 | | | 33.582 | | | 33.535 | | | 33.553 | |
| 161.501 | -0.168 | 0.13 | 161.461 | -0.167 | 0.07 | 161.470 | -0.166 | 0.10 | 161.442 | -0.166 | 0.03 | 161.469 | -0.165 | 0.13 |
| | -27.058 | | | -26.881 | | | -26.861 | | | -26.746 | | | -26.684 | |
| 161.422 | -0.290 | 0.10 | 161.388 | -0.289 | -0.01 | 161.392 | -0.288 | -0.00 | 161.380 | -0.288 | -0.06 | 161.395 | -0.287 | 0.02 |
| | -46.748 | | | -46.564 | | | -46.486 | | | -46.388 | | | -46.270 | |
| 161.355 | -0.382 | 0.02 | 161.365 | -0.381 | 0.07 | 161.351 | -0.381 | 0.00 | 161.333 | -0.380 | -0.12 | 161.322 | -0.379 | -0.22 |
| | -61.662 | | | -61.514 | | | -61.442 | | | -61.348 | | | -61.190 | |
| 161.327 | -0.472 | 0.15 | 161.303 | -0.471 | 0.03 | 161.298 | -0.471 | -0.00 | 161.294 | -0.470 | -0.04 | 161.311 | -0.469 | 0.10 |
| | -76.180 | | | -76.031 | | | -75.986 | | | -75.812 | | | -75.605 | |
| 161.253 | -0.534 | -0.01 | 161.238 | -0.534 | -0.12 | 161.254 | -0.533 | -0.02 | 161.248 | -0.532 | -0.09 | 161.239 | -0.530 | -0.21 |
| | -86.230 | | | -86.138 | | | -85.963 | | | -85.766 | | | -85.576 | |
| 161.225 | -0.582 | 0.03 | 161.204 | -0.580 | -0.12 | 161.208 | -0.580 | -0.12 | 161.217 | -0.578 | -0.05 | 161.213 | -0.577 | -0.12 |
| | -93.883 | | | -93.597 | | | -93.509 | | | -93.312 | | | -93.148 | |

STD. DEVIATION OF CURVE ACROSS ONE DIAGONAL 0.10 MM.

CURVE VALUES , INTERPOLATED LINE POINTS AND TARGET HEIGHTS

| P.D. | TAN.Q | LINE | TARGET | LINE | TARGET | LINE | TARGET | LINE | TARGET | LINE | TARGET |
|---|---|---|---|---|---|---|---|---|---|---|---|
| 161.175 | 0.636 | 4.64805 | 4.6505 | 4.81624 | 4.8177 | 4.99805 | 4.9983 | 5.24627 | 5.2445 | 5.55375 | 5.5487 |
| 161.216 | 0.587 | 4.56133 | 4.5639 | 4.71628 | 4.7176 | 4.88337 | 4.8834 | 5.11182 | 5.1109 | 5.39476 | 5.3890 |
| 161.264 | 0.522 | 4.44754 | 4.4495 | 4.58485 | 4.5856 | 4.73308 | 4.7340 | 4.93567 | 4.9346 | 5.18629 | 5.1815 |
| 161.324 | 0.429 | 4.28383 | 4.2858 | 4.39563 | 4.3958 | 4.51653 | 4.5163 | 4.68169 | 4.6812 | 4.88617 | 4.8832 |
| 161.373 | 0.333 | 4.11508 | 4.1159 | 4.20079 | 4.2017 | 4.29339 | 4.2940 | 4.41999 | 4.4187 | 4.57677 | 4.5745 |
| 161.419 | 0.208 | 3.89449 | 3.8957 | 3.94607 | 3.9468 | 4.00194 | 4.0015 | 4.07832 | 4.0770 | 4.17270 | 4.1715 |
| 161.430 | -0.166 | 3.22437 | 3.2220 | 3.17225 | 3.1718 | 3.11612 | 3.1159 | 3.03927 | 3.0410 | 2.94428 | 2.9475 |
| 161.392 | -0.288 | 3.00419 | 3.0013 | 2.91794 | 2.9170 | 2.82502 | 2.8251 | 2.69790 | 2.6997 | 2.54064 | 2.5452 |
| 161.350 | -0.381 | 2.83580 | 2.8332 | 2.72363 | 2.7226 | 2.60256 | 2.6024 | 2.43695 | 2.4384 | 2.23191 | 2.2369 |
| 161.299 | -0.471 | 2.67191 | 2.6690 | 2.53421 | 2.5328 | 2.38575 | 2.3848 | 2.18276 | 2.1847 | 1.93160 | 1.9382 |
| 161.257 | -0.533 | 2.55795 | 2.5546 | 2.40267 | 2.4000 | 2.23533 | 2.2349 | 2.00633 | 2.0093 | 1.72274 | 1.7302 |
| 161.221 | -0.580 | 2.47187 | 2.4674 | 2.30321 | 2.3018 | 2.12139 | 2.1211 | 1.87286 | 1.8760 | 1.56497 | 1.5721 |

COMPOSITE CURVE CONSTANTS R*R*-0.2687 + 161.452 = P.D.

CURVE VALUES FOR PLOTTING

| | | | | | | | | | |
|---|---|---|---|---|---|---|---|---|---|
| 0.05 | 161.450 | 0.10 | 161.445 | 0.15 | 161.436 | 0.20 | 161.424 | 0.25 | 161.408 |
| 0.30 | 161.389 | 0.35 | 161.366 | 0.40 | 161.340 | 0.45 | 161.310 | 0.50 | 161.277 |
| 0.55 | 161.240 | 0.60 | 161.200 | 0.65 | 161.156 | 0.70 | 161.109 | | |

STD. DEVIATION OF COMPOSITE CURVE 0.10 MM. HEIGHT AT THE WIRES

CAMERA 113D  DIAGONAL 500-100  OBJECT DISTANCE 2,3M

PLATE 33 NOMINAL P.D. 161.15 APPROX. DIST. TO 1ST WIRE 1.790

DEFINED P.P. 198.033 200.500  SELECTED P.P. 197.991

PLATE Y COORD. OF IMAGE LINES  200.155  200.066  199.916  199.832  199.731

| | | | | | |
|---|---|---|---|---|---|
| PRINCIPAL POINT ON WIRES | 3.54190 | 3.53878 | 3.53552 | 3.53110 | 3.52540 |
| RESIDUALS OF FITTED LINE | -0.02 | 0.05 | 0.01 | -0.08 | 0.04 |

STD. DEVIATION 0.05  SLOPE -0.011032

| POINTS | CONSTANTS OF UPPER AND LOWER RADIAL LINES M' | M" | N' | N" | COORDINATES OF S L | H |
|---|---|---|---|---|---|---|
| 1 13 | 0.606985 | 4.64827 | -0.608466 | 2.47197 | -1.79053 | 3.56145 |
| 2 12 | 0.558568 | 4.56156 | -0.560534 | 2.55818 | -1.79016 | 3.56163 |
| 3 11 | 0.495042 | 4.44782 | -0.496934 | 2.67208 | -1.79011 | 3.56164 |
| 4 10 | 0.403516 | 4.28404 | -0.405345 | 2.83604 | -1.79018 | 3.56168 |
| 5 9 | 0.309178 | 4.11529 | -0.311360 | 3.00440 | -1.79020 | 3.56180 |
| 6 8 | 0.186060 | 3.89476 | -0.188322 | 3.22460 | -1.79004 | 3.56170 |

RESIDUALS OF LINE HEIGHTS  STD.DEV.

| | | | | | |
|---|---|---|---|---|---|
| -0.03 | 0.15 | -0.16 | 0.01 | 0.03 | 0.11 |
| -0.01 | -0.04 | 0.04 | 0.05 | -0.04 | 0.04 |
| 0.04 | -0.03 | -0.02 | 0.01 | 0.01 | 0.03 |
| -0.04 | 0.11 | -0.09 | 0.02 | 0.00 | 0.07 |
| -0.01 | -0.01 | 0.02 | 0.01 | -0.01 | 0.01 |
| -0.05 | 0.06 | -0.02 | 0.03 | -0.02 | 0.04 |
| -0.01 | 0.07 | -0.04 | -0.05 | 0.04 | 0.05 |
| 0.01 | -0.07 | 0.05 | 0.07 | -0.05 | 0.06 |
| -0.04 | 0.04 | 0.05 | -0.08 | 0.03 | 0.06 |
| 0.01 | 0.02 | -0.02 | -0.03 | 0.02 | 0.02 |
| -0.00 | 0.01 | 0.04 | -0.09 | 0.04 | 0.05 |
| -0.07 | 0.06 | -0.00 | 0.06 | -0.05 | 0.06 |

| | | | |
|---|---|---|---|
| WEIGHTED MEAN COORDINATES OF S | -1.79024 | 3.56162 | SLOPE OF AXIS -2275.4 SECONDS |
| INCREMENTS | -0.00024 | 3.56162 | ITERATION 1 |
| HT. BY EXTENSION OF AXIS EQUATION | | 3.56163 | |


| | | | | | |
|---|---|---|---|---|---|
| PRINCIPAL POINT ON WIRES | 3.54190 | 3.53878 | 3.53552 | 3.53110 | 3.52540 |
| RESIDUALS OF FITTED LINE | -0.02 | 0.05 | 0.01 | -0.08 | 0.04 |

STD. DEVIATION 0.05  SLOPE -0.011032


| POINTS | CONSTANTS OF UPPER AND LOWER RADIAL LINES M' | M" | N' | N" | COORDINATES OF S L | H |
|---|---|---|---|---|---|---|
| 1 13 | 0.506985 | 4.64827 | -0.608467 | 2.47197 | -1.79053 | 3.56145 |
| 2 12 | 0.558568 | 4.56156 | -0.560535 | 2.55818 | -1.79016 | 3.56163 |
| 3 11 | 0.495042 | 4.44782 | -0.496935 | 2.67208 | -1.79010 | 3.56164 |
| 4 10 | 0.403516 | 4.28404 | -0.405345 | 2.83604 | -1.79018 | 3.56168 |
| 5 9 | 0.309178 | 4.11529 | -0.311360 | 3.00440 | -1.79020 | 3.56180 |
| 6 8 | 0.186060 | 3.89476 | -0.188323 | 3.22460 | -1.79004 | 3.56170 |


RESIDUALS OF LINE HEIGHTS  STD.DEV.

| | | | | | |
|---|---|---|---|---|---|
| -0.03 | 0.15 | -0.16 | 0.01 | 0.03 | 0.11 |
| -0.01 | -0.04 | 0.04 | 0.05 | -0.04 | 0.04 |
| 0.04 | -0.03 | -0.02 | 0.01 | 0.01 | 0.03 |
| -0.04 | 0.11 | -0.09 | 0.02 | 0.00 | 0.07 |
| -0.01 | -0.01 | 0.02 | 0.01 | -0.01 | 0.01 |
| -0.05 | 0.06 | -0.02 | 0.03 | -0.02 | 0.04 |
| -0.01 | 0.07 | -0.04 | -0.05 | 0.04 | 0.05 |
| 0.01 | -0.07 | 0.05 | 0.07 | -0.05 | 0.06 |
| -0.04 | 0.04 | 0.05 | -0.08 | 0.03 | 0.06 |
| 0.01 | 0.02 | -0.02 | -0.03 | 0.02 | 0.02 |
| -0.00 | 0.01 | 0.04 | -0.09 | 0.04 | 0.05 |
| -0.07 | 0.06 | -0.00 | 0.06 | -0.05 | 0.06 |


| | | | |
|---|---|---|---|
| WEIGHTED MEAN COORDINATES OF S | -1.79023 | 3.56162 | SLOPE OF AXIS -2275.4 SECONDS |
| INCREMENTS | 0.00000 | 0.00000 | ITERATION 2 |
| HT. BY EXTENSION OF AXIS EQUATION | | 3.56163 | |

SEC.SQD.W = 1.000122  TAN.W = -0.011032

CAMERA 113D  DIAGONAL 500-100  OBJECT DISTANCE 1,6M

PLATE 11 NOMINAL P.D. 166.03 APPROX. DIST. TO 1ST WIRE 1.171

DEFINED P.P. 199.711 201.017  SELECTED P.P. 199.622

PLATE Y COORD. OF IMAGE LINES 200.438 200.277 200.144 200.039 199.808

| | | | | | |
|---|---|---|---|---|---|
| PRINCIPAL POINT ON WIRES | 3.09188 | 3.09111 | 3.08993 | 3.08847 | 3.08691 |
| RESIDUALS OF FITTED LINE | -0.03 | -0.03 | 0.08 | 0.01 | -0.03 |

STD. DEVIATION 0.05  SLOPE -0.005177

| POINTS | CONSTANTS OF UPPER AND LOWER RADIAL LINES M' | M" | N' | N" | COORDINATES OF S L | H | RESIDUALS OF LINE HEIGHTS | STD.DEV. |
|---|---|---|---|---|---|---|---|---|
| 1 13 | 0.589796 | 3.78973 | -0.590901 | 2.40544 | -1.17244 | 3.09823 | 0.08 -0.14 0.08 -0.03 0.01 | 0.09 |
| | | | | | | | -0.10 0.06 0.05 0.05 -0.06 | 0.07 |
| 2 12 | 0.542539 | 3.73342 | -0.543490 | 2.46108 | -1.17155 | 3.09781 | -0.15 0.08 0.17 -0.08 -0.02 | 0.12 |
| | | | | | | | -0.05 0.03 0.05 -0.02 -0.01 | 0.04 |
| 3 11 | 0.484204 | 3.66512 | -0.484164 | 2.53088 | -1.17129 | 3.09797 | -0.11 0.05 0.10 0.01 -0.05 | 0.08 |
| | | | | | | | -0.14 0.13 0.11 0.08 -0.08 | 0.11 |
| 4 10 | 0.393222 | 3.55851 | -0.394201 | 2.63642 | -1.17103 | 3.09804 | -0.07 -0.02 0.10 0.07 -0.08 | 0.08 |
| | | | | | | | -0.06 0.06 -0.01 0.05 -0.04 | 0.05 |
| 5 9 | 0.301778 | 3.45111 | -0.301432 | 2.74494 | -1.17070 | 3.09782 | -0.05 0.01 0.07 -0.02 -0.02 | 0.05 |
| | | | | | | | -0.05 0.02 0.05 0.02 -0.04 | 0.04 |
| 6 8 | 0.181580 | 3.31045 | -0.182614 | 2.88425 | -1.17026 | 3.09796 | -0.03 -0.03 0.07 0.02 -0.03 | 0.05 |
| | | | | | | | -0.03 0.03 -0.02 0.03 -0.02 | 0.03 |

| | | | |
|---|---|---|---|
| WEIGHTED MEAN COORDINATES OF S | -1.17143 | 3.09799 | SLOPE OF AXIS -1067.9 SECONDS |
| INCREMENTS | -0.00043 | 3.09799 | ITERATION 1 |
| HT. BY EXTENSION OF AXIS EQUATION | | 3.09792 | |

| | | | | | |
|---|---|---|---|---|---|
| PRINCIPAL POINT ON WIRES | 3.09188 | 3.09111 | 3.08993 | 3.08847 | 3.08691 |
| RESIDUALS OF FITTED LINE | -0.03 | -0.03 | 0.08 | 0.01 | -0.03 |

STD. DEVIATION 0.05  SLOPE -0.005177

| POINTS | CONSTANTS OF UPPER AND LOWER RADIAL LINES M' | M" | N' | N" | COORDINATES OF S L | H | RESIDUALS OF LINE HEIGHTS | STD.DEV. |
|---|---|---|---|---|---|---|---|---|
| 1 13 | 0.589799 | 3.78973 | -0.590902 | 2.40544 | -1.17243 | 3.09823 | 0.08 -0.14 0.08 -0.03 0.01 | 0.09 |
| | | | | | | | -0.10 0.06 0.05 0.05 -0.06 | 0.07 |
| 2 12 | 0.542541 | 3.73341 | -0.543491 | 2.46108 | -1.17154 | 3.09780 | -0.15 0.08 0.16 -0.08 -0.02 | 0.12 |
| | | | | | | | -0.05 0.03 0.05 -0.02 -0.01 | 0.04 |
| 3 11 | 0.484207 | 3.66512 | -0.484165 | 2.53088 | -1.17128 | 3.09797 | -0.11 0.05 0.10 0.01 -0.05 | 0.08 |
| | | | | | | | -0.14 0.13 0.11 0.08 -0.08 | 0.11 |
| 4 10 | 0.393224 | 3.55851 | -0.394203 | 2.63642 | -1.17102 | 3.09804 | -0.07 -0.02 0.10 0.07 -0.08 | 0.08 |
| | | | | | | | -0.06 0.06 -0.01 0.05 -0.04 | 0.05 |
| 5 9 | 0.301779 | 3.45111 | -0.301432 | 2.74494 | -1.17070 | 3.09782 | -0.05 0.01 0.07 -0.02 -0.02 | 0.05 |
| | | | | | | | -0.05 0.02 0.05 0.02 -0.04 | 0.04 |
| 6 8 | 0.181581 | 3.31045 | -0.182614 | 2.88425 | -1.17025 | 3.09795 | -0.03 -0.03 0.07 0.02 -0.03 | 0.05 |
| | | | | | | | -0.02 0.03 -0.02 0.03 -0.02 | 0.03 |

| | | | |
|---|---|---|---|
| WEIGHTED MEAN COORDINATES OF S | -1.17142 | 3.09799 | SLOPE OF AXIS -1067.9 SECONDS |
| INCREMENTS | 0.00001 | -0.00000 | ITERATION 2 |
| HT. BY EXTENSION OF AXIS EQUATION | | 3.09792 | |

SEC.SQD.W = 1.000027  TAN.W = -0.005177

CAMERA 113D DIAGONAL 300-700 OBJECT DISTANCE 2,3M

PLATE -34 NOMINAL P.D. 161.15 APPROX. DIST. TO 1ST WIRE 1.790

DEFINED P.P. 197.567 199.863 SELECTED P.P. 197.476

PLATE Y COORD. OF IMAGE LINES 200.171 200.069 199.916 199.821 199.717

PRINCIPAL POINT ON WIRES 3.53640 3.53234 3.52808 3.52216 3.51467
RESIDUALS OF FITTED LINE 0.02 0.04 -0.04 -0.07 0.06 STD. DEVIATION 0.06 SLOPE -0.014545

| POINTS | CONSTANTS OF UPPER AND LOWER RADIAL LINES M' | M" | N' | N" | COORDINATES OF S L | H | RESIDUALS OF LINE HEIGHTS | STD.DEV. |
|---|---|---|---|---|---|---|---|---|
| 1 13 | 0.606642 | 4.64846 | -0.608798 | 2.47215 | -1.79055 | 3.56224 | -0.02 0.10 -0.12 0.03 0.01<br>-0.06 0.01 0.07 0.00 -0.03 | 0.08<br>0.05 |
| 2 12 | 0.558266 | 4.56173 | -0.560839 | 2.55835 | -1.79016 | 3.56234 | 0.01 -0.00 -0.01 -0.01 0.01<br>-0.03 0.17 -0.10 -0.14 0.10 | 0.01<br>0.13 |
| 3 11 | 0.494695 | 4.44801 | -0.497199 | 2.67222 | -1.79030 | 3.56236 | 0.03 0.05 -0.08 -0.07 0.07<br>-0.04 0.03 0.01 0.04 -0.03 | 0.07<br>0.04 |
| 4 10 | 0.403236 | 4.28420 | -0.405694 | 2.83623 | -1.78998 | 3.56242 | -0.03 0.08 -0.02 -0.07 0.04<br>0.02 -0.08 0.04 0.05 -0.03 | 0.06<br>0.05 |
| 5 9 | 0.308930 | 4.11543 | -0.311551 | 3.00451 | -1.79041 | 3.56231 | -0.05 0.06 0.00 0.01 -0.02<br>-0.03 0.00 0.03 0.02 -0.02 | 0.04<br>0.03 |
| 6 8 | 0.185826 | 3.89489 | -0.188566 | 3.22474 | -1.78997 | 3.56226 | -0.02 0.05 0.02 -0.09 0.04<br>-0.04 0.07 -0.05 0.02 -0.01 | 0.06<br>0.05 |

WEIGHTED MEAN COORDINATES OF S -1.79027 3.56232 SLOPE OF AXIS -2999.9 SECONDS
INCREMENTS -0.00027 3.55232 ITERATION 1
HT. BY EXTENSION OF AXIS EQUATION 3.56245

PRINCIPAL POINT ON WIRES 3.53639 3.53234 3.52807 3.52216 3.51467
RESIDUALS OF FITTED LINE 0.02 0.04 -0.04 -0.07 0.06 STD. DEVIATION 0.06 SLOPE -0.014545

| POINTS | CONSTANTS OF UPPER AND LOWER RADIAL LINES M' | M" | N' | N" | COORDINATES OF S L | H | RESIDUALS OF LINE HEIGHTS | STD.DEV. |
|---|---|---|---|---|---|---|---|---|
| 1 13 | 0.506642 | 4.64846 | -0.608799 | 2.47215 | -1.79055 | 3.56224 | -0.02 0.10 -0.12 0.03 0.01<br>-0.06 0.01 0.07 0.00 -0.03 | 0.08<br>0.05 |
| 2 12 | 0.558266 | 4.56173 | -0.560840 | 2.55835 | -1.79015 | 3.56234 | 0.01 -0.00 -0.01 -0.01 0.01<br>-0.03 0.17 -0.10 -0.14 0.10 | 0.01<br>0.13 |
| 3 11 | 0.494696 | 4.44801 | -0.497199 | 2.67223 | -1.79030 | 3.56236 | 0.03 0.05 -0.08 -0.07 0.07<br>-0.04 0.03 0.01 0.04 -0.03 | 0.07<br>0.04 |
| 4 10 | 0.403236 | 4.28420 | -0.405694 | 2.83623 | -1.78998 | 3.56242 | -0.03 0.08 -0.02 -0.07 0.04<br>0.02 -0.08 0.04 0.05 -0.03 | 0.06<br>0.05 |
| 5 9 | 0.308930 | 4.11543 | -0.311552 | 3.00451 | -1.79041 | 3.56232 | -0.05 0.06 0.00 0.01 -0.02<br>-0.03 0.00 0.03 0.02 -0.02 | 0.04<br>0.03 |
| 6 8 | 0.185826 | 3.89489 | -0.188567 | 3.22474 | -1.78997 | 3.56226 | -0.02 0.05 0.02 -0.09 0.04<br>-0.04 0.07 -0.05 0.02 -0.01 | 0.06<br>0.05 |

WEIGHTED MEAN COORDINATES OF S -1.79027 3.56232 SLOPE OF AXIS -2999.9 SECONDS
INCREMENTS 0.00000 0.00000 ITERATION 2
HT. BY EXTENSION OF AXIS EQUATION 3.56245
SEC.SQD.W = 1.000212 TAN.W = -0.014545

CAMERA 113D  DIAGONAL 300-700  OBJECT DISTANCE 1,6M

PLATE -12 NOMINAL P.D. 166.03 APPROX. DIST. TO 1ST WIRE 1.175

DEFINED P.P. 199.665 200.067  SELECTED P.P. 199.490

PLATE Y COORD. OF IMAGE LINES  200.292  200.102  199.933  199.821  199.563

PRINCIPAL POINT ON WIRES  3.09731  3.09714  3.09688  3.09671  3.09639
RESIDUALS OF FITTED LINE  -0.03  0.00  0.07  -0.03  -0.00  STD. DEVIATION  0.04  SLOPE  -0.000925

| POINTS | CONSTANTS OF UPPER AND LOWER RADIAL LINES M' | M" | N' | N" | COORDINATES OF S L | H | RESIDUALS OF LINE HEIGHTS | STD.DEV. |
|---|---|---|---|---|---|---|---|---|
| 1 13 | 0.588088 | 3.79033 | -0.589652 | 2.40500 | -1.17626 | 3.09858 | 0.01 -0.07 0.10 -0.06 0.01 | 0.07 |
| | | | | | | | -0.08 0.05 0.04 0.04 -0.05 | 0.06 |
| 2 12 | 0.540770 | 3.73404 | -0.542533 | 2.46075 | -1.17538 | 3.09843 | -0.12 0.08 0.12 -0.10 0.01 | 0.10 |
| | | | | | | | -0.02 -0.00 0.04 -0.01 -0.01 | 0.02 |
| 3 11 | 0.482647 | 3.66566 | -0.483262 | 2.53056 | -1.17517 | 3.09847 | -0.08 0.05 0.06 -0.01 -0.02 | 0.06 |
| | | | | | | | -0.14 0.15 0.00 0.04 -0.05 | 0.10 |
| 4 10 | 0.391945 | 3.55896 | -0.393500 | 2.63617 | -1.17486 | 3.09848 | -0.06 -0.00 0.07 0.04 -0.06 | 0.06 |
| | | | | | | | -0.05 0.07 -0.04 0.04 -0.03 | 0.05 |
| 5 9 | 0.300607 | 3.45153 | -0.301023 | 2.74479 | -1.17470 | 3.09841 | -0.04 0.01 0.05 -0.03 -0.00 | 0.03 |
| | | | | | | | -0.05 0.02 0.05 0.00 -0.02 | 0.04 |
| 6 8 | 0.180823 | 3.31072 | -0.182397 | 2.88417 | -1.17435 | 3.09837 | -0.01 -0.01 0.03 -0.01 -0.00 | 0.02 |
| | | | | | | | -0.03 0.02 0.02 0.00 -0.01 | 0.02 |

WEIGHTED MEAN COORDINATES OF S  -1.17531  3.09848  SLOPE OF AXIS  -190.9 SECONDS
INCREMENTS  -0.00031  3.09848  ITERATION 1
HT. BY EXTENSION OF AXIS EQUATION  3.09836

PRINCIPAL POINT ON WIRES  3.09731  3.09714  3.09688  3.09671  3.09639
RESIDUALS OF FITTED LINE  -0.03  0.00  0.07  -0.03  -0.00  STD. DEVIATION  0.04  SLOPE  -0.000925

| POINTS | CONSTANTS OF UPPER AND LOWER RADIAL LINES M' | M" | N' | N" | COORDINATES OF S L | H | RESIDUALS OF LINE HEIGHTS | STD.DEV. |
|---|---|---|---|---|---|---|---|---|
| 1 13 | 0.588089 | 3.79033 | -0.589653 | 2.40500 | -1.17626 | 3.09858 | 0.01 -0.07 0.10 -0.06 0.01 | 0.07 |
| | | | | | | | -0.08 0.05 0.04 0.04 -0.05 | 0.06 |
| 2 12 | 0.540771 | 3.73404 | -0.542534 | 2.46075 | -1.17538 | 3.09843 | -0.11 0.08 0.12 -0.09 0.01 | 0.10 |
| | | | | | | | -0.02 -0.00 0.04 -0.01 -0.01 | 0.02 |
| 3 11 | 0.482648 | 3.66566 | -0.483262 | 2.53056 | -1.17516 | 3.09847 | -0.08 0.05 0.06 -0.01 -0.02 | 0.06 |
| | | | | | | | -0.14 0.14 0.00 0.04 -0.05 | 0.10 |
| 4 10 | 0.391947 | 3.55896 | -0.393501 | 2.63617 | -1.17486 | 3.09848 | -0.06 -0.00 0.07 0.04 -0.06 | 0.06 |
| | | | | | | | -0.05 0.07 -0.04 0.04 -0.03 | 0.05 |
| 5 9 | 0.300607 | 3.45153 | -0.301023 | 2.74479 | -1.17470 | 3.09840 | -0.04 0.01 0.05 -0.03 -0.00 | 0.03 |
| | | | | | | | -0.05 0.02 0.05 0.00 -0.02 | 0.04 |
| 6 8 | 0.180823 | 3.31072 | -0.182397 | 2.88417 | -1.17434 | 3.09837 | -0.00 -0.01 0.03 -0.01 -0.00 | 0.02 |
| | | | | | | | -0.03 0.02 0.02 0.00 -0.01 | 0.02 |

WEIGHTED MEAN COORDINATES OF S  -1.17530  3.09847  SLOPE OF AXIS  -190.9 SECONDS
INCREMENTS  0.00000  -0.00000  ITERATION 2
HT. BY EXTENSION OF AXIS EQUATION  3.09836
SEC.SQD.W = 1.000001  TAN.W = -0.000925

APPENDIX C1.

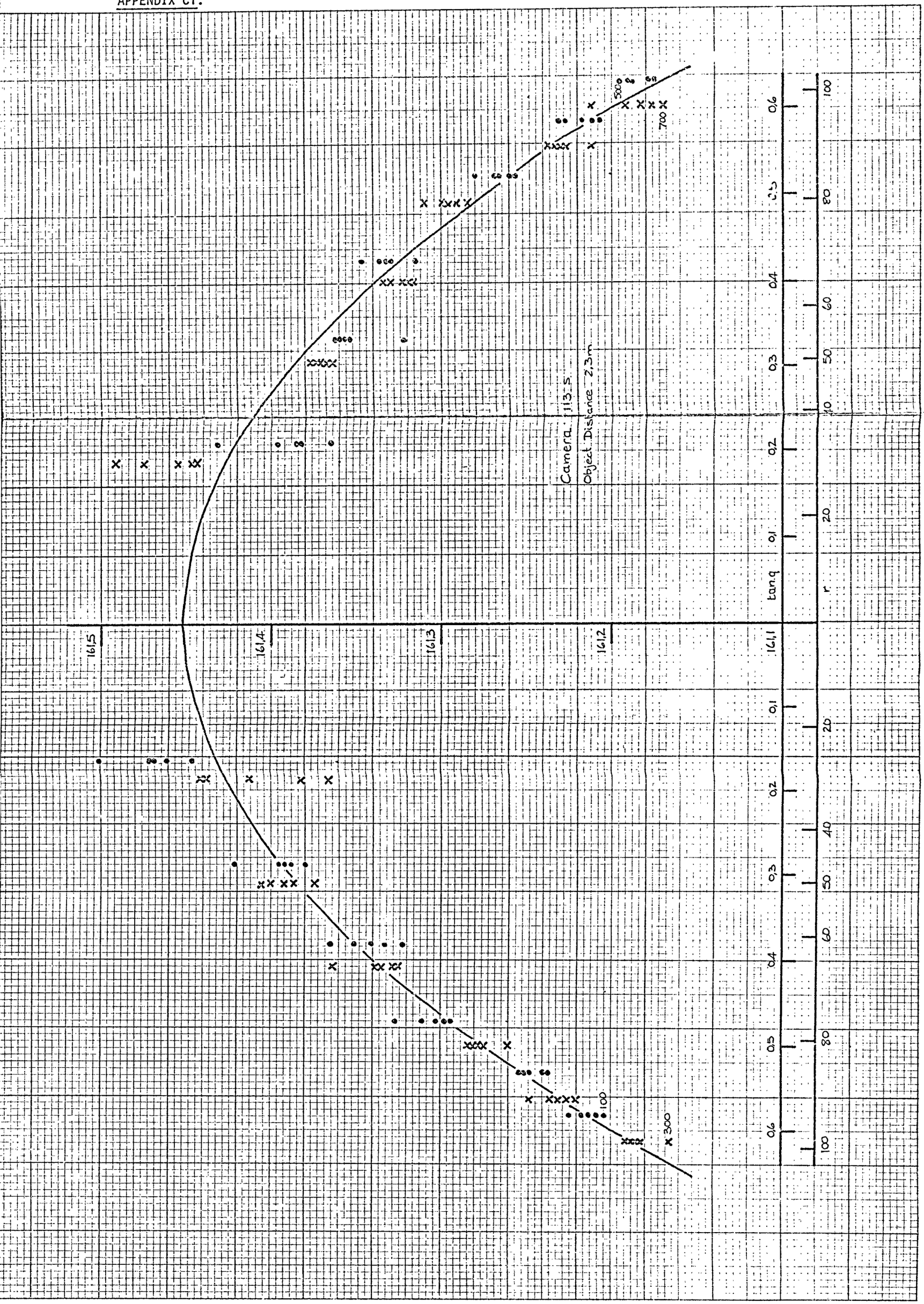
Camera 113 S
Object Distance 2,3m
tanq
r
161,1
161,2
161,3
161,4
161,5
0,1
0,2
0,3
0,4
0,5
0,6
20
40
50
60
80
100
300
500
700

APPENDIX C2.

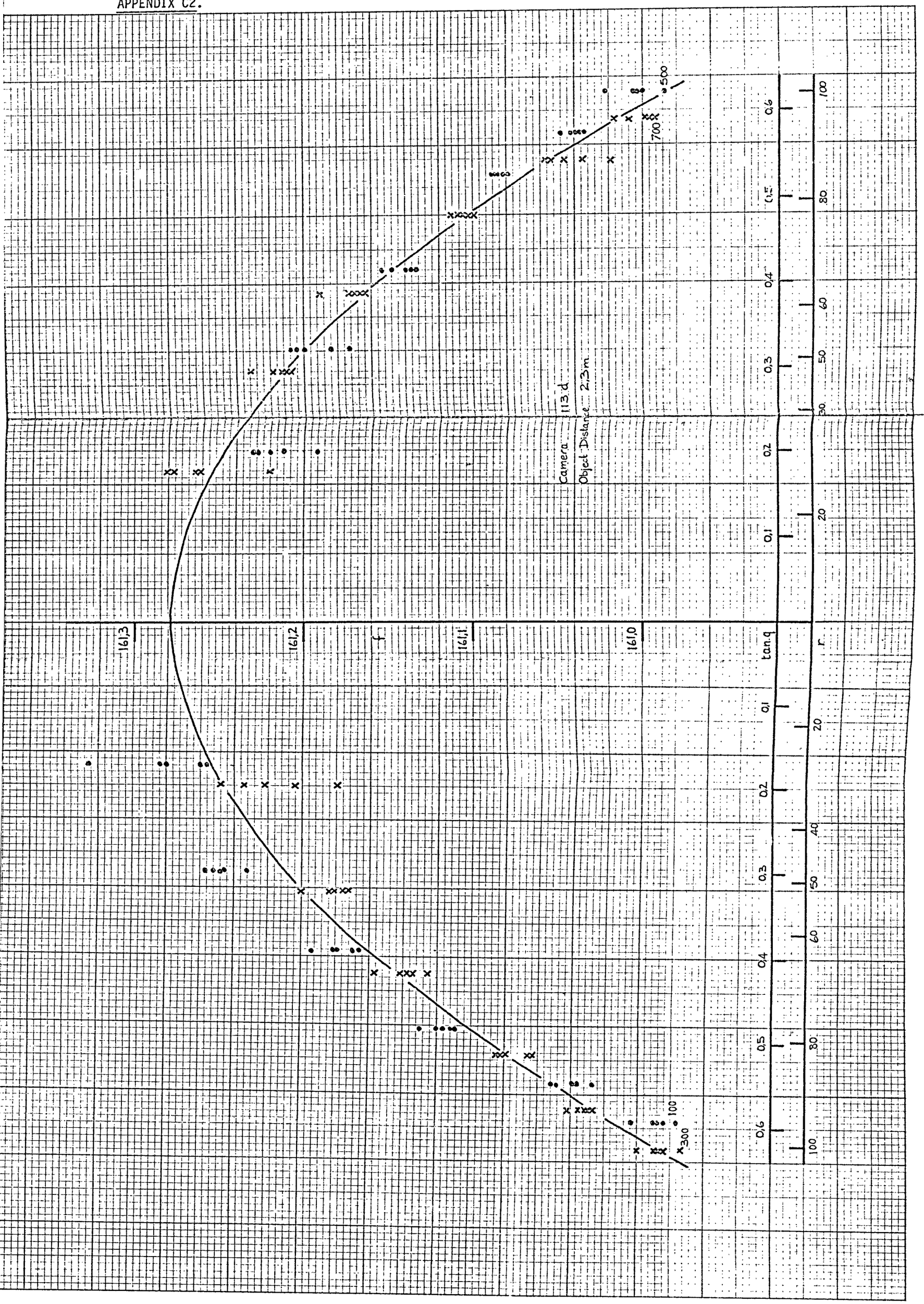
Camera 113.d
Object Distance 2,3m
f
161,3
161,2
161,1
161,0
tan.q
r
0,1
0,2
0,3
0,4
0,5
0,6
20
30
40
50
60
80
100
300
500
700

APPENDIX C3.

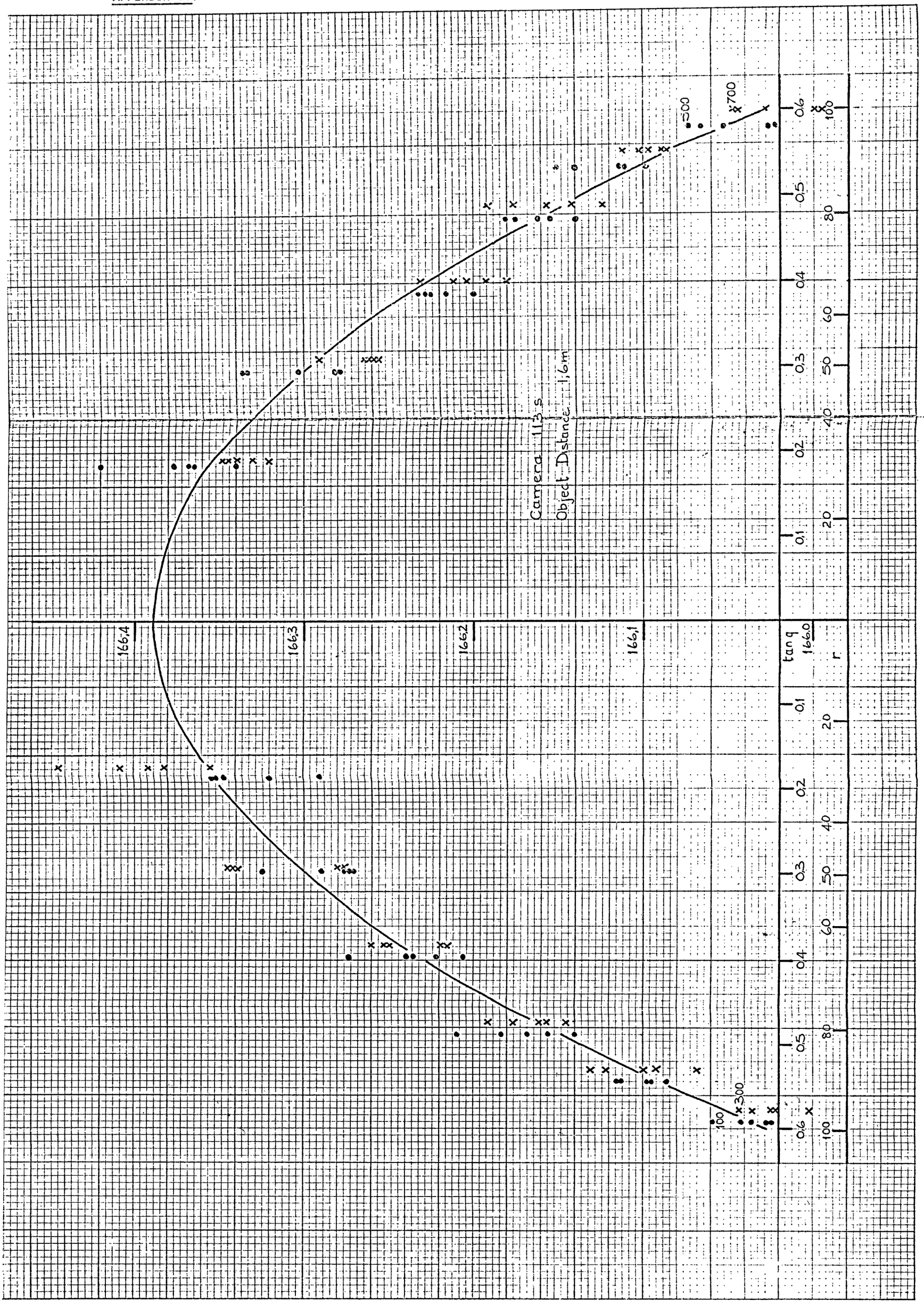
Camera 11.2 s
Object Distance 1.6m
166.4
166.3
166.2
166.1
166.0
tan q
r
300
700
0.1
0.2
0.3
0.4
0.5
0.6
20
40
50
60
80
100

APPENDIX C4.

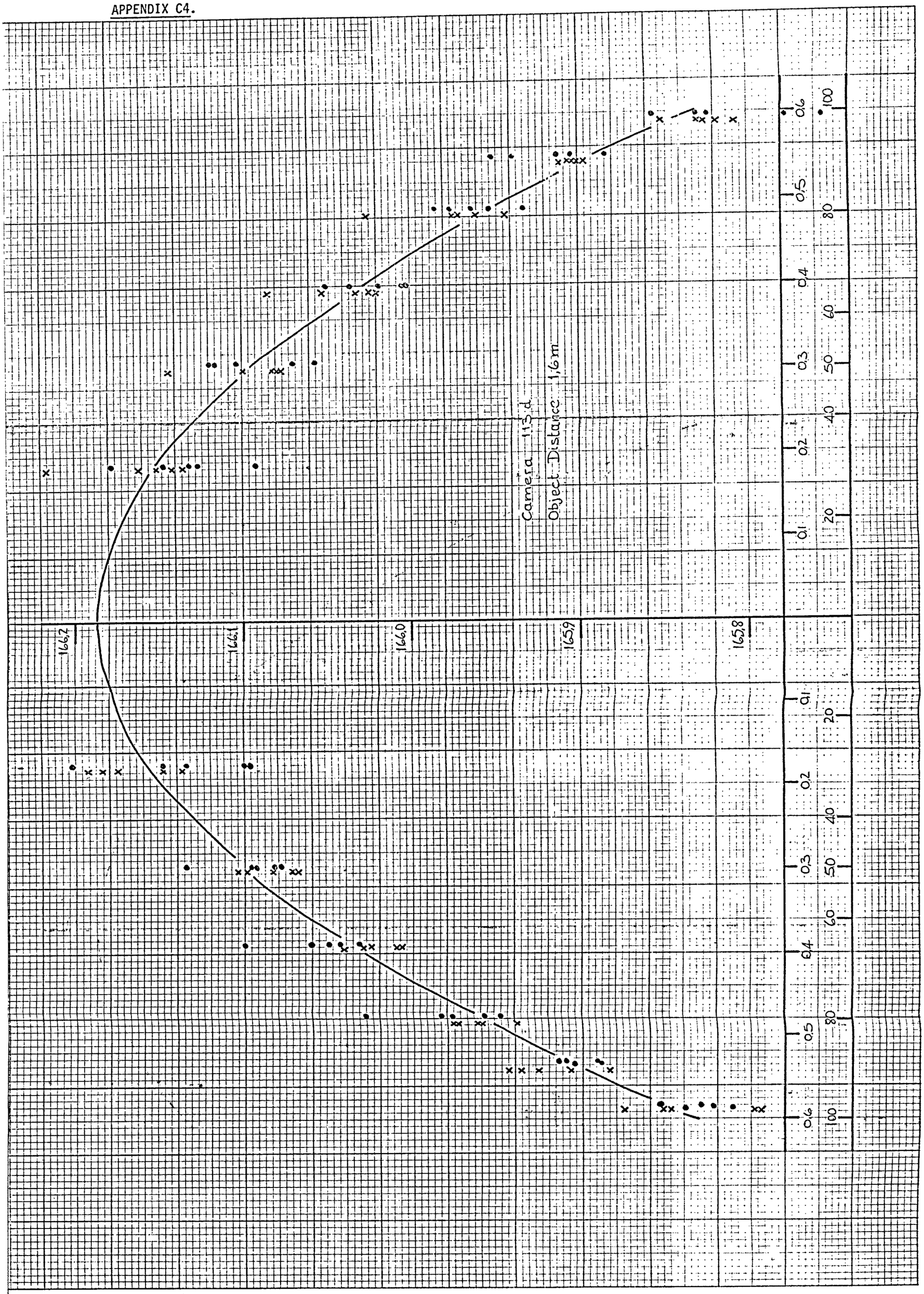
Camera 113 d
Object Distance 1,6 m
1662
1661
1660
1659
1658
0,1
0,2
0,3
0,4
0,5
0,6
20
40
50
60
80
100